ANISOTROPY IN ARENES

ANISOTROPY IN ARENES:
CALCULATION OF NMR CHEMICAL SHIFTS

By

ARVIND AGARWAL

A Thesis

Submitted to the Faculty of Graduate Studies

In Partial Fulfilment of the Requirements

for the Degree

Master of Science

McMaster University

December 1976

To

My Parents

MASTER OF SCIENCE (1976)
(Chemistry)

McMASTER UNIVERSITY
Hamilton, Ontario

TITLE: Anisotropy in Arenes: Calculation of NMR Chemical Shifts

AUTHOR: Arvind Agarwal, M.Sc. (I.I.T. Kanpur, India)

SUPERVISOR: Dr. M. J. McGlinchey

NUMBER OF PAGES: x, 104

ABSTRACT

The local anisotropic shielding contribution to proton NMR chemical shifts, due to electron circulation around each carbon, in benzene is calculated on the basis of the free electron in a loop model. The circulating current was estimated from the experimentally measured ^{13}C shielding tensors. The ring current contribution is recalculated, using the Waugh and Fessenden approach but no loop separation is assumed.

The sum of the local anisotropic and ring current contributions in conjunction with an appropriately chosen standard shift predict chemical shift values which compare favourably with experimental values for benzene and toluene. The predicted chemical shifts for the methylene protons of [9]-paracyclophane are given.

Contour maps of the local anisotropic contributions in various planes in and around a benzene ring are presented. Also presented is a contour map for the ring current contribution, similar to the Johnson and Bovey plot, with the assumption there is no separation of the current loops.

ACKNOWLEDGEMENTS

I would like to take this opportunity to express my deep gratitude and heartfelt thanks to my supervisor, Dr. M. J. McGlinchey, for his infinite patience, interest and help during the course of this work. The help of my friends and especially the members of our research group, in particular John Fletcher, is gratefully acknowledged. Mention must also be made of Jack Barnes, a summer student, for his help in the initial stages of the work. Help in computer programming from Dr. D. P. Santry is greatly appreciated.

Special thanks are due to Mrs. Jan Gallo for typing the thesis with speed and accuracy.

Financial support, in the form of an Assistantship, from the Chemistry Department, McMaster University, is gratefully acknowledged.

TABLE OF CONTENTS

LIST OF TABLES

LIST OF FIGURES

LIST OF COMPUTER PROGRAMMES

CHAPTER I

INTRODUCTION

1.1 HISTORICAL

1.1.1 Magnetic Anisotropy

Since the detection of molecular diamagnetic anisotropy in experiments on magnetic birefringence (1,2), it has now become well established that the majority of organic molecules exhibit anisotropic diamagnetic behaviour in the presence of an external magnetic field.

Raman and Krishnan (3), used the large positive values of magnetic birefringence of aromatic compounds to conclude that they possess large diamagnetic anisotropy. They then pointed out that when such magnetically anisotropic molecules are arranged in a regular manner, as in a crystal, the crystal as a whole exhibits diamagnetic anisotropy; on the other hand, in liquids and gases, only the average susceptibility is measured due to the rapid tumbling of molecules. The magnitude of the differences between the diamagnetic susceptibilities, in different directions, will depend on the relative orientation of the molecules in the unit cell (4).

The diamagnetic susceptibilities of a large number of benzenoid hydrocarbons, as single crystals, have been measured (4-10). All the benzenoid hydrocarbons were found to have the diamagnetic susceptibility along the axis perpendicular to the rings (χ_3), to be much larger than the susceptibilities along either of the other two axes in the plane of the rings (χ_1, χ_2). The susceptibility data for the series, benzene,

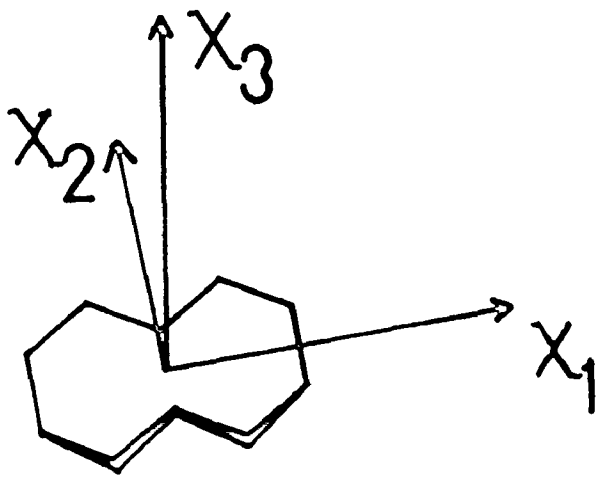

naphthalene and anthracene, (see Table 1.1), show that χ_1 and χ_2 are more or less constant for all three but χ_3 increases, additively, as the number of rings increases (11).

TABLE 1-1: Principal Diamagnetic Susceptibilities for Benzene Naphthalene and Anthracene (11)

Compound	$-\chi_1 \times 10^6$ esu	$-\chi_2 \times 10^6$ esu	$-\chi_3 \times 10^6$ esu
	37.3	37.3	91.2
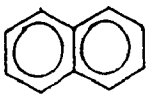	39.4	43.0	187.2
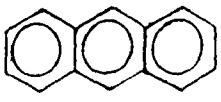	45.9	52.7	272.5

Diamagnetic susceptibility can be considered to arise due to Larmor precession of electrons in orbits around each atom. Ehrenfest (12) first used the Larmor precession of electrons in orbits including many nuclei to explain the unusually large diamagnetic anisotropy observed in crystals of bismuth. Raman (13) extended this concept to explain the large diamagnetic susceptibility of graphite, perpendicular to the plane of the hexagonal carbon rings. The same concept of Larmor precession of electrons was then extended further, by Raman and Krishnan (3), to explain the large diamagnetic susceptibility values of χ_3 for aromatic compounds.

Pauling (14) developed the idea into a semiclassical quantitative form for calculating the contribution to the magnetic susceptibility of electrons moving in loops. London (15,16) presented a quantum mechanical interpretation of the theory of diamagnetic anisotropy which supported Pauling's work and established the first theoretical explanation for the phenomenon presently known as the ring current.

1.1.2 NMR Chemical Shifts

Nuclear Magnetic Resonance (NMR) spectroscopy is a technique whereby a nucleus is used as a probe to investigate the local magnetic environment in a molecule. The basic theory of the phenomenon of NMR has been reviewed a number of times (17-19).

The nuclei of certain isotopes possess a spin which causes these nuclei to behave as tiny magnets with a magnetic moment μ. Due to the quantization of spin angular momentum, in an external field a spinning nucleus assumes only a discrete set of orientations which

depend on I the spin quantum number. Protons have I = 1/2 and hence assume only two orientations which have energies $\pm \mu H_0$ where H_0 is the external field (20). It is well established that the energy of a system in a magnetic field is proportional to the applied field hence, for a proton in an external field, the energy level splitting can be represented as follows:

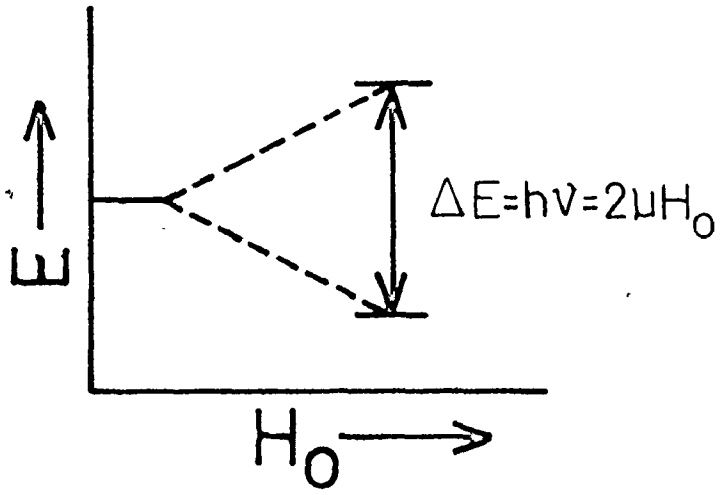

NMR signals are observed when the protons absorb energy and flip from one spin state to the other. In practice it is found easier to have the spectrometer operate at a constant frequency and vary the field until resonance conditions prevail.

The nucleus of an isolated atom, in an external magnetic field, feels a different magnetic field strength than the applied field due to circulation of electrons in a manner which creates a secondary magnetic field opposing the primary field. This circulation, known as Larmor precession, causes the diamagnetic shielding due to the opposing field; the NMR chemical shifts are a measure of this shielding. The

chemical shift of a nucleus N is given as σ_N such that H_N, the magnetic field at the nucleus is given by (17-20)

$$H_N = H_o - H_o \cdot \sigma_N = H_o(1-\sigma_N) \qquad (1\text{-}1)$$

Lamb (21) derived an expression to calculate the diamagnetic shielding, but his formula was found to be valid only for isolated atoms which have unhindered, spherical motion of electrons. Ramsey (22) corrected for hindrance to electron motion around atoms in molecules, and his formula had two terms which became similar to the Lamb formula (21), when averaged over all directions (19, p. 168). In effect, the second term of the Ramsey formula (22) was the paramagnetic correction for hindrance to electron motion.

Even the Ramsey formula (22) is good for only the smallest of molecules. In large molecules, the two terms both become large and cancel each other (19, p. 169). Hence, for large systems, the total diamagnetic shielding must be approximated by a number of contributing factors.

Saika and Slichter (23) first suggested the following division of the diamagnetic shielding into separate contributing factors:

i) The diamagnetic term for the atom under observation. This is easily estimated from the Lamb formula (21).

ii) The paramagnetic term which corrects for the hindrance to the motion of electrons around an atom in a molecule.

iii) The diamagnetic and paramagnetic contribution from other atoms in the molecule on the atom being observed.

Later, Pople (24) showed that interatomic flow of electrons

could be a large contributing factor, particularly for molecules where electrons can flow around in closed loops. Hence the fourth factor is added.

iv) The interatomic current contribution.

McConnell (25) and Pople (26) have discussed the quantum mechanical derivations for the various contributing terms.

1.2 PROTON CHEMICAL SHIFTS

The range of chemical shifts for protons has been found to be of the order of 10^{-5} to 10^{-6}. Since different instruments with different frequencies and field strengths will give different chemical shifts, it is desirable to have a parameter which is independent of the instrumentation. The parameter commonly used to represent chemical shifts is δ, where δ is defined as follows (20)

$$\delta = (H_r - H_s)/H_r \qquad (1\text{-}2)$$

H_r being the resonance field strength for the reference compound and H_s being the resonance field strength for the sample.

The reference compound most commonly used for protons is tetramethylsilane (TMS) which gives a single, sharp absorption line at a higher field than most other protons absorb (20).

As previously outlined in Section 1.1.2, the shielding for an atom in a molecule can be visualized as the sum of four contributing factors. Since there are no low lying p orbitals in hydrogen it has an approximately spherical electron density, even in molecules, thus the local paramagnetic term for protons is small and hence neglected (19).

The other three factors are discussed individually in the following sections.

1.2.1 The Local Diamagnetic Contribution

Due to the fact that the electron density around a hydrogen atom can be considered approximately spherical, the diamagnetic shielding in an external field can be calculated from the Lamb formula (21):

$$\sigma_{1d} = \frac{e^2}{3mc^2}\int(\rho/r)dr, \qquad (1\text{-}3)$$

where e is the electronic charge; m is the mass of an electron; c is the velocity of light; ρ is the electron density; and r is the distance in atomic units.

The electron density ρ for hydrogen may be approximately defined as

$$\rho = \lambda\psi_{1s}^2 = \lambda\frac{e^{-2r}}{\pi}, \qquad (1\text{-}4)$$

where λ is the effective number of electrons in the 1s orbit.

Upon substituting for ρ and the physical constants in (1-3), the value of σ_{1d} was found to be (27)

$$\sigma_{1d} = 17.8\lambda \times 10^{-6} \qquad (1\text{-}5)$$

Variations in electron density around the hydrogen will thus cause an experimentally observable change in the screening constant and hence in the chemical shift. This change can be correlated with the electronegativities of the halide atom in methyl halides (28).

1.2.2 Local Anisotropic Effect

In an external magnetic field, H_0, electrons around an atom Y, circulate to produce a secondary or induced field. This induced field, if not isotropic, will change the screening constant of any neighbouring hydrogens. The change can be positive or negative depending on the direction of the H-Y bond with respect to the applied field, viz., if the H-Y bond is parallel to H_0, then the secondary field due to Y, felt at H will be such that it opposes H_0 and so provides a positive increment to the shielding. In contrast, if the H-Y bond is perpendicular to H_0, the hydrogen will get a negative increment to its shielding constant (29). There will, of course, be two possible perpendicular orientations.

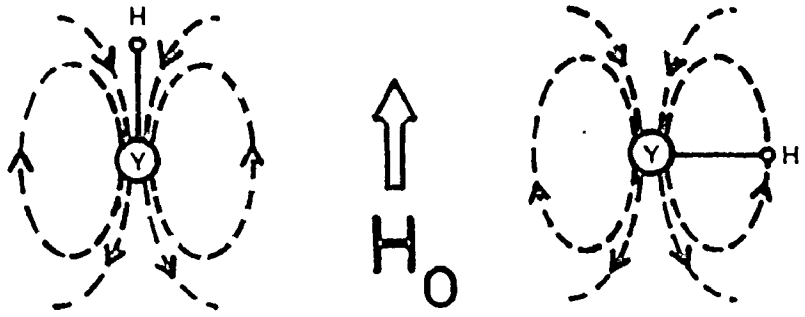

The change in shielding constant due to magnetic anisotropy of Y can be calculated if the susceptibilities are known. McConnell (25) derived an equation for calculating the change in σ for an axially symmetric system,

$$\Delta\sigma = \frac{\Delta\chi_Y}{3R^3}(1-3\cos^2\gamma)_{av} \qquad (1\text{-}6)$$

where R is the distance of the hydrogen from Y; γ is the angle between R and the symmetry axis; $\Delta\chi_Y$ is the anisotropy in the susceptibility of Y

$$\Delta\chi_Y = \chi_Y^{\parallel} - \chi_Y^{\perp} \qquad (1\text{-}7)$$

and $\chi_Y^{\parallel}$, $\chi_Y^{\perp}$ are susceptibilities parallel and perpendicular to the symmetry axis. The $(1-3\cos^2\gamma)$ in (1-6) is the average over time so as to account for possible intramolecular motions which may cause γ to change.

In effect, McConnell (25), replaced the atom Y by a point dipole and then calculated the resulting magnetic field. If the system is not axially symmetric, the change in shielding is given by (30)

$$\Delta\sigma = [(1-3\cos^2\gamma_x)\chi_Y^{\parallel} + (1-3\cos^2\gamma_y)\chi_Y^{\perp} + (1-3\cos^2\gamma_z)\chi_Y'^{\perp}]/3R^3 \qquad (1\text{-}8)$$

where x, y, z axes correspond to the directions of $\chi_Y^{\parallel}$, $\chi_Y^{\perp}$ and $\chi_Y'^{\perp}$, respectively and γ_x, γ_y and γ_z are the angles R makes with the respective axes.

This dipole approach is an approximation which does not take into account the size and shape of the electron charge distribution hence is totally inadequate for distances comparable to dimensions of electron distribution.

Experimental measurement of the magnetic susceptibility is very difficult and hence few are known. Narasimhan and Rogers (30) have used NMR shift results to predict the magnetic susceptibilities of proton neighbours.

A more accurate approximation is where the electron distribution is regarded as a loop carrying the induced current. The current is directly calculated from Larmor's theorem and its associated magnetic field is thus derived. This method has the advantage that it does not require a priori knowledge of diamagnetic anisotropies (18, p. 74). A more detailed analysis and use of this method will be discussed later for predicting proton chemical shifts.

Accurate quantum mechanical methods for calculating the diamagnetic anisotropy are only possible for the simplest molecules, such as the hydrogen molecule (31). Order of magnitude values of $\chi^{\parallel}$, $\chi^{\perp}$ and $\chi'^{\perp}$ can be obtained from approximate quantum mechanical methods for larger systems (32-35).

1.2.3 Ring Current Effect

The ring current effect arises due to the delocalized circulation of electrons around a ring of bonded atoms. Ehrenfest (12) was the first to recognize that such an interatomic circulation of electrons would cause large diamagnetic anisotropies. The effect of this delocalized circulation is well illustrated in aromatic molecules. In an external magnetic field H_0, the π electrons of aromatic compounds will circulate

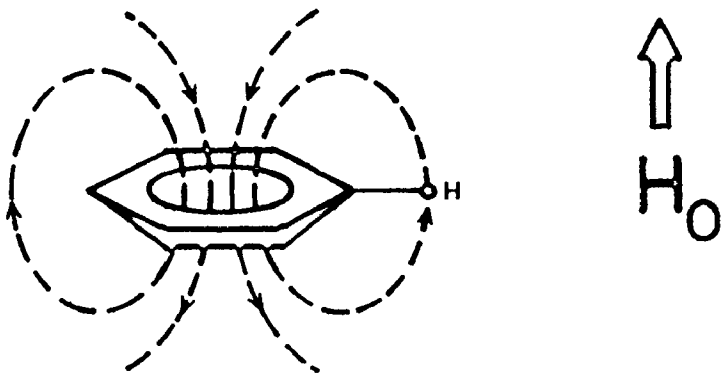

such that the induced magnetic field opposes the applied field. As can be seen from the figure above, the effect at the proton is to augment H_o and hence, during NMR experiments, cause the protons to appear at very low fields. This circulation would also account for the large diamagnetic anisotropies of aromatic compounds.

A number of workers have advanced theories accounting for the anomalous chemical shifts of aromatic compounds due only to ring currents, but with varying amounts of success.

Pople (24,36) on the basis of Pauling's (14) classical method, used the dipole approach, similar to the one used for local anisotropic contribution, to calculate the ring current contribution. There are several drawbacks to this approach; firstly, the distance of the proton from the dipole is comparable to the radius of circulation of electrons; secondly, and more serious, the dipole method does not predict upfield shifts for protons inside the ring as has been experimentally proven for [4n + 2]-annulenes (37), where n > 2 -- benzene being a [6]-annulene.

Waugh and Fessenden (38) used another classical approach to the same problem. They calculated the magnetic field components at a given point due to the current in a loop with radius equal to radius of the benzene ring. The induced magnetic field components in cylindrical coordinates can be calculated from magnetostatics (39,40). The induced magnetic field will have two components,

$$H'_\rho = \frac{2\mu I z}{\rho[(a+\rho)^2 + z^2]^{1/2}} \left[-K + \frac{a^2 + \rho^2 + z^2}{(a-\rho)^2 + z^2} E\right] \qquad (1\text{-}9)$$

$$H'_z = \frac{2\mu I}{[(a+\rho)^2 + z^2]^{1/2}} \left[K + \frac{a^2 - \rho^2 - z^2}{(a-\rho)^2 + z^2} E\right] \qquad (1\text{-}10)$$

where μ is the permeability of the medium; I is the current; a is the radius of circulation; ρ is the radial distance from the center of the ring to the proton, and z is the perpendicular distance from the center of the ring to the proton; K and E are complete elliptical integrals of the first and second kind, respectively, with the argument

$$k^2 = \frac{4a\rho}{(a+\rho)^2 + z^2} \tag{1-11}$$

K and E are easily evaluated because they can be expanded as infinite power series in k^2:

$$K = \frac{\pi}{2}\left[1 + \left(\frac{1}{2}\right)^2 k^2 + \left(\frac{1.3}{2.4}\right)^2 k^4 + \left(\frac{1.3.5}{2.4.6}\right)^2 k^6 + \ldots\right] \tag{1-12}$$

$$E = \frac{\pi}{2}\left[1 - \left(\frac{1}{2}\right)^2 k^2 - \left(\frac{1.3}{2.4}\right)^2 \frac{k^4}{3} - \left(\frac{1.3.5}{2.4.6}\right)^2 \frac{k^6}{5} - \ldots\right] \tag{1-13}$$

Waugh and Fessenden (38) used these formulae with a current appropriate for 6 electrons, in benzene, being given by (24)

$$I = -6\left(\frac{e^2 \vec{H}_o \cdot \vec{n}}{4\pi mc\mu}\right) \tag{1-14}$$

where $\vec{H}_o$ is the applied field and $\vec{n}$ is a unit vector perpendicular to the plane of the loop. Since, during NMR experiments, all orientations of the molecule are possible the expectation value of H'_{eff}, the effective field, in the direction of H_o is required

$$H'_{eff} = \frac{1}{H_o} \int \vec{H}_o \cdot \vec{H}' d\omega \tag{1-15}$$

Hence, because $\vec{H}_o \cdot \vec{H}'_\rho = H_o H'_\rho \cos(90°) = 0$, H'_ρ can be omitted from the calculations. Thus

$$H'_{eff} = \frac{6e^2H_o}{6\pi mc^2} \frac{I}{[(a+\rho)^2 + z^2]^{1/2}} \left[K + \frac{a^2 - \rho^2 - z^2}{[(a-\rho)^2 + z^2]} E\right] \qquad (1\text{-}16)$$

$$\Delta\sigma = \text{chemical shift change} = \frac{H'_{eff}}{H_o}$$

$$\therefore \quad \Delta\sigma = \frac{e^2}{\pi mc^2} G \qquad (1\text{-}17)$$

where G is simply a geometric factor dependent only on ρ and z for a given 'a'.

Evaluation for the aromatic protons in benzene predicted $\Delta\sigma \simeq 2.7$ ppm which was too large compared to the desired $\Delta\sigma = 1.5$ ppm. The choice of $\Delta\sigma = 1.5$ ppm as the required shift came from using vinylic protons of 1,3-cyclohexadiene as the reference protons; now, this rather arbitrary choice of standard deserves closer examination and it will be necessary to return to this problem later. To make their theory fit Waugh and Fessenden (38) separated the current into two loops, above and below the plane of the ring, 1.28 Å apart. There is no theoretical

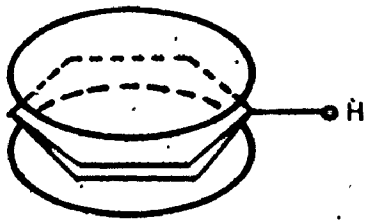

justification for the separation, it is totally empirical and may be unnecessary in the light of later data. This method did have success in the sense it predicted an upfield shift for protons inside or over the ring. To demonstrate this upfield shift prediction, Waugh and

Fessenden (38) compared their calculated shifts for the methylene protons in [10]-paracyclophane to experimental shifts. These latter shifts, obtained from a poorly resolved 40 MHz NMR spectrum, were later shown to have been incorrectly assigned (41). There is, however, poor correlation between the predicted shift based on ring currents only and the accurate experimental values for [10]-paracyclophane obtained at 220 MHz (41). This approach also fails to predict correctly chemical shifts in condensed polycyclic aromatic compounds.

Johnson and Bovey (42) tabulated the calculations of Waugh and Fessenden (38) and plotted a contour map of chemical shifts.

Hoarau (43) suggested that the sigma bond in benzene could also contribute to the total diamagnetic anisotropy. Dailey (44) used the sigma bond contribution to resolve the paradox that calculated diamagnetic anisotropies were too low while calculated chemical shifts too high though both were directly related.

Quantum mechanical approaches to predicting chemical shifts due to ring currents have had varying amounts of success. Pople (45) and McWeeny (46) extended London's (15,16) molecular orbital (MO) method for the ring current effect on diamagnetism to its effect on chemical shifts. Hall and Hardisson (47) improved on McWeeny's (46) method by using a self consistent field (SCF) MO method. The variable electronegativity SCFMO (VESCFMO) approach (48) has been used for heterocyclic aromatic compounds though estimates for the effect of the hetero atom are imprecise. All these methods gave estimates of about 2.5 ppm as the benzene shift as did the Waugh and Fessenden (38) approach before separating the circulations. Hence to fit the required

1.5 ppm, the values have had to be scaled by a factor of about 0.6, this factor being called an empirical scaling factor until a better calculation or explanation could be found.

More recently, Haigh and Mallion (49-51) and Roberts (52) have made further improvements which give reasonably good values when compared to experimental values.

Musher (53) challenged the whole concept of ring currents and instead claimed that the whole effect could be attributed to the symmetry of the system and there was no need for artificial separation into various effects. Gaidis and West (54) supported the need for ring current concept with some experimental evidence which Musher (55) countered by saying that his theory was an "anti-theory", which could not be related to experimental evidence. The situation with regards to Musher's opinion is best summarized by Haddon, Haddon and Jackman (56), viz., " ... there is little excuse for the substitution of dogmatic iconoclasm for reasoned criticism".

1.3 JUSTIFICATION FOR THIS WORK

Classical and quantum mechanical methods have been applied widely to calculate chemical shifts and diamagnetic anisotropies, e.g., for polycyclic aromatic hydrocarbons (36,44,45,47,49-52,57-62); for non-benzenoid aromatics (63,64); heterocyclic aromatic compounds (48,63,65,66); and even biological systems (67). The Johnson-Bovey (42) tables are the most routinely used, e.g., References (68-71); they are even used as corner-stones of conformational analysis, e.g., (72). The results of these calculations have been only moderately

successful when compared to experimental values.

However, using a combination of local anisotropic and ring current contributions to the chemical shift, it was found that the predicted and observed chemical shifts for [10]-paracyclophane -- the very model compound for which data were unjustifiably claimed to support the free electron ring current theory (38) -- are now in excellent agreement (41). In the light of this, it was deemed reasonable to present isoshielding contour maps depicting local anisotropic and ring current contributions to the shifts of protons in the neighbourhood of an aromatic ring.

It is our hope that these contour maps will replace the widely used but somewhat inadequate Johnson-Bovey (42) tables presently used somewhat indiscriminately by organic and physical organic chemists.

CHAPTER 2

ANISOTROPY CALCULATIONS

2.1 HISTORICAL

The importance of local anisotropic contributions, for aromatic hydrocarbons, was first pointed out by Berthier et al. (57); Pople (73) deduced that local anisotropic contributions for benzene protons could account for as much as 30% of the total shift. Dailey (44) noted that the inclusion of the local anisotropic effects could solve the paraxodical results obtained for the diamagnetic susceptibility of benzene and the chemical shift of protons in benzene. The estimation of local anisotropic contributions for aromatic compounds was difficult because there was no reasonable way to derive a value for the current flowing around each carbon. However, Pople (33) and Tillieu (35) used two methods to give estimates for the principal diamagnetic susceptibilities of a carbon-carbon double bond. Jackman and Sternhell (18, p. 85) used those methods to plot contour maps of chemical shifts due to a carbon-carbon double bond. Contour maps of chemical shifts due to carbonyl groups are also plotted (18, p. 89) based on Pople's (33) method of estimation of susceptibilities.

Finally, in 1972 Pines, Gibby and Waugh (74), by using Proton-Enhanced Nuclear Induction Spectroscopy, measured the ^{13}C shielding tensors for benzene in the solid state and hence obtained three values --

one for each of the principal axes of circulation of electrons. Since the ^{13}C shielding tensors are directly related to the current around each carbon, it became possible to get reliable estimates of the local anisotropic contributions to the proton NMR chemical shifts. The first measurement for benzene was done at -50°C and showed the two in-plane tensors to be equal. Subsequent experiments using durene (1,2,4,5-tetramethylbenzene) and pentamethylbenzene have shown all the three tensors to be different in value (75,76).

Barfield, Grant and Ikenberry (77) used these ^{13}C shielding tensors for benzene (74) to calculate the local anisotropic contribution in condensed polycyclic aromatic hydrocarbons using the free electron in a loop model similar to the Waugh and Fessenden (38) approach for ring currents. Since Barfield et al. (77) used outdated ^{13}C tensors (74) to estimate the local anisotropic contributions to the chemical shift, their results are now of qualitative interest only. Calculations done on [10]-paracyclophane, using the latest ^{13}C tensors available for estimating the local anisotropic contributions (75,76), gave good correlation between the calculated and experimental chemical shifts of the methylene protons (41).

We have now plotted contour maps for the local anisotropic contribution to chemical shifts of protons in the vicinity of a benzene ring, using the same formalism as Barfield et al. (77) used. The ring current contour map plot by Johnson and Bovey (42) is also recalculated with the assumption that there is no separation of the current loop.

2.2 DERIVATIONS

2.2.1 Field Due to a Circular Loop

The derivation of equation (1-10) can be done from basic electrostatics (39) as shown below.

Define a vector $\vec{B}$ as the magnetic field at a point. Since there are no sources or sinks of magnetic nature

$$\therefore \quad \vec{\nabla}\cdot\vec{B} = 0 \tag{2-1}$$

where

$$\vec{\nabla} = \frac{\partial}{\partial x}\hat{i} + \frac{\partial}{\partial y}\hat{j} + \frac{\partial}{\partial z}\hat{k}$$

$\hat{i}$, $\hat{j}$, $\hat{k}$ being unit vectors along the x, y, z axes respectively.

We know

$$\oint\vec{B}\cdot d\vec{s} = \mu I \tag{2-2}$$

where $d\vec{s}$ represents the line integral; μ is the permeability; and I is the total current.

But,

$$I = \int\vec{i}\cdot\vec{n}dS$$

($\therefore$ by definition

$$\vec{i} = \frac{d\vec{I}}{dS} \tag{2-3}$$

where $\vec{i}$ is the current density; $\vec{n}$ is the unit normal vector; dS is the surface integral. Hence substitute (2-3) into (2-2)

$$\therefore \quad \oint\vec{B}\cdot d\vec{s} = \mu\int\vec{i}\cdot\vec{n}dS \tag{2-4}$$

By Stokes' theorem

$$\oint\vec{B}\cdot d\vec{s} = \int_S \vec{\nabla}\times\vec{B}\cdot\vec{n}dS = \mu\int\vec{i}\cdot\vec{n}dS$$

$$\therefore \quad \vec{\nabla} \times \vec{B} = \mu \vec{i} \tag{2-5}$$

Define $\vec{A}$ as the magnetostatic vector potential such that

$$\vec{\nabla} \times \vec{A} = \vec{B} \quad \text{and} \quad \vec{\nabla} \cdot \vec{A} = 0$$

Now

$$\vec{\nabla} \times (\vec{\nabla} \times \vec{A}) = \vec{\nabla}(\vec{\nabla} \cdot \vec{B}) - (\vec{\nabla} \cdot \vec{\nabla})\vec{A}$$

$$= -\nabla^2 \vec{A} \qquad (\because \quad \vec{\nabla} \cdot \vec{A} = 0 \quad \text{given}) \tag{2-6}$$

But

$$\vec{\nabla} \times \vec{A} = B \quad \text{(given)}$$

$$\therefore \quad \vec{\nabla} \times (\vec{\nabla} \times \vec{A}) = \vec{\nabla} \times \vec{B} = \mu \vec{i} \tag{2-7}$$

$\therefore$ From (2-6) and (2-7)

$$\nabla^2 \vec{A} = -\mu \vec{i} \tag{2-8}$$

or

$$\hat{i}\nabla^2 A_x + \hat{j}\nabla^2 A_y + \hat{k}\nabla^2 A_z = -\mu(\hat{i} i_x + \hat{j} i_y + \hat{k} i_z)$$

$\therefore$ A_x, A_y and A_z all satisfy Poisson's equation

$$\nabla^2 V = -\rho/\epsilon \tag{2-9}$$

where V is potential; ρ is density; and ϵ is a constant.

But we know

$$V = \frac{1}{4\pi\epsilon} \int_v \rho \frac{dv}{r} \tag{2-10}$$

$\therefore$ (2-10) is a solution of (2-9). Hence applying (2-10) to A_x, A_y, A_z Get

$$A_x = \mu \int_v i_x \frac{dv}{r} \tag{2-11a}$$

$$A_y = \mu \int_v i_y \frac{dv}{r} \tag{2-11b}$$

$$A_z = \mu \int_v i_z \frac{dv}{r} \tag{2-11c}$$

where dv is volume integral; r is distance. Equations (2-11a,b,c) can be written vectorially as:

$$\vec{A} = \mu \int_v \vec{i} \frac{dv}{r} \tag{2-11}$$

Consider a thin wire. Outside the wire, $\vec{i} = 0$ and in a thin wire of cross-sectional area dS, we get

$$i_x dv = idSdx = Idx \tag{2-12a}$$

$$i_y dv = idSdy = Idy \tag{2-12b}$$

$$i_z dv = idSdz = Idz \tag{2-12c}$$

Putting equations (2-12a,b,c) into (2-11), we get

$$\vec{A} = \mu \oint \frac{I d\vec{s}}{r} \tag{2-12}$$

Now consider a loop carrying a uniform current I, from symmetry we know that the magnitude of $\vec{A}$ is independent of ϕ in spherical polar coordinates.

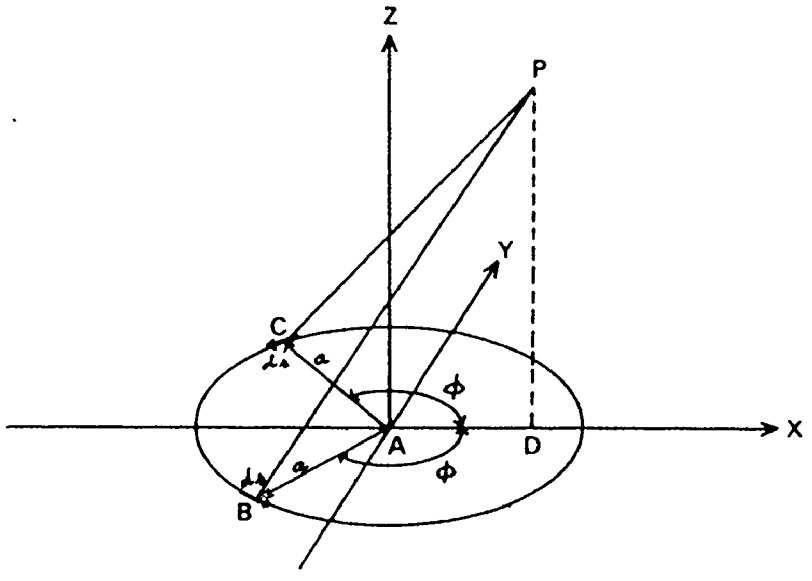

Therefore, choose P such that it lies in the xz plane where $\phi = 0$. Equidistant elements of length ds at $+\phi$ and $-\phi$ are paired, the resultant is normal to ρz, where ρ = AD and z = DP on the diagram above. Thus $\vec{A}$ has only one component A_ϕ. Hence in (2-12)

$$\vec{ds} = ds_\phi$$

and

$$ds_\phi = a\cos\phi d\phi \tag{2-13}$$

$$r = BP = CP = ((BD)^2 + (DP)^2)^{1/2}$$

But, $$DP = z$$

and $$BD^2 = AB^2 + AD^2 - 2AB \cdot AD \cdot \cos\phi$$

$$= a^2 + \rho^2 - 2a\rho\cos\phi$$

$$\therefore \quad r = (a^2 + \rho^2 + z^2 - 2a\rho\cos\phi)^{1/2} \tag{2-14}$$

Put (2-13) and (2-14) in (2-12) with I = constant

$$\therefore \quad A_\phi = \mu I \oint \frac{ds_\phi}{r} = 2\mu I \int_o^\pi \frac{a\cos\phi d\phi}{(a^2 + \rho^2 + z^2 - 2a\rho\cos\phi)} \tag{2-15}$$

Let $$\phi = 2\theta$$

$$\therefore \quad \cos\phi = 2\sin^2\theta - 1 \tag{2-16}$$

Substitute (2-16) in (2-15)

$$\therefore \quad A_\phi = 2\mu I \int_o^{\pi/2} \frac{a(2\sin^2\theta - 1)d\theta}{[(a + \rho)^2 + z^2 - 4a\rho\sin^2\theta]^{1/2}}$$

$$= 2\mu I \int_0^{\pi/2} \frac{a(2\sin^2\theta - 1)d\theta}{2a^{1/2}\rho^{1/2}[\frac{(a+\rho)^2 + z^2}{4a\rho} - \sin^2\theta]^{1/2}} \qquad (2\text{-}17)$$

Define

$$k^2 = \frac{4a\rho}{(a+\rho)^2 + z^2} \qquad (2\text{-}18)$$

Substitute (2-18) in (2-17)

$$A_\phi = \mu I \int_0^{\pi/2} \frac{a^{1/2}(2\sin^2\theta - 1)d\theta}{\rho^{1/2}(1/k^2 - \sin^2\theta)^{1/2}}$$

$$= \mu I(\frac{a}{\rho})^{1/2} \int_0^{\pi/2} \frac{k(2\sin^2\theta - 1)d\theta}{(1 - k^2\sin^2\theta)^{1/2}}$$

$$= \mu I(\frac{a}{\rho})^{1/2}[\int_0^{\pi/2} \frac{k2\sin^2\theta d\theta}{(1 - k^2\sin^2\theta)^{1/2}} - \int_0^{\pi/2} \frac{kd\theta}{(1 - k^2\sin^2\theta)^{1/2}}] \qquad (2\text{-}19)$$

From standard integrals (80) we know

$$\int_0^{\pi/2} \frac{1d\theta}{(1 - k^2\sin^2\theta)^{1/2}} = \frac{\pi}{2}(1 + (\frac{1}{2})^2k^2 + (\frac{1.3}{2.4})^2k^4 + (\frac{1.3.5}{2.4.6})^2k^6 + \ldots) = K \qquad (2\text{-}20)$$

Thus (2-19) becomes

$$A_\phi = \mu I(\frac{a}{\rho})^{1/2}[\int_0^{\pi/2} \frac{2k\sin^2\theta d\theta}{(1 - k^2\sin^2\theta)^{1/2}} - kK]$$

Rearranging the integral gives

$$A_\phi = \mu I(\frac{a}{\rho})^{1/2}[\int_0^{\pi/2} \frac{2}{k}\frac{(1 - (1 - k^2\sin^2\theta))d\theta}{(1 - k^2\sin^2\theta)^{1/2}} - kK]$$

$$= \mu I\left(\frac{a}{\rho}\right)^{1/2}\left[\int_0^{\pi/2} \frac{2}{k} \frac{1d\theta}{(1 - k^2\sin^2\theta)^{1/2}} - \int_0^{\pi/2} \frac{2}{k}(1 - k^2\sin^2\theta)^{1/2}d\theta - kK\right] \quad (2\text{-}21)$$

We know from standard integrals (80)

$$\int_0^{\pi/2} (1 - k^2\sin^2\theta)^{1/2}d\theta = \frac{\pi}{2}\left(1 - \left(\frac{1}{2}\right)^2 k^2 - \left(\frac{1.3}{2.4}\right)^2\frac{k^4}{3} - \left(\frac{1.3.5}{2.4.6}\right)^2\frac{k^6}{5} - \ldots\right)$$

$$= E \quad (2\text{-}22)$$

Substitute (2-22) and (2-20) in (2-21)

$$A_\phi = I\left(\frac{a}{\rho}\right)^{1/2}\left[\frac{2}{k}K - \frac{2}{k}E - kK\right]$$

$$= \frac{2\mu I}{k}\left(\frac{a}{\rho}\right)^{1/2}\left[\left(1 - \frac{k^2}{2}K\right) - E\right] \quad (2\text{-}23)$$

To get the field, by definition

$$\vec{B} = \vec{\nabla} \times \vec{A}$$

In spherical coordinates we know

$$B_\rho = -\frac{1}{\rho}\frac{\partial}{\partial z}(\rho A_\phi) + \frac{1}{\rho}\frac{\partial}{\partial \phi}(A_z) \quad (2\text{-}24a)$$

$$B_\phi = \frac{\partial}{\partial z}(A\rho) - \frac{\partial}{\partial \rho}(A_z) \quad (2\text{-}24b)$$

$$B_z = -\frac{1}{\rho}\frac{\partial}{\partial \phi}(A\rho) + \frac{1}{\rho}\frac{\partial}{\partial \rho}(\rho A_\phi) \quad (2\text{-}24c)$$

But

$$A_\rho = A_z = 0$$

$\therefore$

$$B_\rho = -\frac{\partial}{\partial z}A_\phi \quad \text{and} \quad B_z = \frac{1}{\rho}\frac{\partial}{\partial \rho}(\rho A_\phi)$$

Substituting for A_ϕ from (2-23) gives

$$B_\rho = \frac{2\mu I z}{\rho[(a+\rho)^2 + z^2]^{1/2}} \left[-K + \frac{a^2 + \rho^2 + z^2}{(a-\rho)^2 + z^2} E\right] \qquad (2\text{-}25a)$$

$$B_z = \frac{2\mu I}{[(a+\rho)^2 + z^2]^{1/2}} \left[K + \frac{a^2 - \rho^2 - z^2}{(a-\rho)^2 + z^2} E\right] \qquad (2\text{-}25b)$$

Since, in an applied field perpendicular to B_ρ (along B_z), the interaction will be of the form

$$H_{eff} = \vec{H}_o \cdot \vec{B} = H_o B_z \cos 0° + H_o B \cos 90°$$

$$= H_o B_z$$

Hence, only B_z need be calculated. Thus (2-25b) is identical to equation (1-10) with $B_z = H'_z$

In general,

$$B_z = C \times G \qquad (2\text{-}26)$$

where C is a constant denoting the current and G is the geometric factor dependent on ρ and z for a given 'a'.

2.2.2 Local Anisotropic Contributions

The three ^{13}C shielding tensors, measured by Waugh's group (74-76), can be visualized as arising due to three mutually perpendicular circulations of electrons around each carbon. Since the measured tensors are known to be along the three principal molecular axes (74-76), the circulations of electrons will be in the three principal molecular planes. Figure 2.1 shows the circulations and the corresponding tensors; circula-

Figure 2.1 The three circulation loops around each carbon with the respective tensors

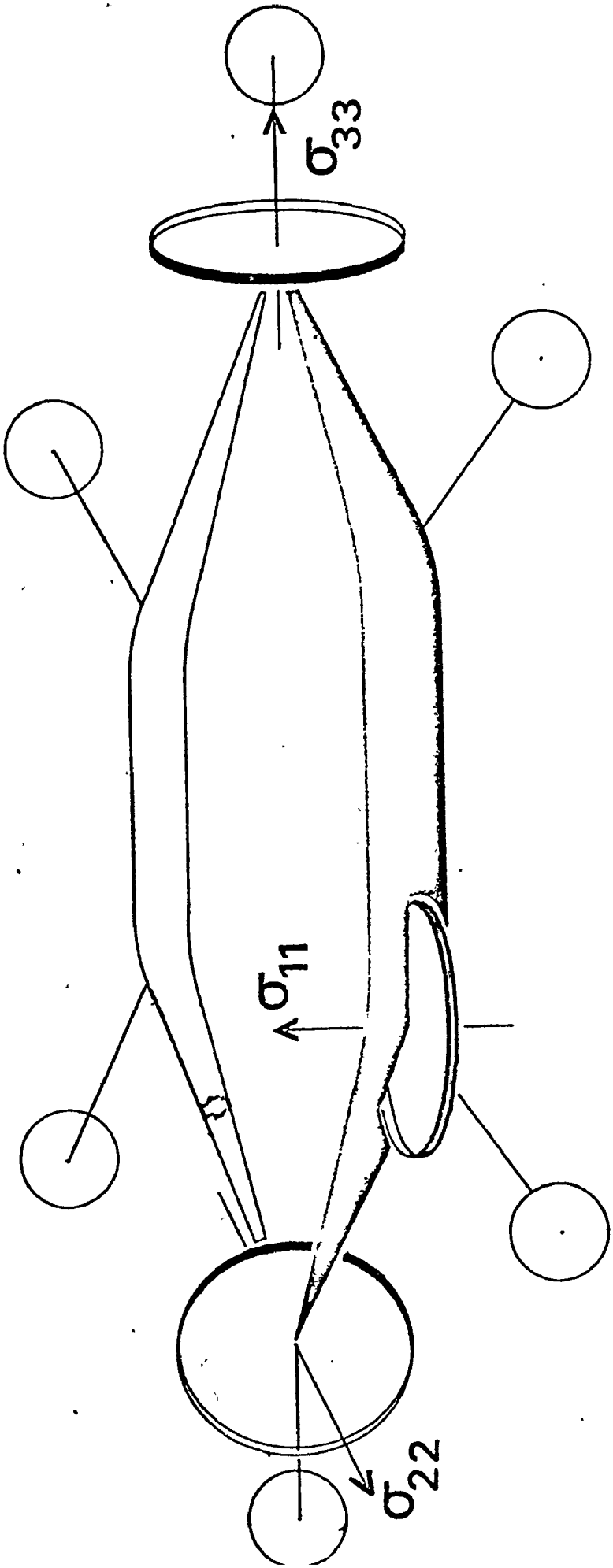
σ_{33}
σ_{11}
σ_{22}

tion in the plane of the ring gives rise to tensor σ^{C}_{11}; circulation in the plane perpendicular to ring which contains the C-H bond gives rise to tensor σ^{C}_{22}; and, circulation in the plane perpendicular to the ring and the C-H bond gives rise to tensor σ^{C}_{33}.

The chemical shift of the protons due to each circulation is given by the following relationship:

$$\sigma^{H}_{i} = \sigma^{C}_{ii} \frac{a}{\pi} G_i \qquad i = 1\text{-}3 \tag{2-27}$$

where G_i is the geometric factor from equation (2-26). This time a, the radius of circulation around the carbon, is taken as the expectation value of the distance of the electrons from the nucleus using Slater's 2p orbitals:

$$a = [\langle \phi_{2p} | r^{-3} | \phi_{2p} \rangle] \tag{2-28}$$

The radial function of the Slater orbital for 2p is as follows (78):

$$\phi_{2p} = re^{-3.25r/2a_0} \tag{2-29}$$

where r is the distance from the nucleus and a_0 is the first Bohr radius (= 0.529 Å) for hydrogen. Substituting (2-29) in (2-28):

$$a = \left[\frac{\int_0^\infty re^{-3.25r/2a_0} \times \frac{1}{r^3} \times re^{-3.25r/2a_0} r^2 dr}{\int_0^\infty (re^{-3.25r/a_0})^2 r^2 dr} \right]^{-\frac{1}{3}}$$

$$= \left[\frac{\int_0^\infty re^{-3.25r/a_0} dr}{\int_0^\infty r^4 e^{-3.25r/a_0} dr} \right]^{-\frac{1}{3}} \neq \left[\frac{(a_0/3.25)^2}{24(a_0/3.25)^5} \right]^{-\frac{1}{3}}$$

$$= \frac{a_0}{3.25}(24)^{1/3} \approx 0.4695 \approx 0.47 \text{ Å}$$

At this level of sophistication, it is assumed that the radius of circulation is the same ($a = 0.47$ Å) in all the three directions.

The radial distance ρ and the perpendicular distance z will differ for each circulation. The ρ and z can be calculated as follows:

For σ_{11}: $\rho_1 = ((\Delta x)^2 + (\Delta z)^2)^{1/2}$ and $z_1 = \Delta y$ (2-30a)

For σ_{22}: $\rho_2 = ((\Delta x)^2 + (\Delta y)^2)^{1/2}$ and $z_2 = \Delta z$ (2-30b)

For σ_{33}: $\rho_3 = ((\Delta y)^2 + (\Delta z)^2)^{1/2}$ and $z_3 = \Delta x$ (2-30c)

where Δx, Δy and Δz are the relative distances between the carbon and hydrogen along the x, y, z axes oriented as shown in the diagram below.

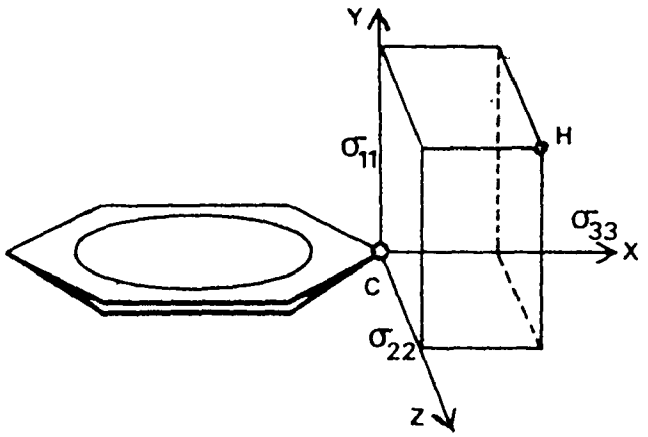

The average local anisotropic contribution, to the proton chemical shift, due to each carbon in the ring will be given by:

$$\sigma^H = \frac{1}{3}(\sigma_1^H + \sigma_2^H + \sigma_3^H) \qquad (2\text{-}31)$$

The total local anisotropic contribution to the chemical shift by the whole benzene ring will be the sum of all the six σ^H's for each carbon. Thus, there are three components for each σ^H and six σ^H's for each ring;

hence, a total of eighteen calculations are required for each proton position.

2.2.3 Ring Current Contribution

The ring current contribution to the chemical shift is given by equation (1-17) where a is the radius of the benzene ring, which is generally taken as 1.39 Å. The ρ and z are calculated with respect to the center of the ring; the evaluation of the physical constants in equation (1-17) gives:

$$\sigma = 8.970 \text{ G} \qquad (2\text{-}32)$$

2.3 COMPUTATION

The actual computation of the values for the local anisotropic shielding and ring current shielding was done on a H.P. 3000 computer by means of a Fortran programme, LARC, written for the purpose.

The programme evaluates K and E, the elliptical integrals, as a sum of the first 29 terms of the infinite series. The number of terms was limited to 29 by machine capabilities and not as a mathematical approximation. The expansion for K and E can be written using a general coefficient as follows (79):

$$K = \frac{\pi}{2}\left[1 + \sum_{N=0}^{\infty}\left(\frac{(2N+1)!}{(N!)^2(4^N)(2N+2)}\right)^2 k^{(2N+2)}\right], \qquad (2\text{-}33a)$$

$$E = \frac{\pi}{2}\left[1 - \sum_{N=0}^{\infty}\left(\frac{(2N+1)!}{(N!)^2(4^N)(2N+2)}\right)^2 \frac{k^{(2N+2)}}{(2N+2)}\right] \qquad (2\text{-}33b)$$

Since the coefficients of $k^{(2N+2)}$ involve factorials, to save computer

time, they are evaluated at the beginning and stored as arrays of 29 terms each, one for K and one for E.

The ^{13}C tensors for local anisotropic contributions, are dependent on the group directly attached to the carbon in the ring; at present, tensors for H, CH_2 and CH_3 as attached groups are the only ones accurately determined (74-76). These tensors are stored as an array which can be expanded when more tensors, for other attached groups, are published. The tensor values are given in Table 2-1. It is necessary to add 71 ppm to the values reported by Waugh (74-76) since they were experimentally measured relative to benzene, but absolute chemical shifts are required. The absolute ^{13}C chemical shift of methane has been calculated to be 205 ppm by Ditchfield (81) who used an ab initio coupled Hartree-Fock scheme with gauge-invariant atomic orbitals. Methane is 134 ppm upfield of benzene and this difference [205-134] is the source of the 71 ppm correction factor.

The programme takes into account the fact that for local anisotropy the axes have to be rotated by 60°, in the plane of the ring, to bring the circulations about each carbon into proper perspective, as seen from the hydrogen.

Initially, the number of hydrogens for which calculations are to be done and the substituent pattern of the ring have to be input. Thence forward, only the coordinates of the hydrogens, with respect to the center of ring, are the inputs. The programme compensates for the fact that for local anisotropic contribution, the circulations are centered on the carbons themselves where as for the ring current contribution, the circulation is about the center of the ring.

Group Attached to C	σ_{11} ppm	σ_{22} ppm	σ_{33} ppm
*H	153	73	-19
**CH	177	32	-20
*CH_2	178	36	-20
*CH_3	179	40	-20

TABLE 2-1. ^{13}C Shielding Tensors for the Various Substituents on the Ring Carbon.

* From References 75, 76.

** Estimated from values for CH_2 and CH_3 groups.

The output gives each σ_i^H, σ^H, the total local anisotropy and the ring current.

Various modifications of the programme LARC were used to generate the tables, of local anisotropic contributions and ring current contributions, for plotting the contour maps. The maps were plotted on a Benson-Lehner plotter using a multi-point plotting subroutine.

The listings of LARC, its various modifications and the plotting routines are given in Appendix A.

Validity of LARC was tested by assuming current loop separation of 1.28 Å and getting 1.5 ppm as the current contribution -- same as obtained by Waugh and Fessenden (38).

CHAPTER 3

RESULTS AND DISCUSSION

3.1 GENERAL

Prior to launching out on a discussion of results, it is necessary to define our system of axes. The benzene ring is oriented such that the y-axis is perpendicular to the plane of the carbon ring; the x-axis passes through carbons 1 and 4; and the z-axis bisects the bonds between the carbons 2 and 3, and the carbons 5 and 6 as shown below:

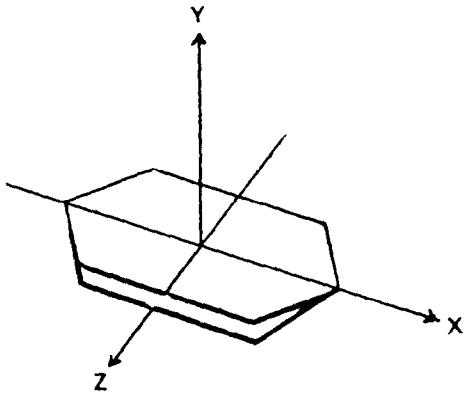

As would be expected for benzene the contour maps for both, local anisotropy and ring current, are symmetric -- the degree of symmetry being dependent on the actual plane being observed. All plots in the xz plane display six-fold symmetry while the plots in the xy and yz planes show symmetry about both the axes which define the plane. Due to the presence of this symmetry, all data were generated for only one quadrant; the other three quadrants being plotted by reflection. There are two plots for each contour map; the first is a single quadrant plot showing all the plotted lines each with its numerical value for the chemical shift, the second is

a plot in all four quadrants which is presented just to show the symmetry and for visual impact.

Detailed discussion of the characteristics of individual plots and their significance is presented in the following sections.

3.2 LOCAL ANISOTROPY

The gross features of the contour maps in the xy plane with z = 0 (Figures 3.1a and 3.1b) and the yz plane with x = 0 (Figures 3.2a and 3.2b) are very similar. Both look like extremely symmetrical butterflies with the shielding (positive chemical shift contribution) zone forming the wings and the deshielding (negative chemical shift contribution) zone the body. A comparison of the deshielding zones for the two maps shows that the xy plane (through the carbons) has a larger area of deshielding. Individual iso-shielding lines are pushed outwards and upwards, e.g., the -1.0 ppm line, in the xy plane extends to 3.16 Å as compared to 2.63 Å for the yz plane along the x and z axes respectively. The maximum height of the -1.0 ppm line, in the xy plane, is about 1.5 Å while for the yz plane it is about 1.3 Å. Hence, in three dimensions, the deshielding zone is not a uniform, level, cylindrically symmetric surface and instead has an undulating surface much like a circular roller-coaster with the dips between the bonds and the peaks at the carbons. The point group of the deshielding zone still remains D_{6h} in spite of its undulatory surface.

There are two consequences of the increased deshielding area over the carbon -- the first and most obvious is that the shielding zone, over the carbons, is reduced both in area and in the maximum value of shielding. The occurrence of greater shielding above and below the

carbon-carbon internuclear axis, i.e., above and below the ring plane, is entirely consistent with the conventional view of the sp^2 hybridized carbon in benzene with a delocalized π system formed by the overlap of the 2p atomic orbitals. The presence of a π system is further supported by the fact that, between the bonds, the maximum shielding value occurs at a height of about 0.5 Å above the ring plane and at a distance of about 1.2 Å (Figure 3.2a) -- which is the distance from the ring center to one of the hexagonal sides. The greater shielding between the carbons also lends support to the concept of bond anisotropy which has been discussed for many years (17, p. 86).

The second consequence is seen in the contour maps for the xz plane, at y = 0.5 Å (Figures 3.4a and 3.4b), y = 1.0 Å (Figures 3.5a and 3.5b) and y = 1.5 Å (Figures 3.6a and 3.6b), in which the maximum shielding or deshielding areas appear as islands. These islands give the contour maps, in all four quadrants, a distinct pizza-like appearance. The islands of maximum shielding lie between neighbouring carbons and the islands of maximum deshielding lie on an axis along the C-H bond direction outside the ring of carbons.

A distinctly different feature of the xy plane with z = 0.0 Å and the xz plane with y = 0.0 Å (Figure 3.3a and 3.3b), is the presence of ∞ chemical shift contribution lines which arise due to the breakdown of the expression for G_i in equation (2-27). The expression for G_i is:

$$G_i = \frac{1}{[(a+\rho_i)^2 + z_i^2]^{1/2}} \left[K + \frac{a^2 - \rho_i^2 - z_i^2}{(a-\rho_i)^2 + z_i^2} E\right]$$

and, when $\rho = a$ and $z = 0$, then we have the division of zero by zero which

is not defined. It is easily demonstrated that there will be three circles around each carbon at which the expression breaks down. These occur in the xy plane with z = 0.0 Å, xz plane with y = 0.0 Å and the yz plane with x = 1.39 Å. The three circles mentioned above will be the only lines of ∞ around any carbon; for all other points, not lying in any of the above mentioned planes, the expression is valid everywhere and at a distance slightly greater than 0.47 Å forms a surface of zero chemical shift around each carbon. This is not to be confused with the zero chemical shift surface between the shielding and deshielding zones.

Since the contour map for the xz plane with y = 0.5 Å (Figure 3.4a and 3.4b) is so close to these points of discontinuity, some of the features seen in that map may be artifacts of the calculation, but these regions are of no chemical consequence and have been included only for the sake of completeness.

At large distances from the ring center, the contours in the xz plane tend to become circular, thereby showing that the dipolar formula is becoming more and more valid as an approximation. The contour map of the xz plane with y = 2.0 Å (Figures 3.7a and 3.7b) shows no islands or other unusual features -- the contours are all tending to be circles. The higher xz planes, with y = 3.0 Å (Figures 3.8a and 3.8b), with y = 4.0 Å (Figures 3.9a and 3.9b) and with y = 5.0 Å (Figures 3.10a and 3.10b), show even closer approximations to circular contours. The G factor in equation (2-27) can easily be shown to reduce to a form for which the dipole formula is a good approximation at very large distances where $\rho >> a$:

$$G = \frac{1}{[(a+\rho)^2 + z^2]^{1/2}} \left[K + \frac{a^2 - \rho^2 - z^2}{(a-\rho)^2 + z^2} E\right]$$

If $\rho \gg a$

$$G = \frac{1}{(\rho^2+z^2)^{1/2}} \left[K - \frac{(\rho^2+z^2)}{(\rho^2+z^2)} E\right] \tag{3-1}$$

But

$$\rho^2 + z^2 = R^2 \tag{3-2}$$

where R is the direct distance of the hydrogen from the center of the ring. Also

$$k^2 = \frac{4a\rho}{(a+\rho)^2 + z^2} = \frac{4a\rho}{R^2} \tag{2-3}$$

when $\rho \gg a$.

Substituting (3-2) in (3-1)

$$G = \frac{1}{R}(K-E) \tag{3-4}$$

But

$$K = \frac{\pi}{2}\left[1 + \frac{1}{4}k^2 + \frac{9}{64}k^4 + \frac{225}{2304}k^6 + \ldots\right] \tag{3-5a}$$

and

$$E = \frac{\pi}{2}\left[1 - \frac{1}{4}k^2 - \frac{3}{64}k^4 - \frac{45}{2304}k^6 - \ldots\right]. \tag{3-5b}$$

Substituting (3-3) in (3-5a) and (3-5b)

$$K \simeq \frac{\pi}{2}\left[1 + \frac{a\rho}{R^2} + \frac{9a^2\rho^2}{4R^4} + \frac{225a^3\rho^3}{36R^6}\right] \tag{3-6a}$$

$$E \simeq \frac{\pi}{2}\left[1 - \frac{a\rho}{R^2} - \frac{3a^2\rho^2}{4R^4} - \frac{45a^3\rho^3}{36R^6}\right] \tag{3-6b}$$

Substituting (3-6a) and (3-6b) in (3-4)

$$G = \frac{\pi}{2}\frac{1}{R}\left[\frac{2a\rho}{R^2} + \frac{3a^2\rho^2}{R^4} + \frac{15a^3\rho^3}{2R^6}\right]$$

$\therefore$ From (2-27)

$$\sigma^H = \frac{a}{\pi}\frac{\pi}{2}\left[\frac{2a\rho}{R^3} + \frac{3a^2\rho^2}{R^5} + \frac{15a^3\rho^3}{2R^7}\right]\sigma^C \qquad (3\text{-}7)$$

Thus, when $\rho \gg a$, the equation (2-27) reduces to a multipolar expansion. If R is large, then the quadrupole and hexapole corrections will be very small and hence can be neglected, leaving only the dipole approximation

$$\sigma^H = \frac{a^2\rho}{R^3}\sigma^C \qquad (3\text{-}8)$$

A previously derived dipolar formula contains an algebraic error due to mis-evaluation of the elliptical integral power series (77). However, this does not materially effect the conclusions drawn previously, i.e., it is unsafe to calculate chemical shifts for proximate protons using only a dipolar formula (77).

Tables of local anisotropic contributions, corresponding to Figures 3.1 to 3.10, are given in Appendix B (Tables B-1 to B-10). The tables are much abbreviated and are given just as samples. The actual plotting was done from tables generated in increments of 0.1 Å along both the axes defining the plane.

3.3 RING CURRENT

Waugh and Fessenden (38) attributed the entire 1.5 ppm difference

between the vinylic protons of 1,3-cyclohexadiene and benzene to the ring current effect. To make their theory fit, they artificially separated the circulation into two loops above and below the plane of the ring. This separation has now been found to be unnecessary once the local anisotropic contribution is included and a proper standard chosen (41).

Calculations for the [10]-paracyclophane system have shown that the correlation between the experimental ring current, which is defined as:

$$-RC_{Expt.} = \text{Expt. Shift} - \text{Standard Shift} + \text{Local Anisotropic Shift}$$

and the calculated ring current (RC_{Calc}) is the best when the calculations are based on no separation of the current loop. A plot of $RC_{Expt.}$ vs. RC_{Calc} gives a straight line of high correlation coefficient for the methylene protons of [10]-paracyclophane. Ideally, the plot should be a straight line, passing through the origin with a slope giving the effective number of electrons circulating in the loop. Experimentally, however, the line does not pass through the origin -- the intercept corrects for the choice of the standard.

The contour map for the ring current has been replotted (Figures 3.11a and 3.11b) assuming no loop separation. The map is very similar to the Johnson-Bovey (42) plot except that all the lines are moved down by 0.64 Å. A representative set of values are given in Appendix B, Table B-11.

Since the ring current has a cylindrical symmetry in the xy plane, only one plane, viz., the xy plane need be plotted and the distance along the x-axis is really ρ, where ρ is:

$$\rho = (x^2 + z^2)^{1/2}$$

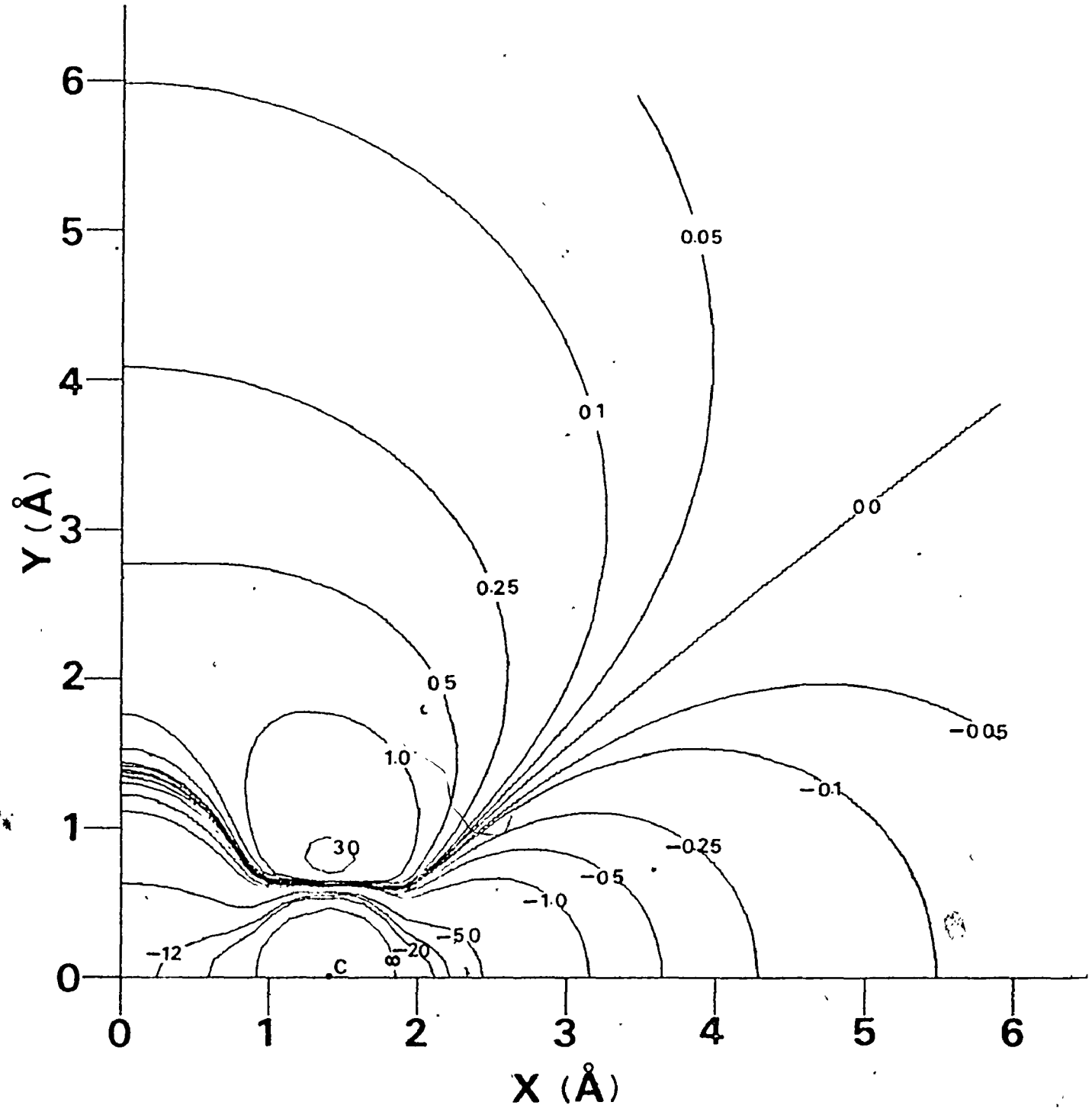

Figure 3.1a Single quadrant of the contour map for the local anisotropic contributions to the chemical shift of protons near benzene in the xy plane with z = 0.0 Å.

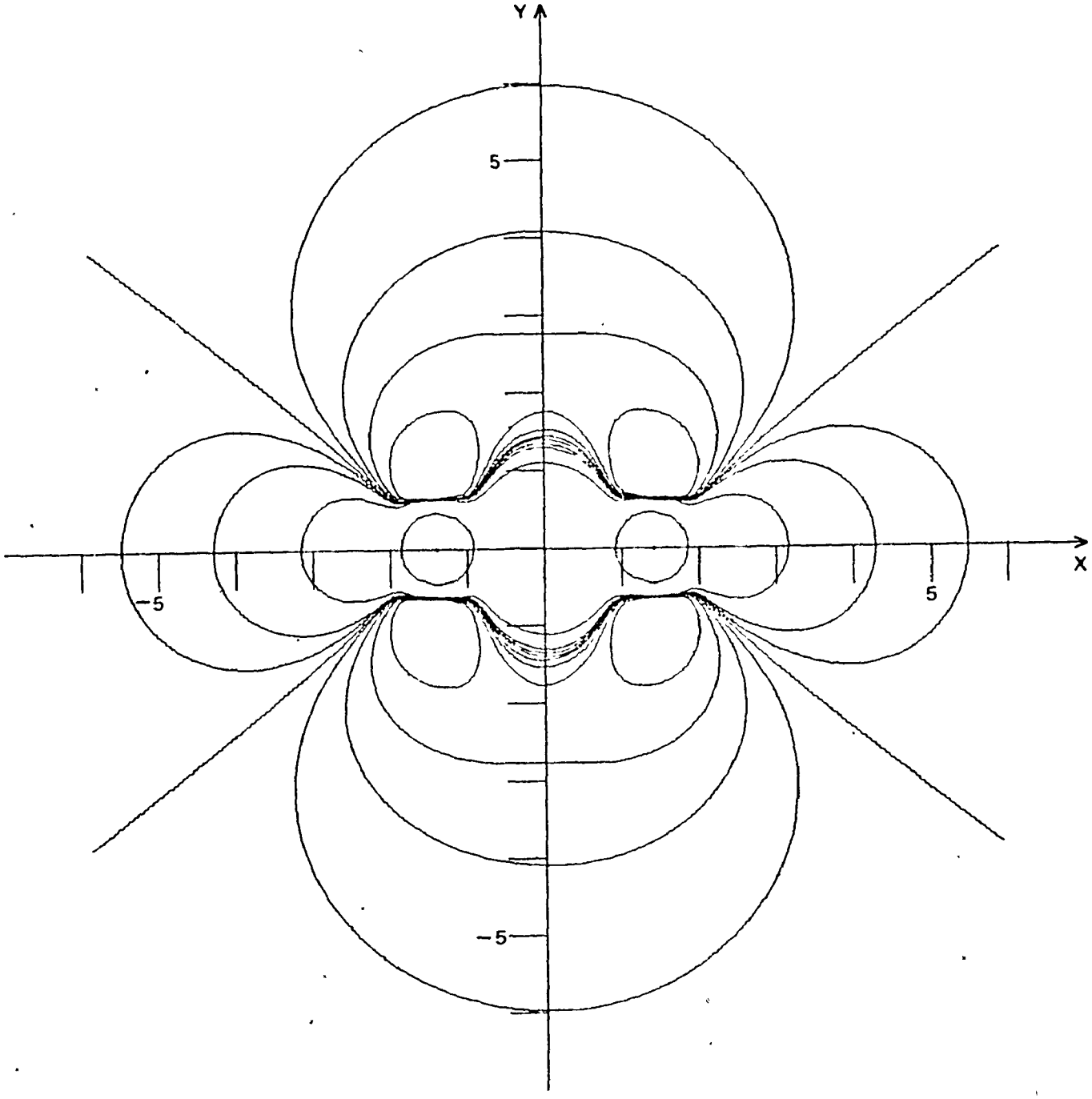

Figure 3.1b Contour map for the local anisotropic contributions to the chemical shift of protons near benzene in the xy plane with z = 0.0 Å.

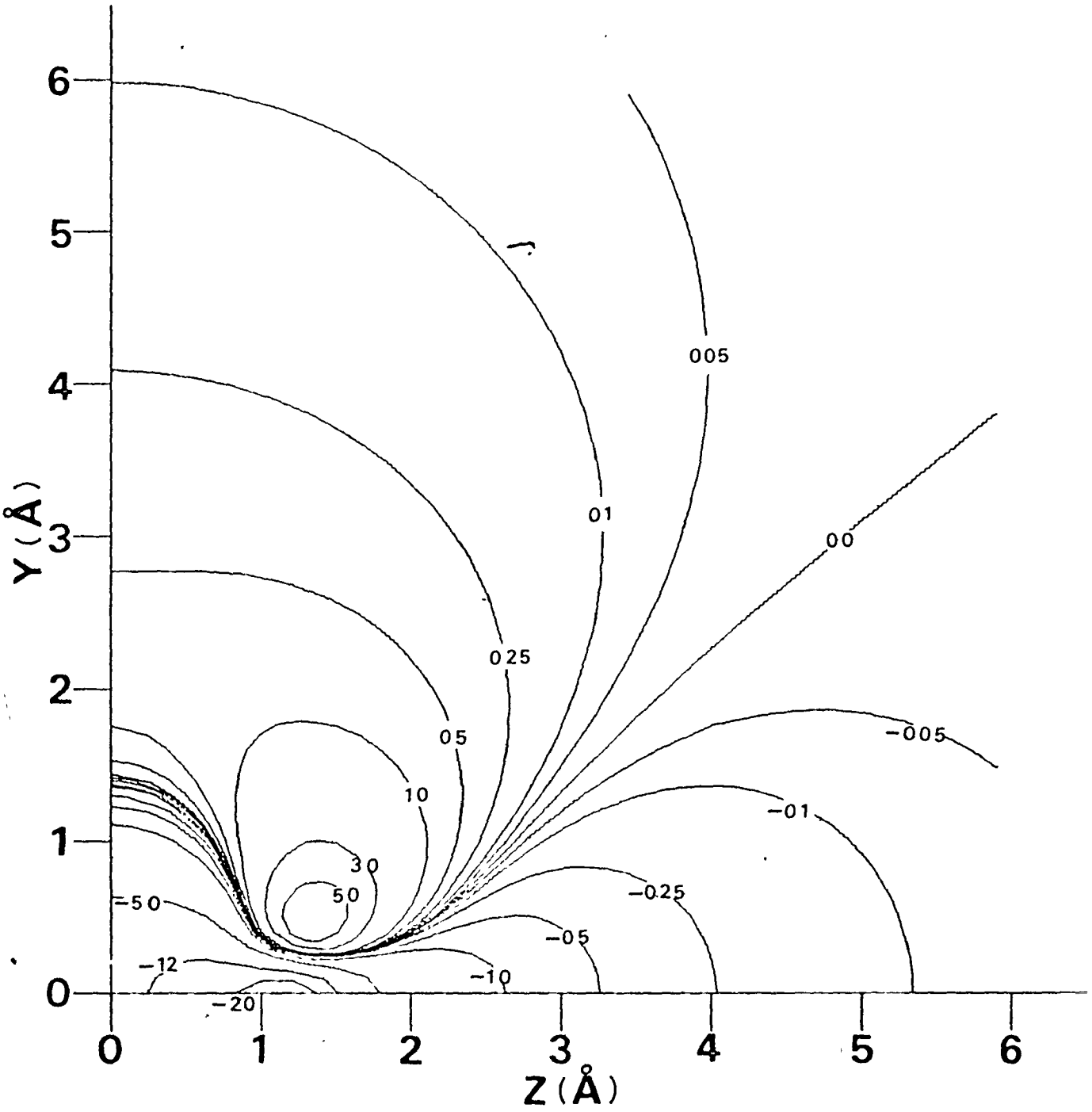

Figure 3.2a Single quadrant of the contour map for the local anisotropic contributions to the chemical shift of protons near benzene in the yz plane with x = 0.0 Å.

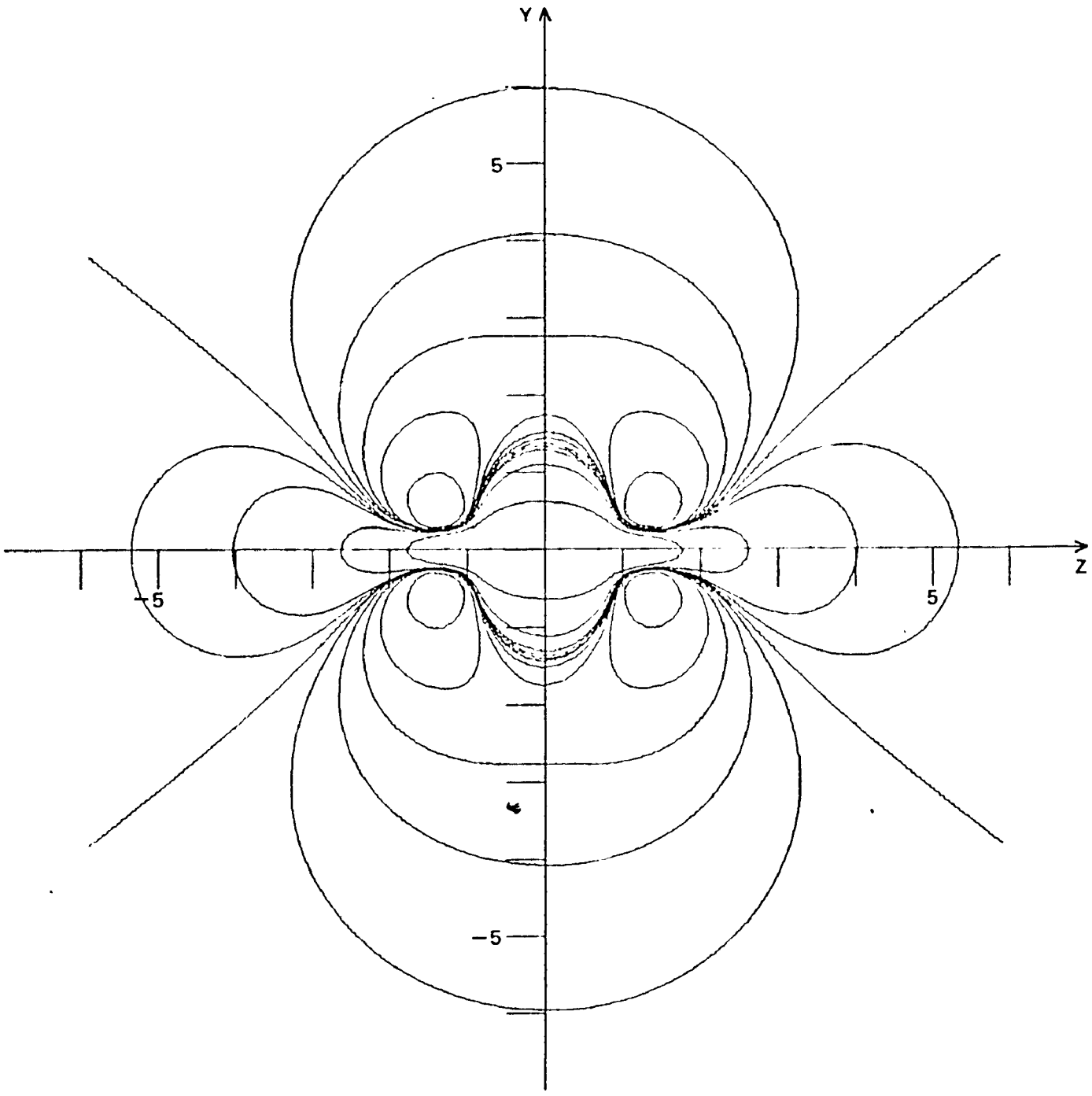

Figure 3.2b Contour map for the local anisotropic contributions to the chemical shift of protons near benzene in the yz plane with x = 0.0 Å.

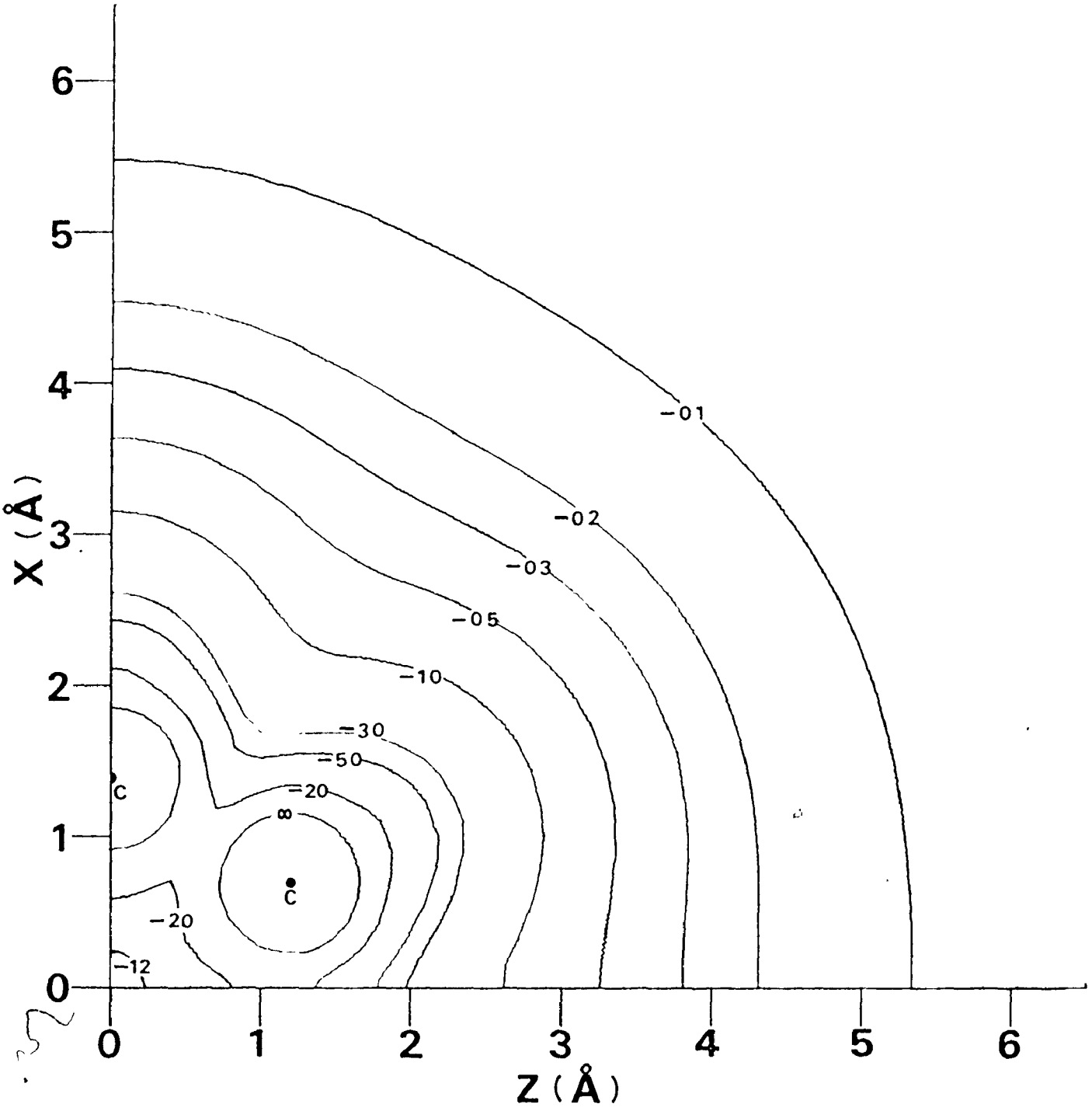

Figure 3.3a Single quadrant of the contour map for the local anisotropic contributions to the chemical shift of protons near benzene in the xz plane with y = 0.0 Å.

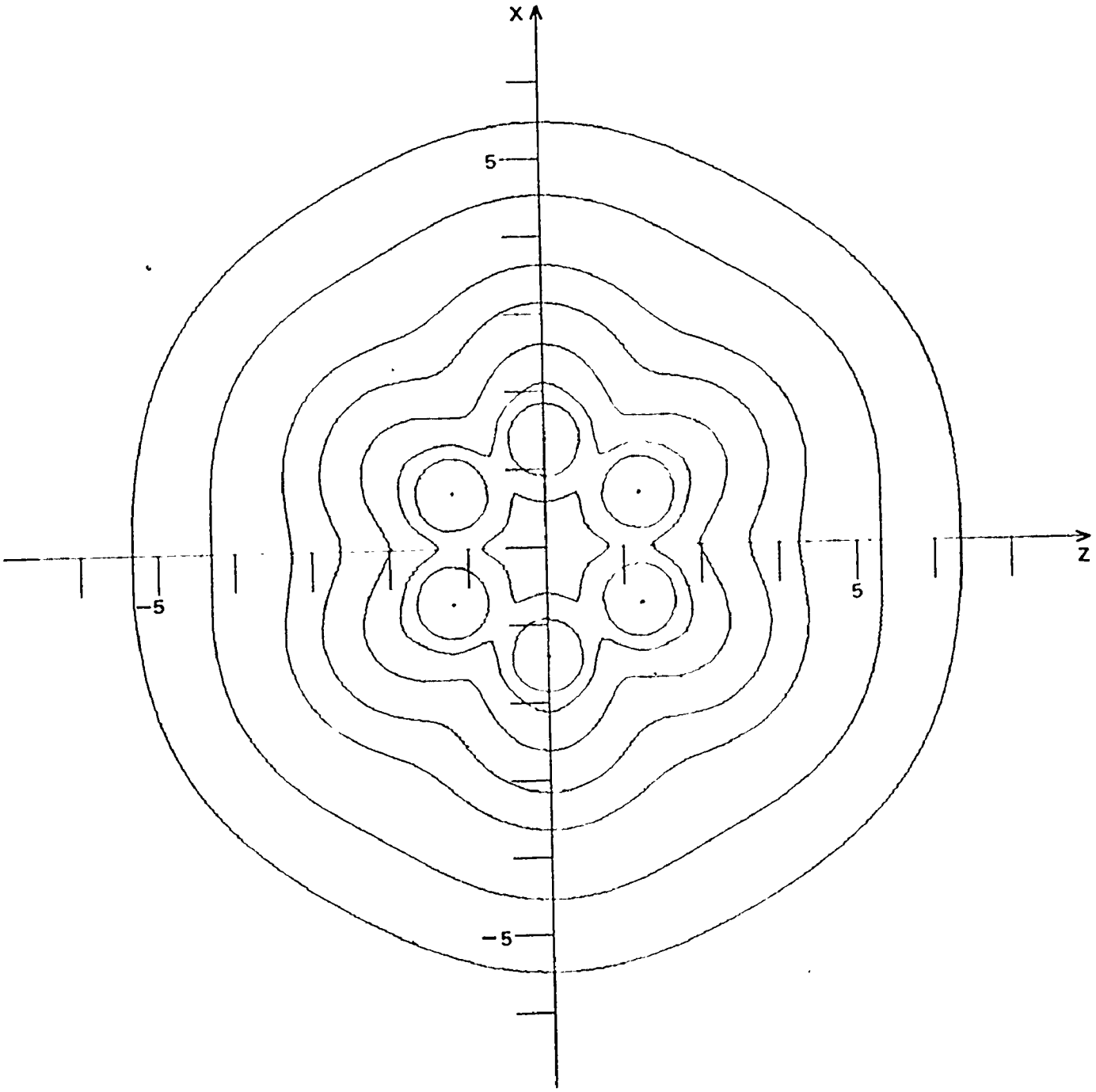

Figure 3.3b Contour map for the local anisotropic contributions to the chemical shift of protons near benzene in the xz plane with y = 0.0 Å.

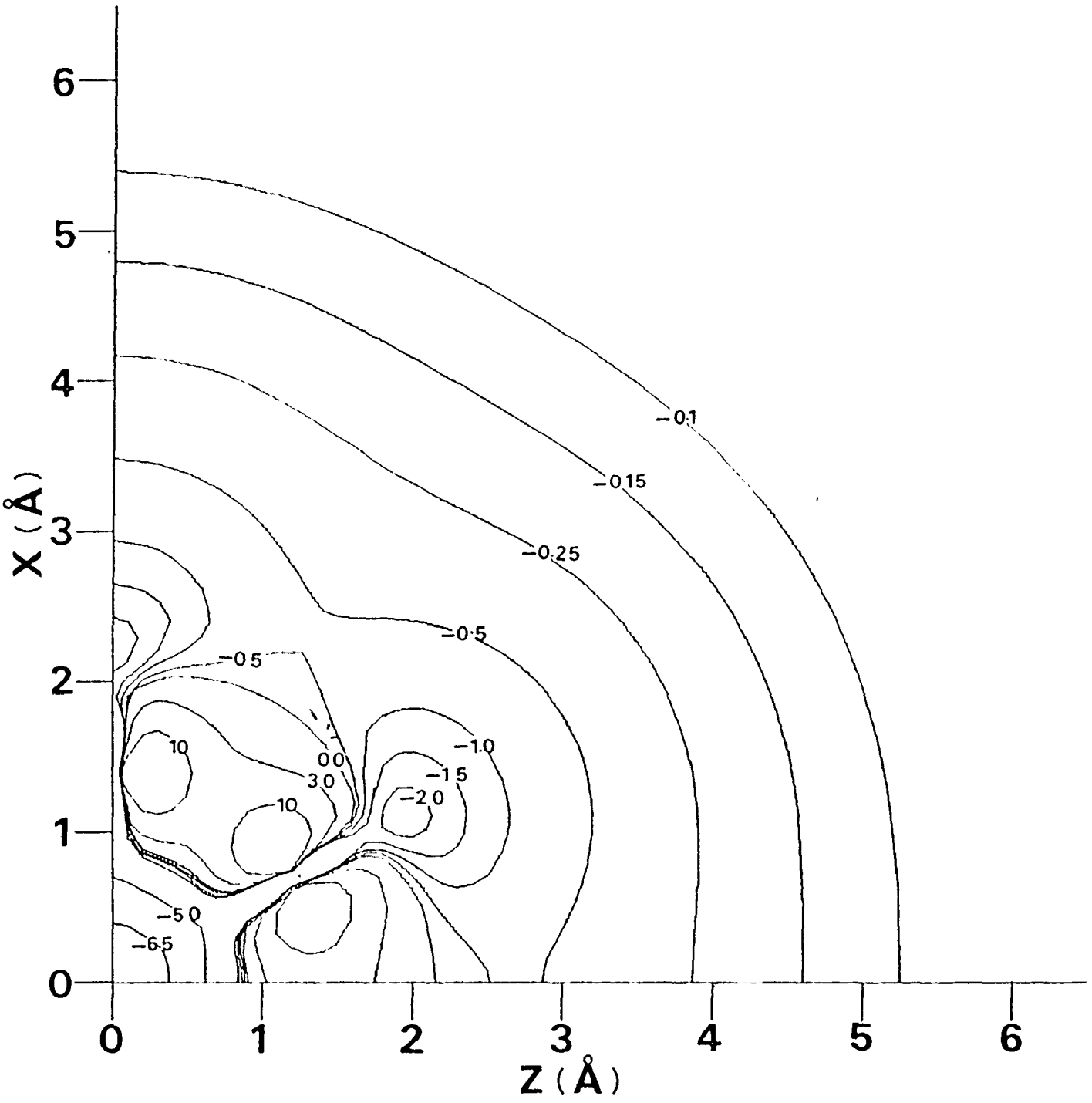

Figure 3.4a Single quadrant of the contour map for the local anisotropic contributions to the chemical shift of protons near benzene in the xz plane with $y = 0.5$ Å.

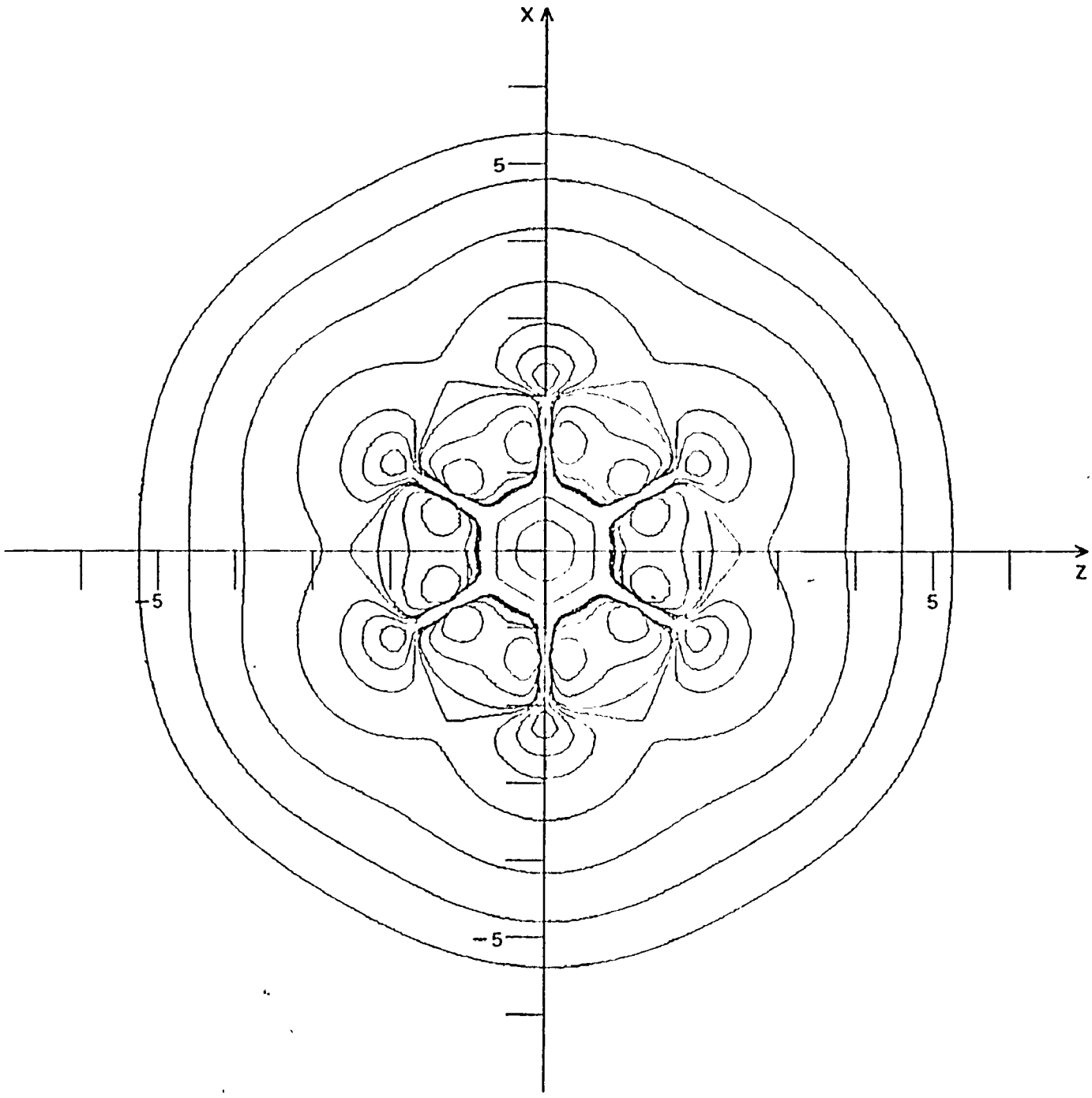

Figure 3.4b Contour map for the local anisotropic contributions to the chemical shift of protons near benzene in the xz plane with y = 0.5 Å.

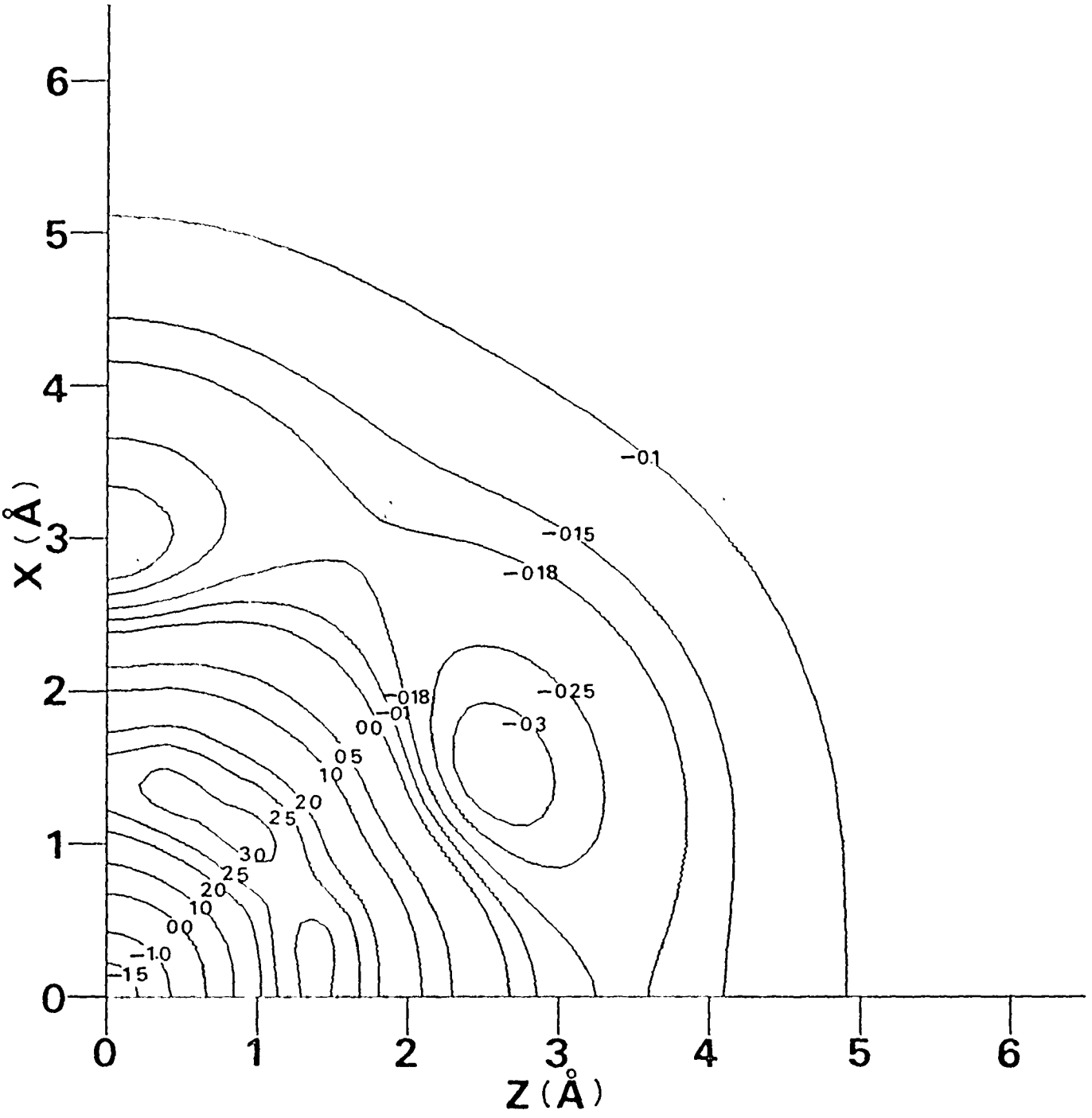

Figure 3.5a Single quadrant of the contour map for the local anisotropic contributions to the chemical shift of protons near benzene in the xz plane with y = 1.0 Å.

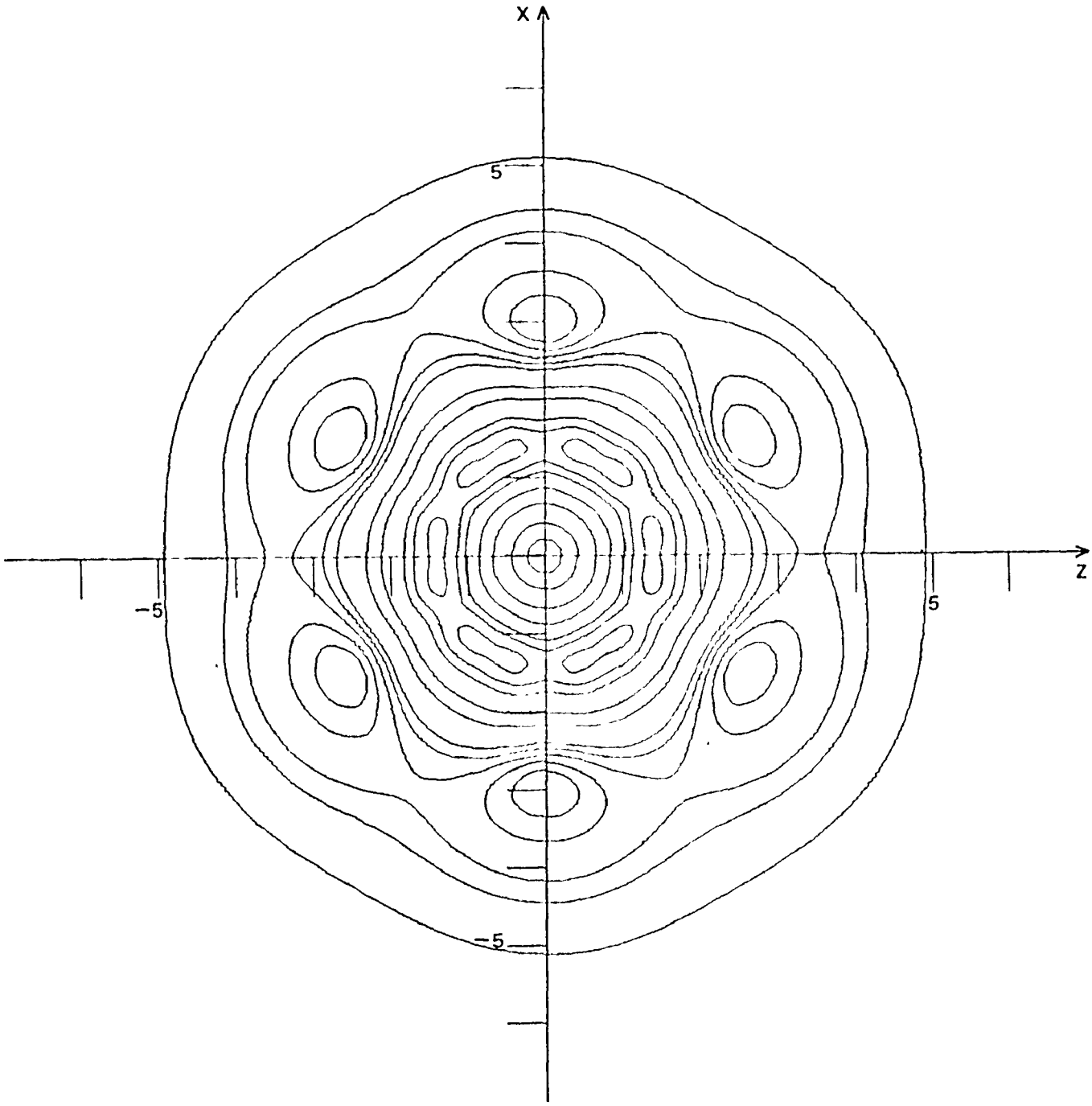

Figure 3.5b Contour map for the local anisotropic contributions to the chemical shift of protons near benzene in the xz plane with y = 1.0 Å.

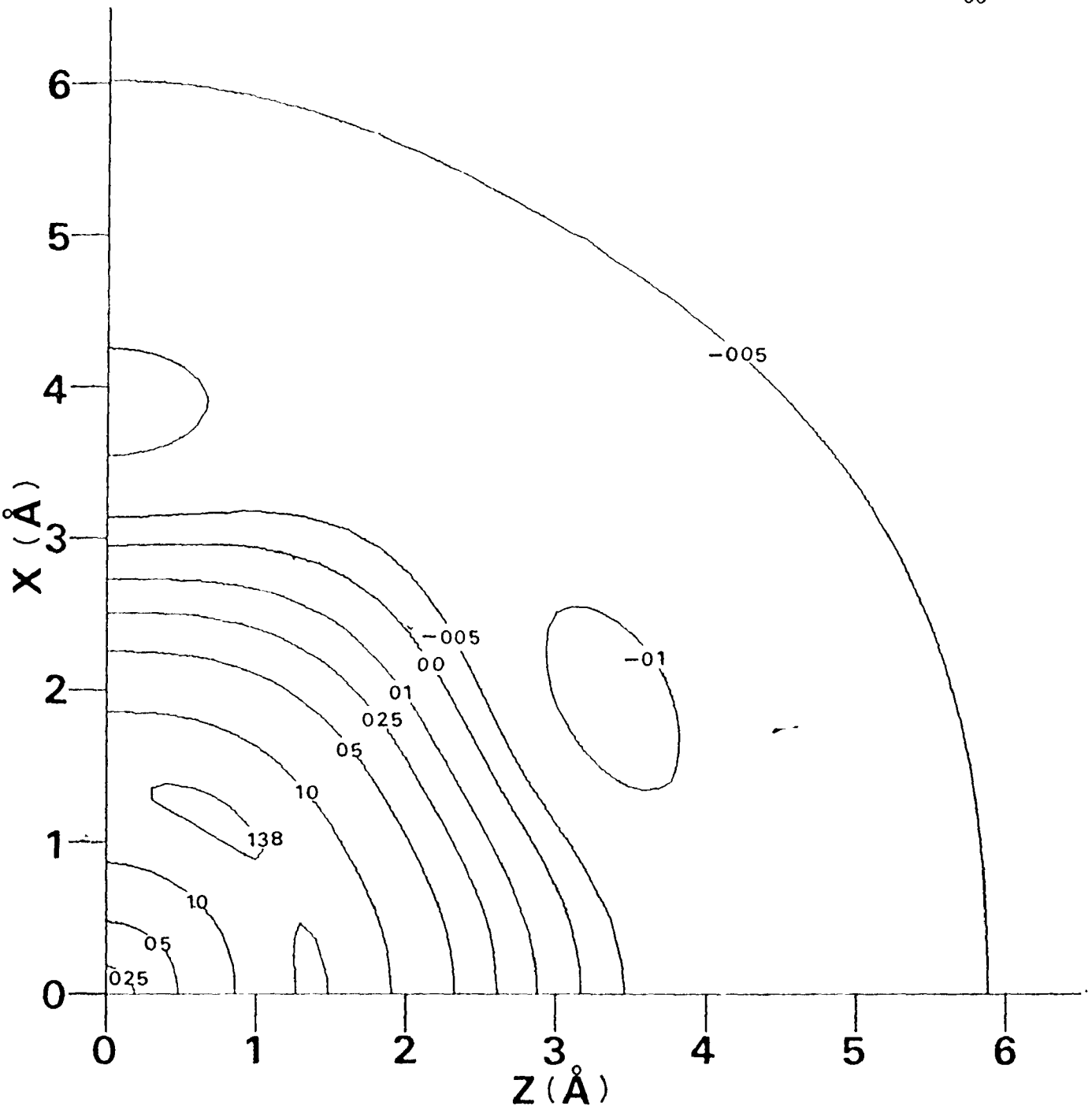

Figure 3.6a Single quadrant of the contour map for the local anisotropic contributions to the chemical shift of protons near benzene in the xz plane with $y = 1.5$ Å.

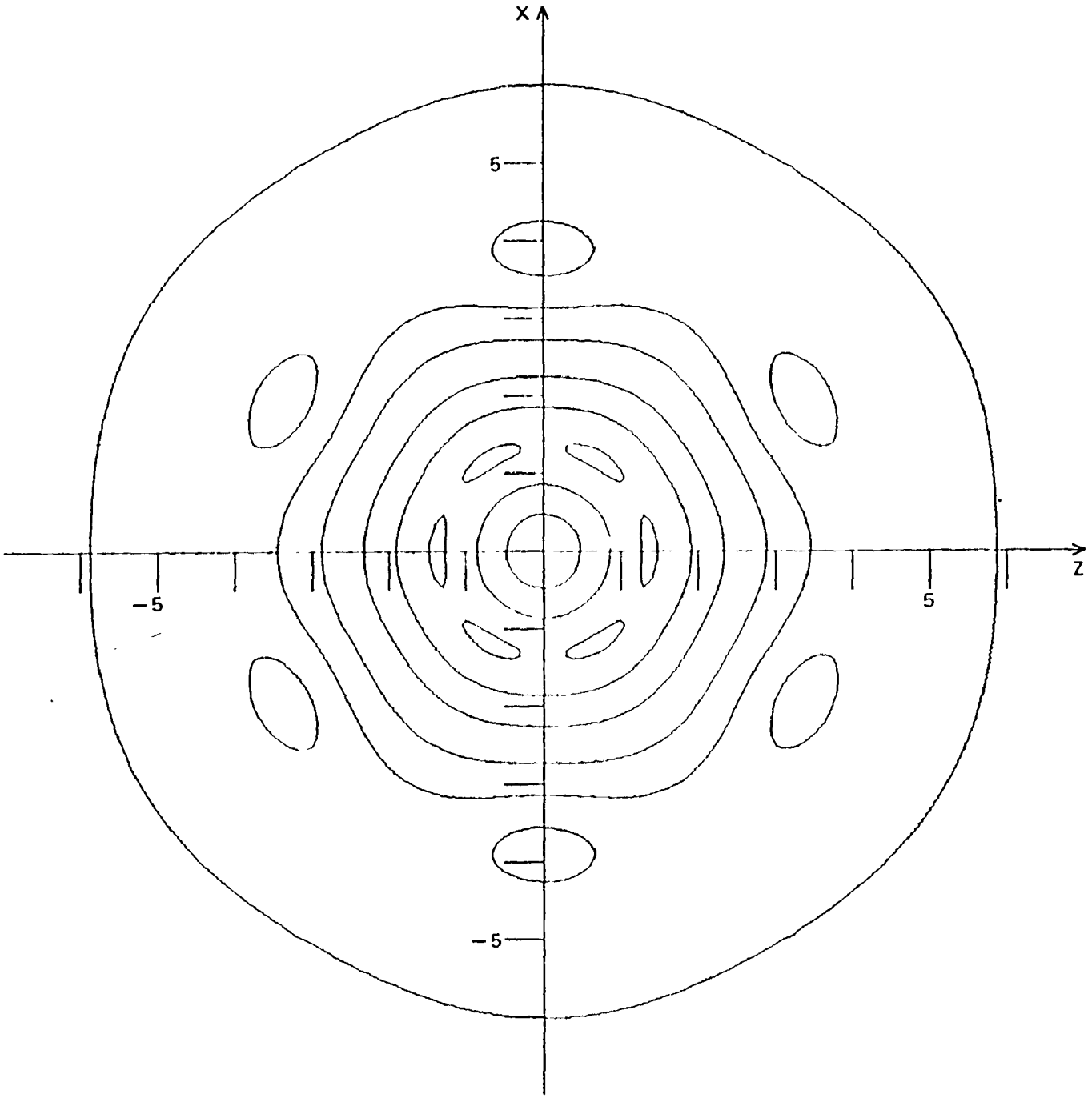

Figure 3.6b Contour map for the local anisotropic contributions to the chemical shift of protons near benzene in the xz plane with y = 1.5 Å.

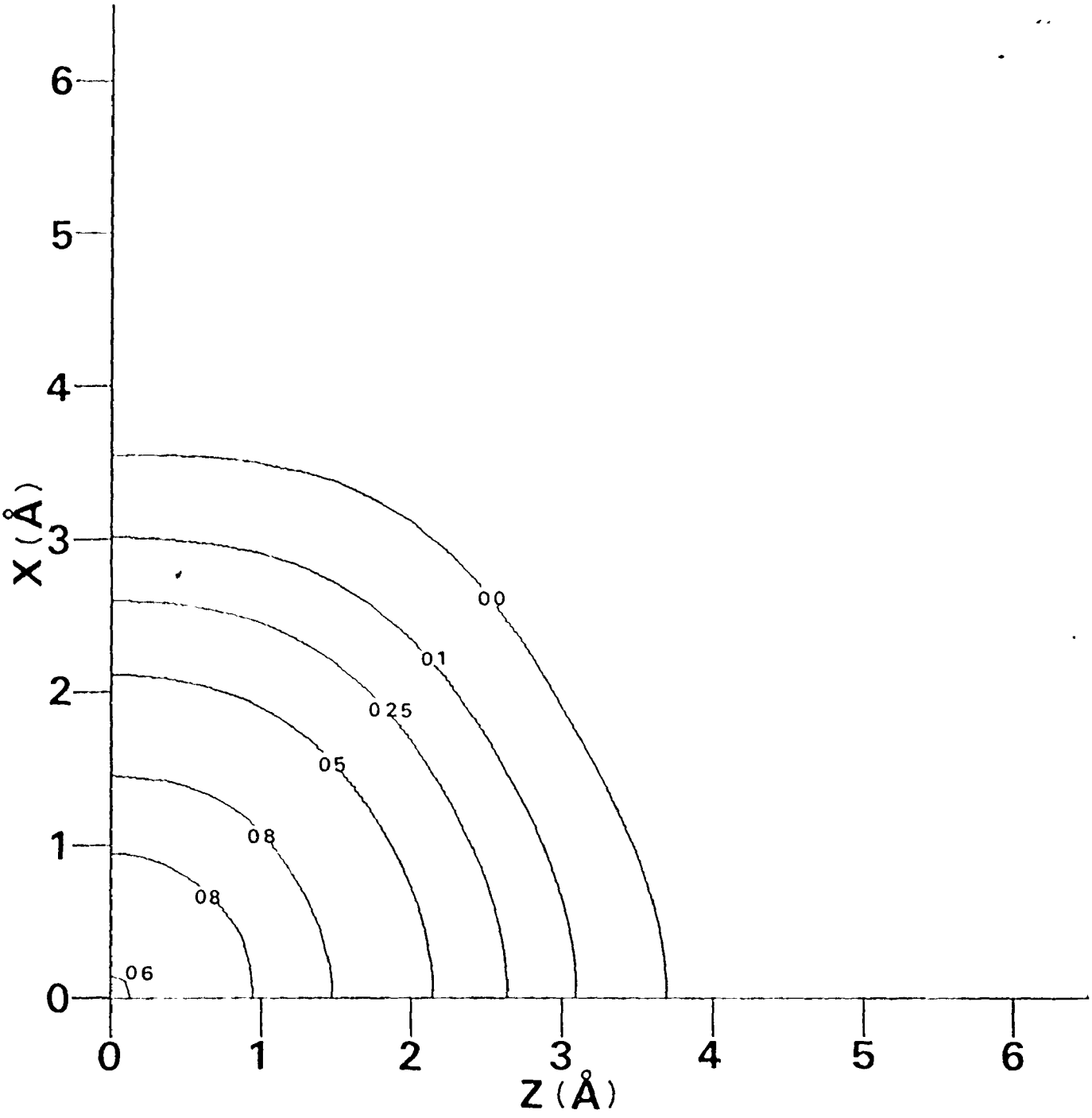

Figure 3.7a Single quadrant of the contour map for the local anisotropic contributions to the chemical shift of protons near benzene in the xz plane with y = 2.0 Å.

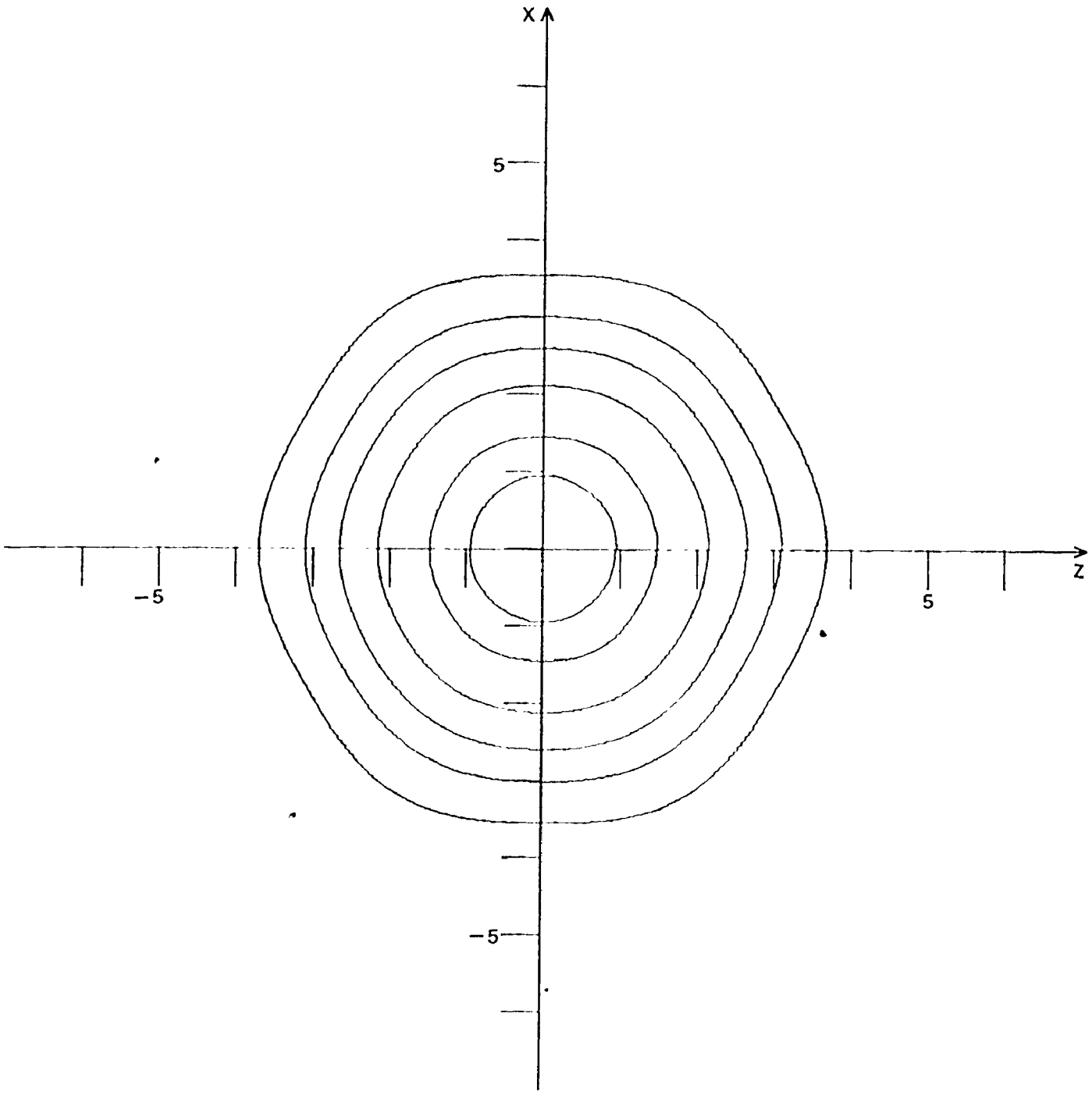

Figure 3.7b Contour map for the local anisotropic contributions to the chemical shift of protons near benzene in the xz plane with y = 2.0 Å.

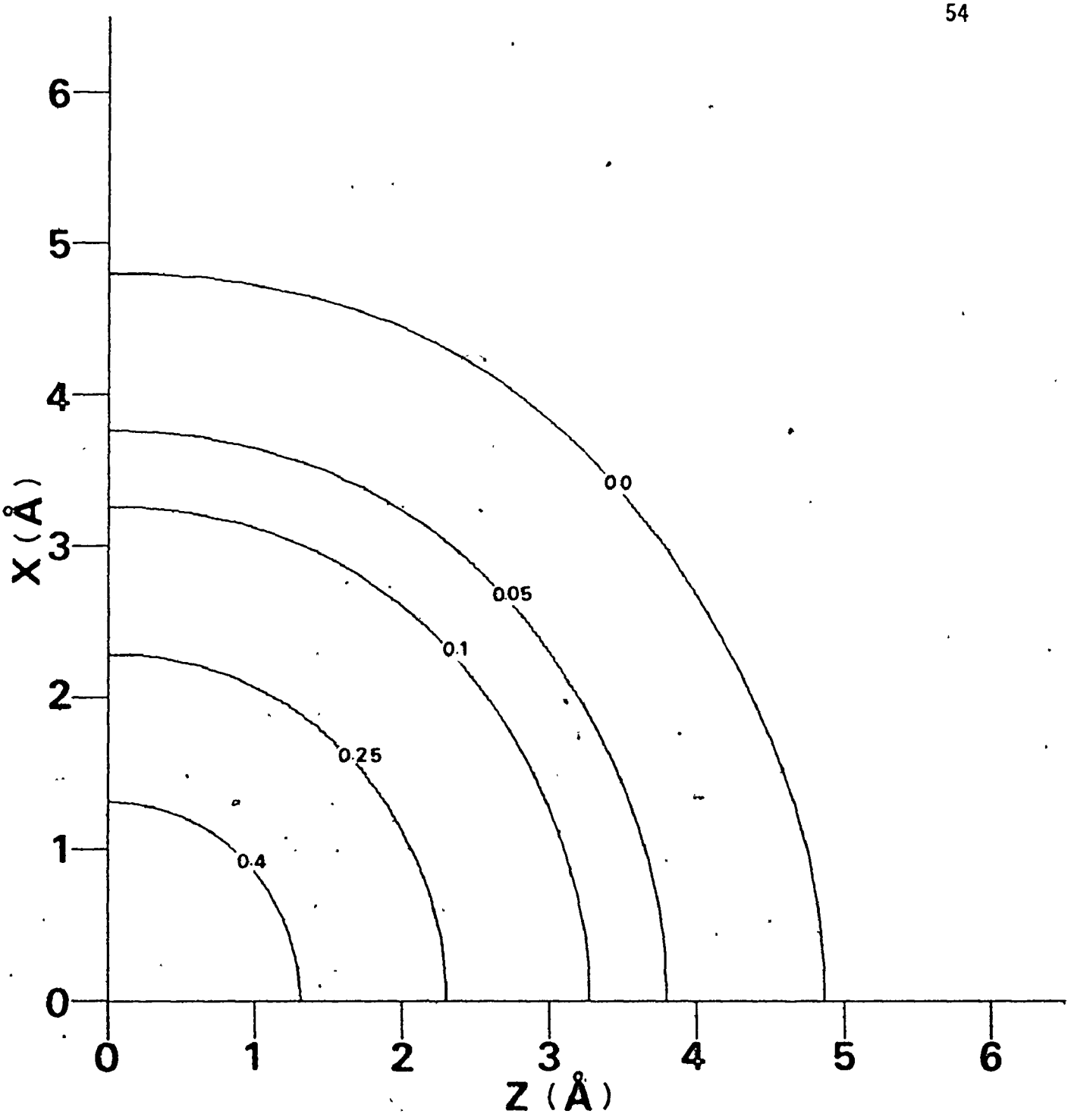

Figure 3.8a Single quadrant of the contour map for the local anisotropic contributions to the chemical shift of protons near benzene in the xz plane with y = 3.0 Å.

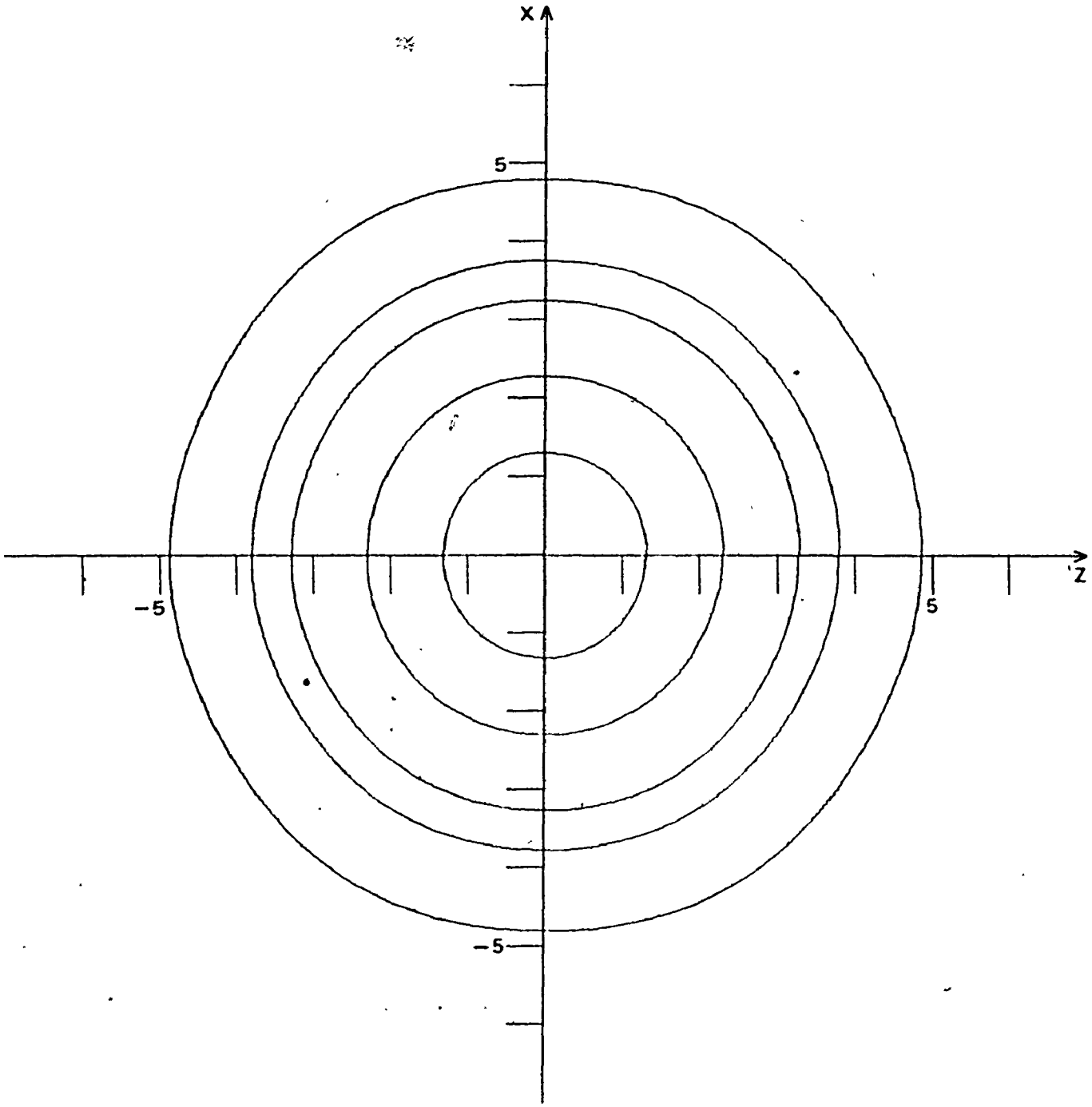

Figure 3.8b Contour map for the local anisotropic contributions to the chemical shift of protons near benzene in the xz plane with y = 3.0 Å.

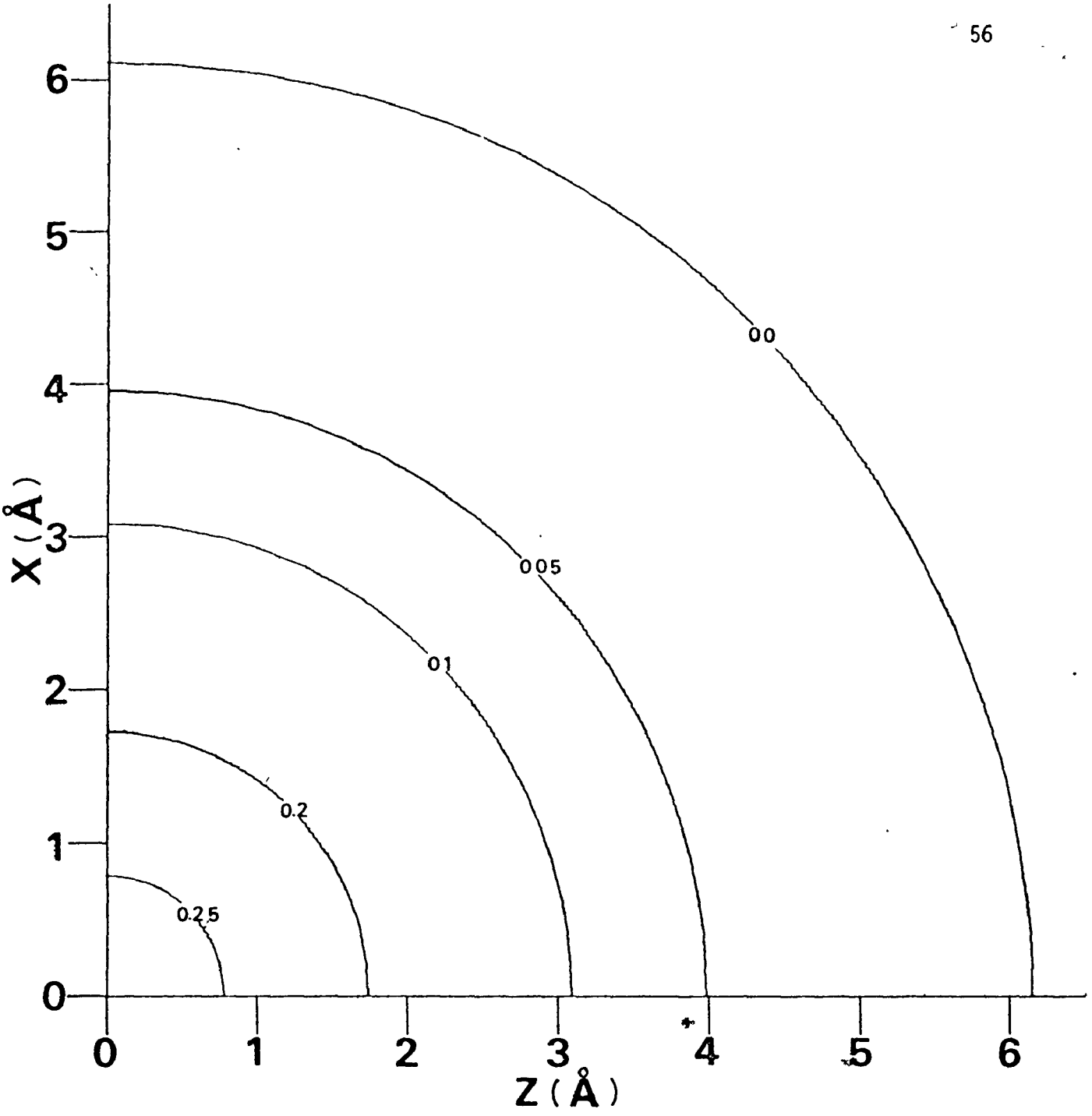

Figure 3.9a Single quadrant of the contour map for the local anisotropic contributions to the chemical shift of protons near benzene in the xz plane with y = 4.0 Å.

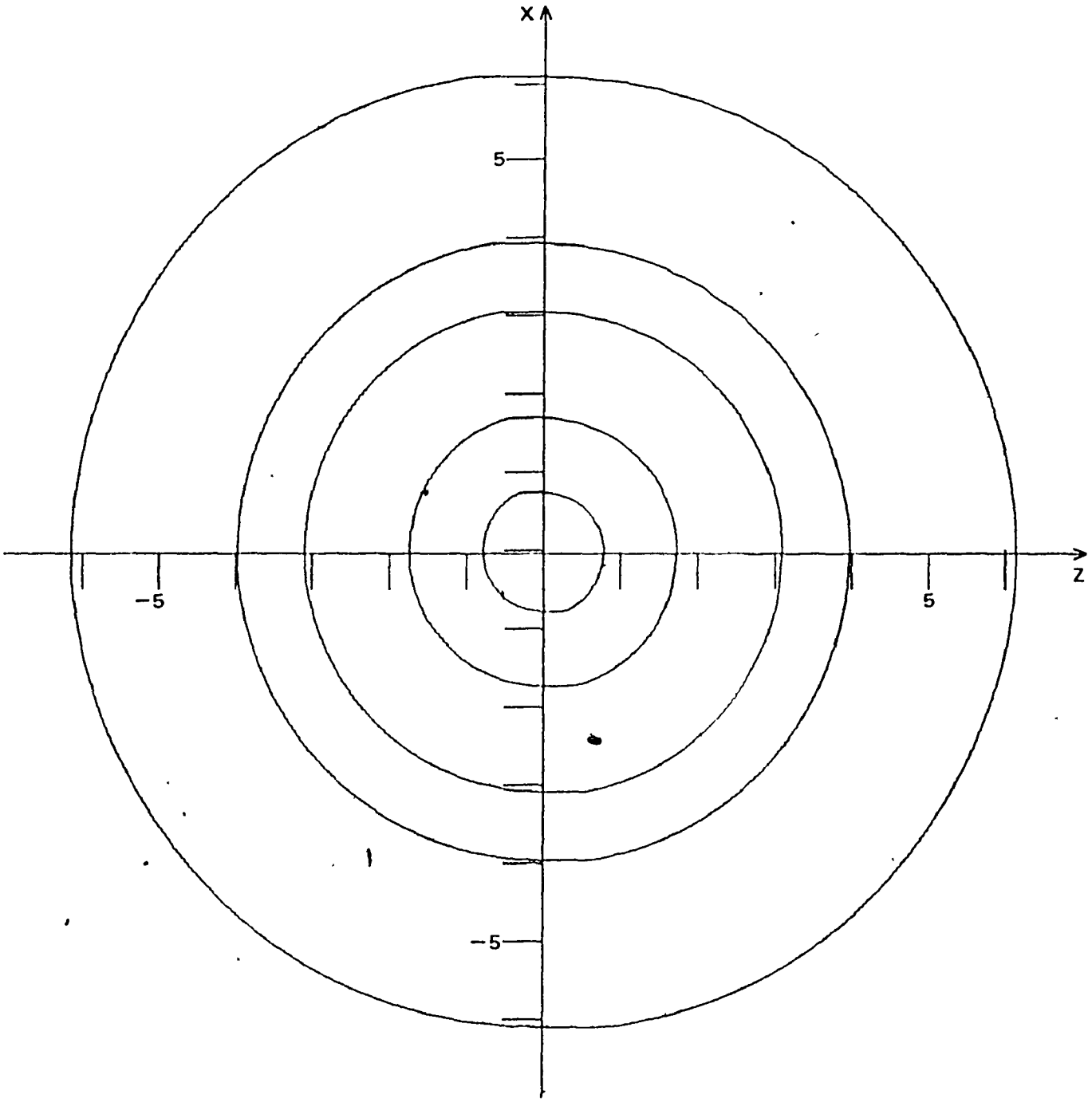

Figure 3.9b Contour map for the local anisotropic contributions to the chemical shift of protons near benzene in the xz plane with y = 4.0 Å.

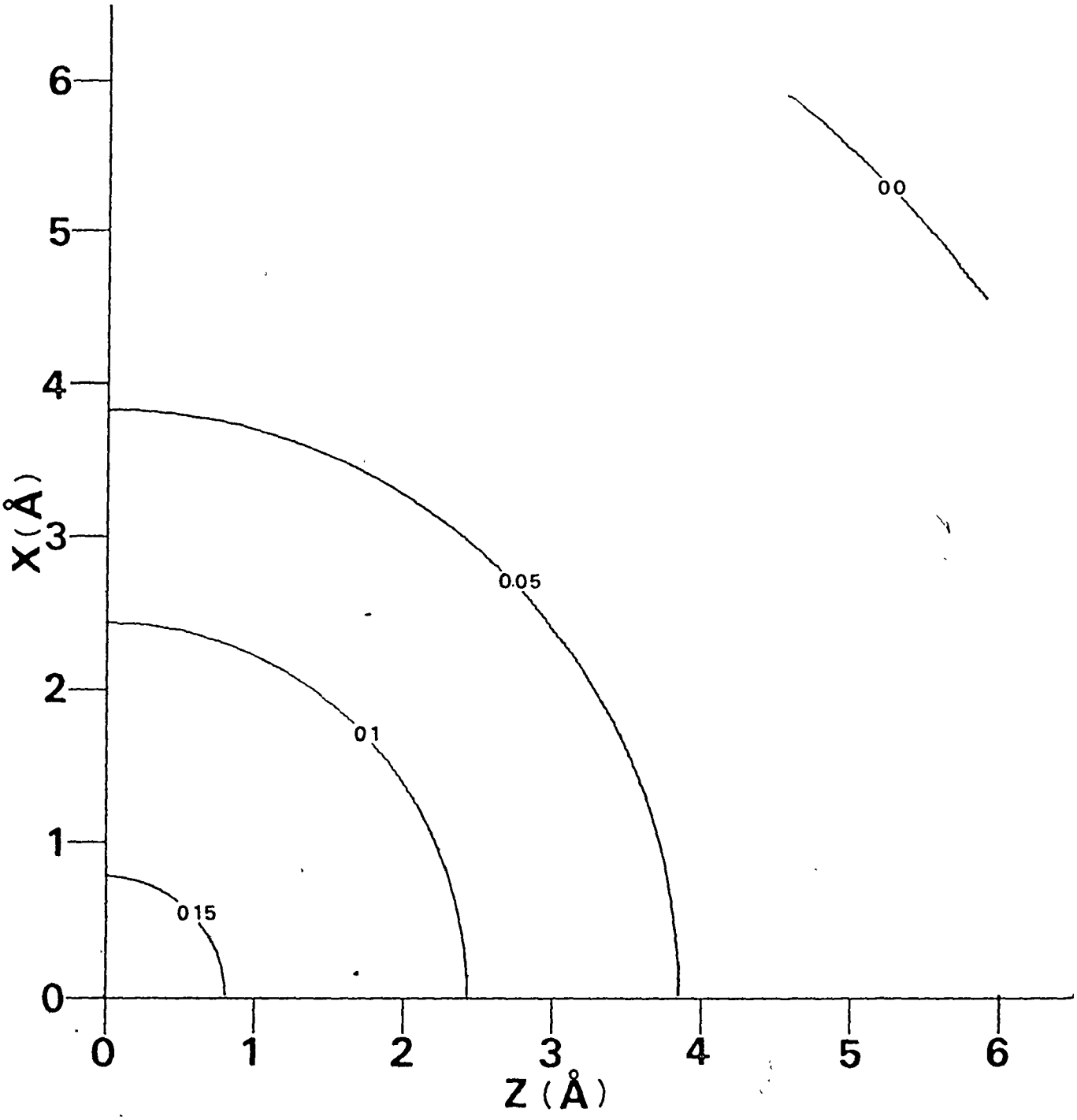

Figure 3.10a Single quadrant of the contour map for the local anisotropic contributions to the chemical shift of protons near benzene in the xz plane with y = 5.0 Å.

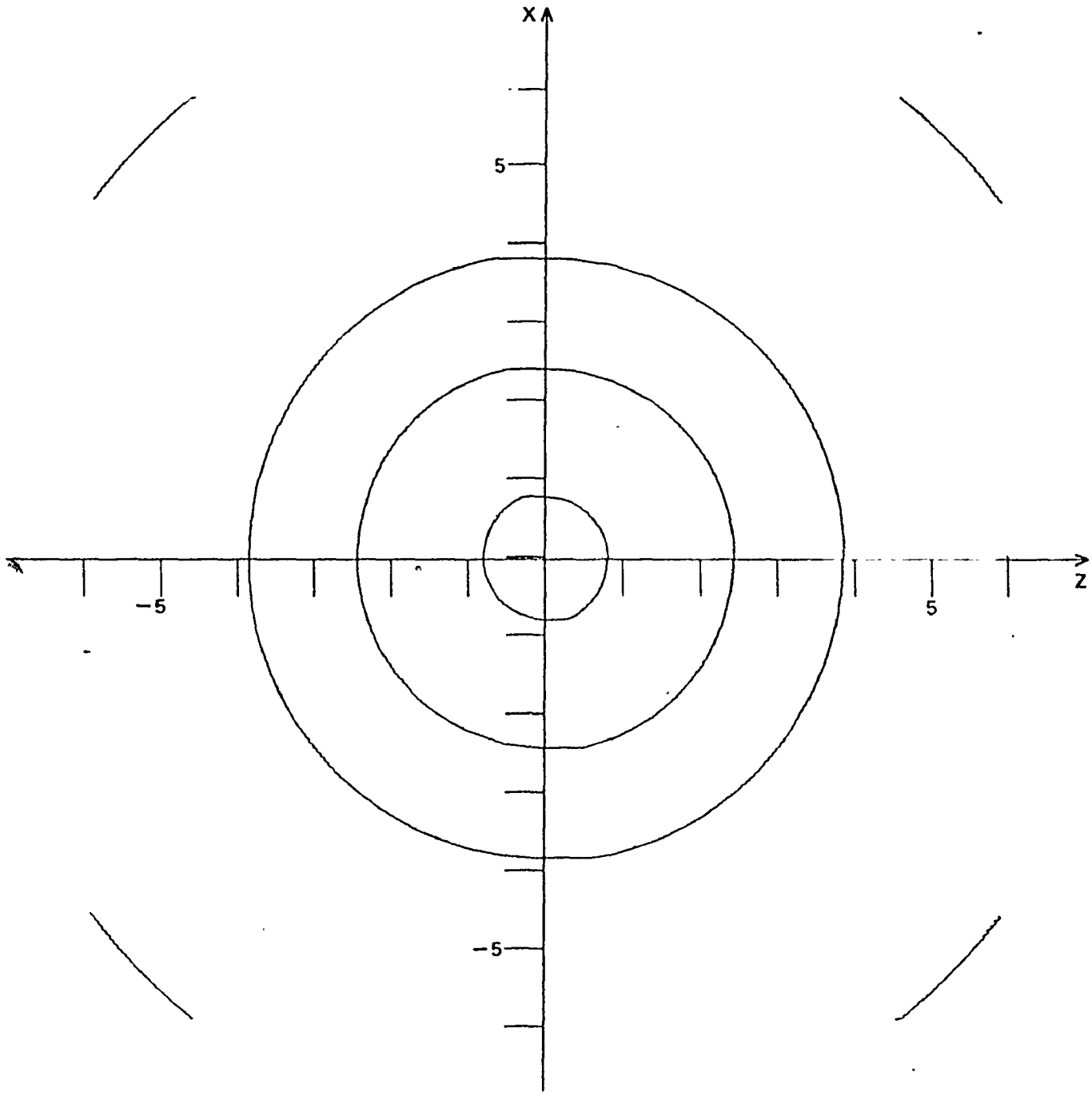

Figure 3.10b Contour map for the local anisotropic contributions to the chemical shift of protons near benzene in the xz plane with y = 5.0 Å.

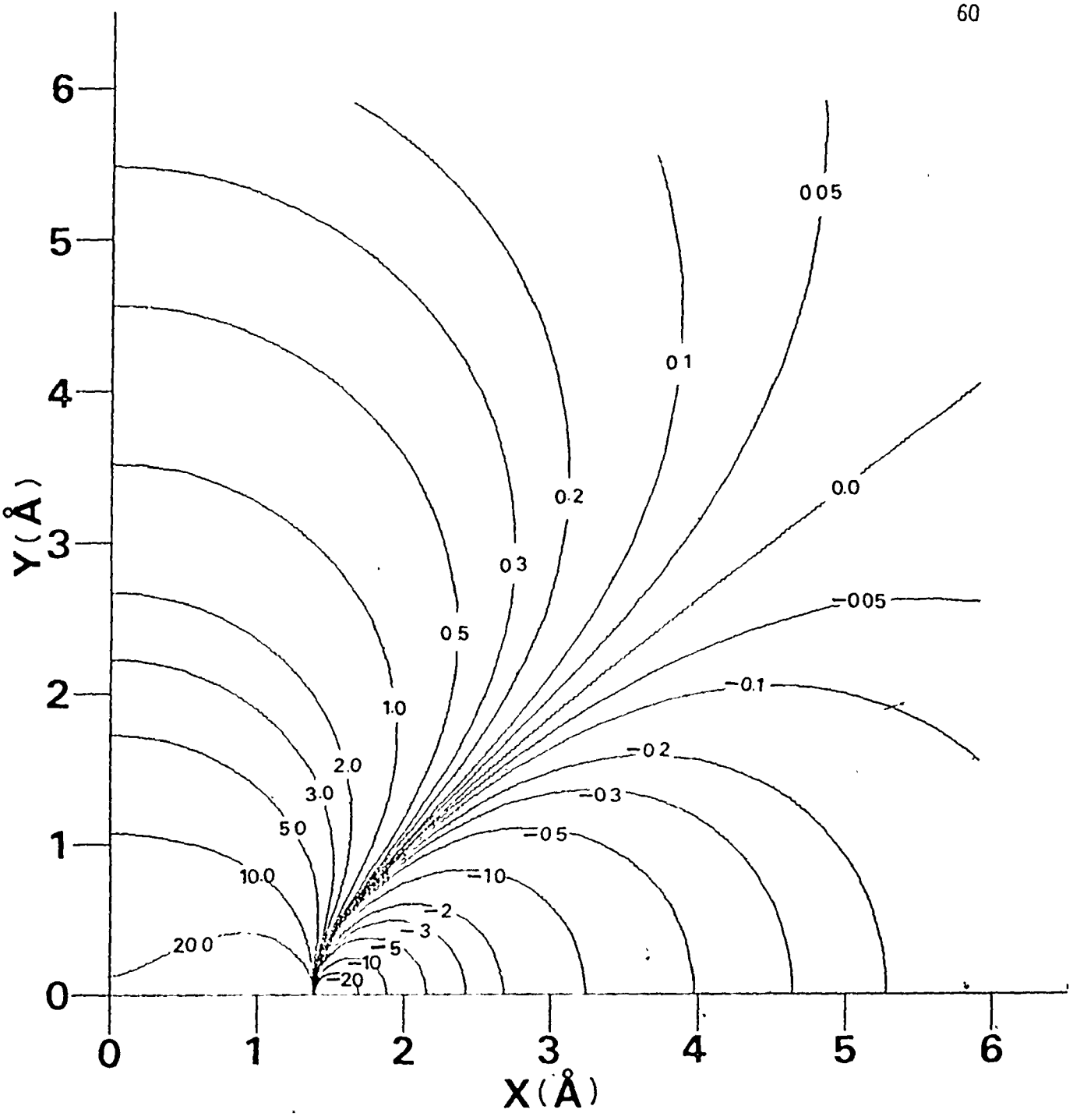

Figure 3.11a Single quadrant of the contour map for the ring current contribution to the chemical shift of protons near benzene in the xy plane with z = 0.0 Å.

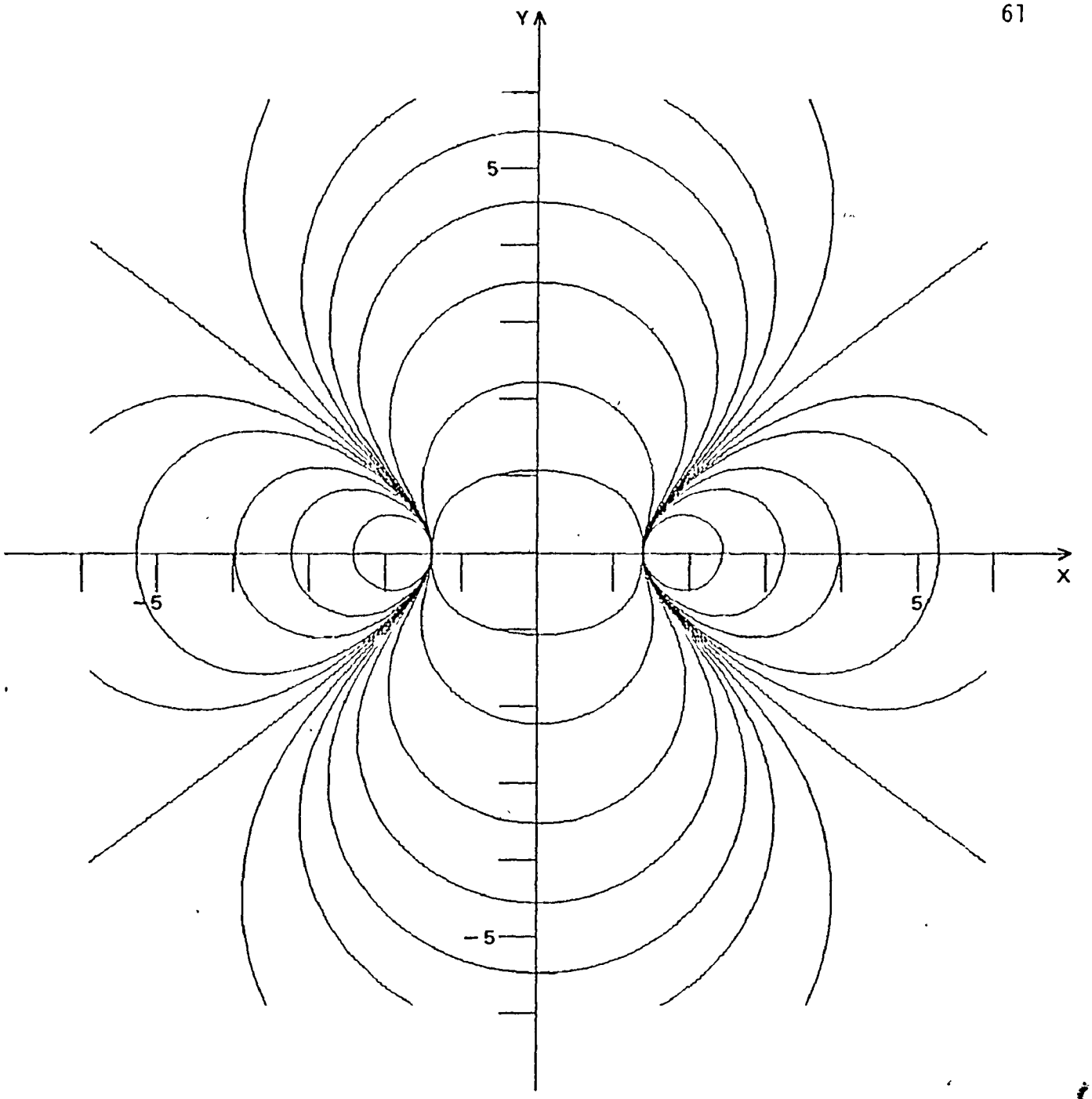

Figure 3.11b Contour map for the ring current contribution to the chemical shift of protons near benzene in the xy plane with z = 0.0 Å.

CHAPTER 4

APPLICATIONS OF LARC

4.1 CALCULATION OF SHIFTS

To get local anisotropic and ring current contributions to the chemical shift of protons from programme LARC, the coordinates of the proton with respect to the center of the ring have to be given. The programme also requires data about ring planarity, viz., which carbons lie out of the plane and, if so, by how much; the substitution pattern around the ring and the number of hydrogens must also be input.

The final shift is given, on the δ scale, by:

$$\text{Calc. shift} = \text{Standard shift} - \text{Local anisotropic shift} - \text{Ring current shift} \quad (4\text{-}1)$$

4.2 BENZENE

Barfield et al. (77) had estimated the local anisotropic contribution to the chemical shift of the aromatic protons in benzene as being 4.18 ppm. Their results are based on ^{13}C tensors which are now known to be inaccurate (74-76). To make their calculations fit to their chosen standard -- cyclohexane, Barfield et al. (77) empirically scaled the ring current contribution and also used a separation of 1.63 Å between the electron circulation loops which is even bigger than the separation Waugh and Fessenden (38) used. Thus we felt it was justified to have another look at the contributions to the benzene proton chemical shift.

Benzene was assumed to have a perfect hexagonal geometry with a

carbon-carbon bond length of 1.39 Å and a carbon-hydrogen bond length of 1.08 Å. It was further assumed that all the carbons and all the hydrogens were coplanar and, since all protons are equivalent, calculations need only be done for one of the protons. Thus, for ease of calculation, the C-H bond was assumed to lie along the x-axis, hence giving the proton the following coordinates with respect to the center of the ring:

$$x = 2.47 \text{ Å}, \quad y = 0.0 \text{ Å}, \quad z = 0.0 \text{ Å}$$

The results obtained from the programme LARC, using the coordinates given above, are listed in Table 4-1.

Table 4-1. Calculated Contributions for Benzene Protons

Atom	LA	RC	LA + RC
H	-4.58	-2.80	-7.38

LA = Local anisotropy; RC = Ring current

If the chemical shift of methane (δ 0.23) (19) is chosen as the standard shift (this molecule having no anisotropic or ring current contribution) then the predicted shift of a benzene proton, from equation (4-1), would be 7.61 ppm which is quite close to the experimental value of δ 7.37 (84).

4.3 TOLUENE

Calculations for toluene (phenylmethane) were based on the assumption that the methyl carbon has a perfect tetrahedral geometry, i.e., all

the H-C-H angles and the C-C-H angles are 109.47°. The phenyl ring was again assumed to have a perfect hexagonal geometry with a C-C bond length of 1.39 Å. The ring carbon to methyl carbon distance was taken as 1.5 Å and the methyl C-H bond distance was assumed to be 1.08 Å. The experimental NMR spectrum shows all the three methyl hydrogens to be equivalent. This equivalence of the protons was employed to simplify calculations.

As an instantaneous picture, the hydrogens can be positioned such that the C(methyl) - H_1 bond lies in the plane of the phenyl ring and the other two hydrogens (H_2,H_3) are equidistant above and below the plane of the ring. Then the predicted shift would be the average of the individual

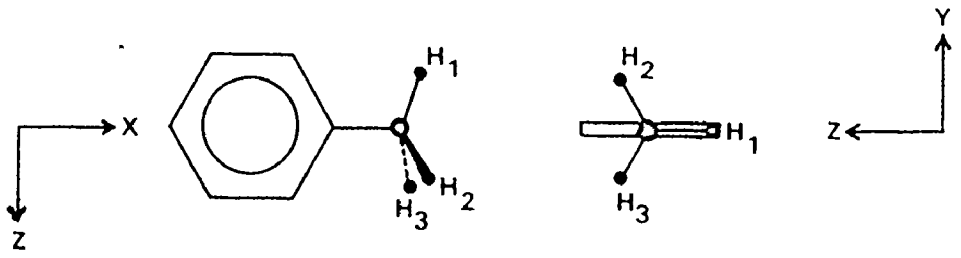

shifts of the three protons. The results are summarized in Table 4-2.

The standard shift for basing the toluene shift was estimated from the equation:

$$^{1}J_{CH} = 6.824\ \delta + 117.1 \qquad (4\text{-}2)$$

where δ is the chemical shift and $^{1}J_{CH}$ is the ^{13}C to H coupling constant. Equation (4-2) was derived by doing a least squares fit on $^{1}J_{CH}$ vs. the proton chemical shift data for compounds for the type CH_3-X where the X group is widely varied. The $^{1}J_{CH}$ data were obtained from Reference 83 and the chemical shifts from Reference 84. The linear regression coef-

Atom	x	y	z	LA	RC	LA + RC
H_1	3.250	0.000	-1.018	-0.56	-0.85	-1.41
H_2	3.250	0.881	0.509	-0.32	-0.59	-0.91
H_3	3.250	-0.881	0.509	-0.32	-0.59	-0.91

Table 4-2 Coordinates and local anisotropic and ring current contributions for the methyl protons of toluene. Average for the three protons = -1.07 ppm.

ficient for equation (4-2) was found to be 0.993.

Substituting $^1J_{CH}$ for toluene as 126.1 Hz (85), the expected or standard shift for toluene would be δ 1.32. Then the predicted shift would be δ 2.39 which is in good agreement with the experimental δ 2.29 (82).

4.4 [9]-PARACYCLOPHANE

The coordinates of the methylene protons in [9]-paracyclophane (Figure 4.1), have been calculated by Allinger (86) by a molecular mechanics method.

The molecular mechanics calculations show that there are three stable conformers, in equilibrium, for [9]-paracyclophane which differ by only a few kcals./mole in terms of the total steric energy (86). The most stable conformer (conformer (i)) has a C_2 symmetry with the ε-carbon up (Figure 4.2) and steric energy 29.01 kcal/mole; the second conformer (conformer (ii)) also has C_2 symmetry but C_ε is down (Figure 4.3) and the steric energy is 30.28 kcal/mole; the highest energy conformer (conformer (iii)) has C_s symmetry with steric energy 32.44 kcal/mole. The benzene ring in all the conformers is distorted -- carbons 1 and 4 are bent up and out of the plane of the ring by 9.16° for conformer (i) and 11.47° for conformer (ii).

In solution, during NMR experiments, the relative abundance of each conformer can be assumed to follow the Boltzman distribution:

$$\frac{N_A}{N_B} = e^{-\Delta E_{AB}/RT} \qquad (4\text{-}3)$$

Applying equation (4-3), the following will be the ratios for the

Figure 4.1 Plan views of [9]-paracyclophane (in the xz plane)

(a) Conformer (i)

(b) Conformer (ii)

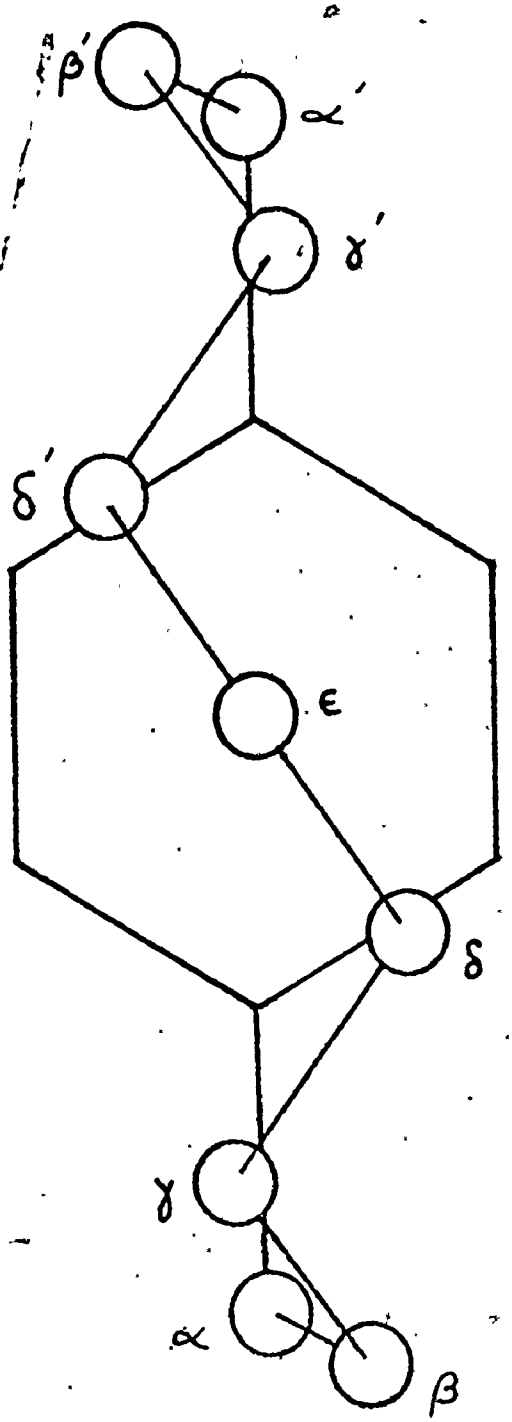

(a)

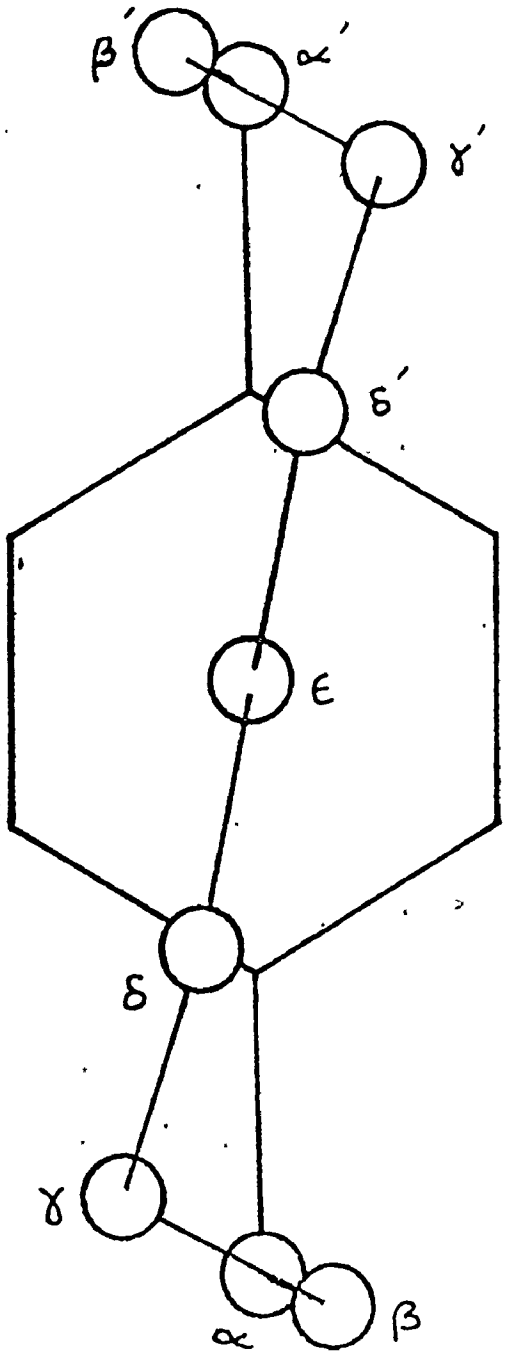

(b)

Figure 4.2 View of conformer (i) of [9]-paracyclophane in the xy plane

Large circles = carbons

Small circles = hydrogens

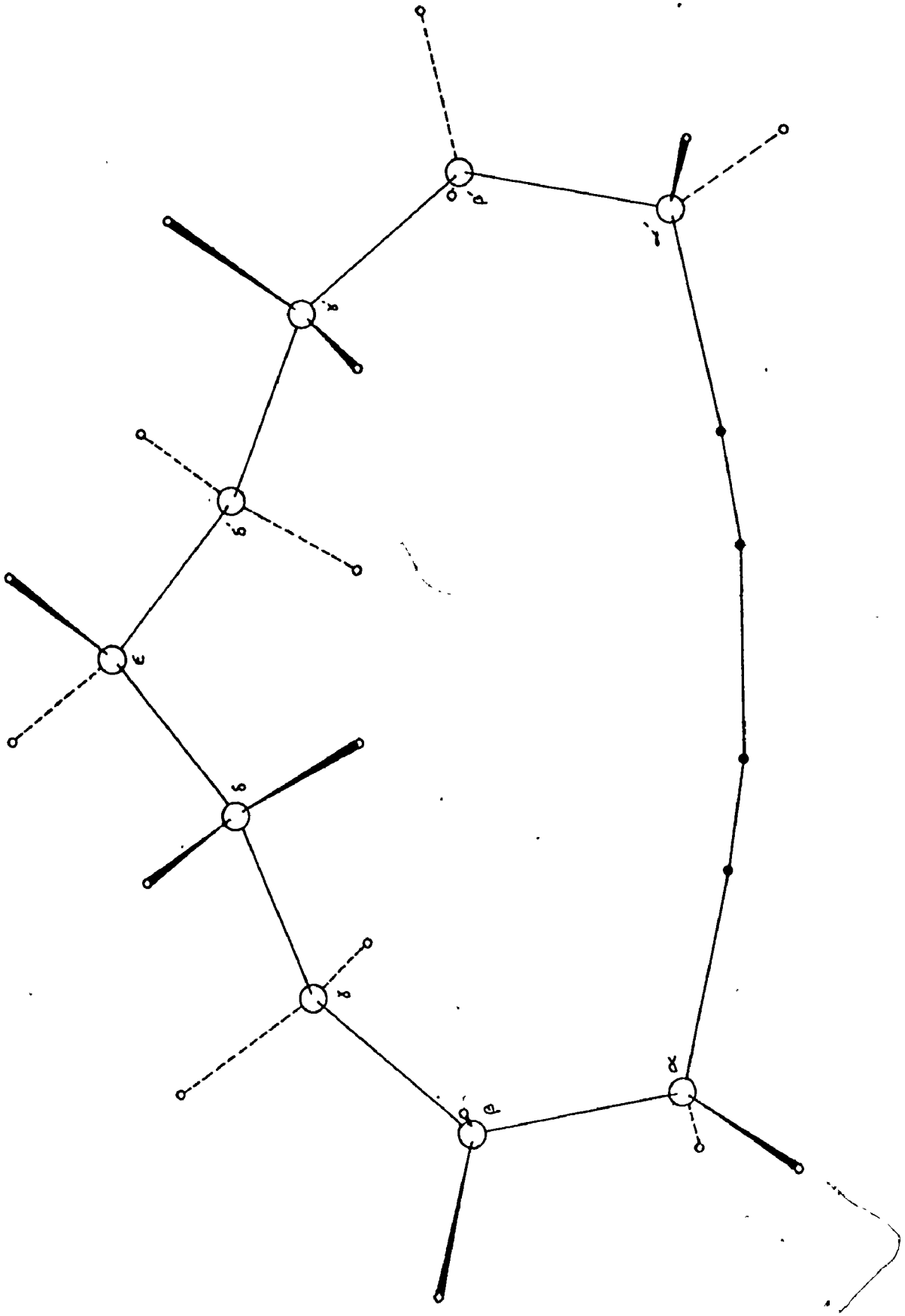
α
β
γ
δ
ε
ζ
η
θ

Figure 4.3 View of conformer (ii) of [9]-paracyclophane in the xy plane

Large circles = carbons

Small circles = hydrogens

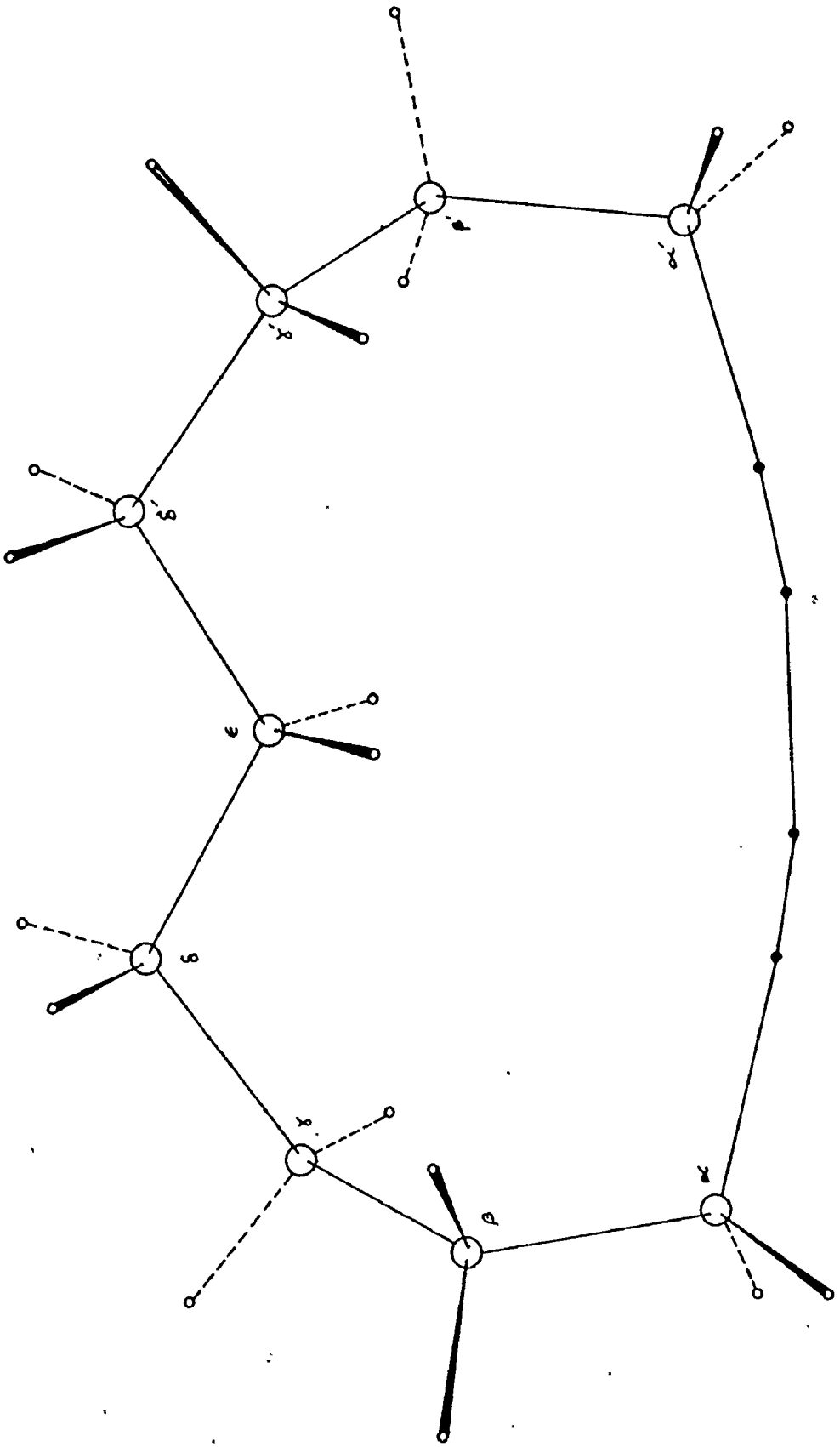

three conformers at 25°C:

$$\frac{N_{(i)}}{N_{(ii)}} = 7.966; \quad \frac{N_{(ii)}}{N_{(iii)}} = 34.105; \quad \frac{N_{(i)}}{N_{(iii)}} = 271.676$$

Thus the abundance of each conformer will be:

$$N_{(i)} = 88.42\%$$

$$N_{(ii)} = 11.25\%$$

$$N_{(iii)} = 0.33\%$$

The observed chemical shifts will be the weighted average of the individual shifts of each conformer. Since the abundance of conformer (iii) is so small, its contribution to the chemical shifts can be neglected.

The calculated shifts for the two protons, of a methylene group, are different because the calculations are based on an instantaneous conformation. In solution, the protons interconvert due to the flexibility of the methylene chain and hence only a single signal will be observed for both the protons.

Results of the calculations are shown in Tables 4-3, 4-4 and 4-5. The standard shift for a methylene proton is taken as 1.36 ppm (41). Since we have been unable to find a high-resolution ^1H NMR spectrum for [9]-paracyclophane, our results are predictions for the expected shifts. The only spectrum available was run at 40 MHz (87) and the only distinguishable methylene protons are the protons attached to C_α. The experimental shift of δ 2.6 compares favourably with our prediction of δ 2.58 for the protons on C_α.

Atom	x	y	z	LA	RC	LA + RC	Average
$H_{\alpha H}$	3.302	0.343	0.985	-0.51	-0.76	-1.27	-1.22
$H_{\alpha L}$	3.391	-0.308	-0.639	-0.40	-0.77	-1.17	
$H_{\beta H}$	4.196	2.113	-0.399	-0.05	-0.09	-0.14	-0.11
$H_{\beta L}$	2.985	1.915	-1.623	-0.01	-0.07	-0.08	
$H_{\gamma H}$	2.846	3.846	0.387	0.14	0.24	0.38	0.70
$H_{\gamma L}$	1.879	2.593	1.083	0.39	0.63	1.02	
$H_{\delta H}$	1.479	4.034	-1.584	0.20	0.37	0.57	1.27
$H_{\delta L}$	0.558	2.602	-1.212	0.63	1.35	1.98	
H_{ϵ}	0.536	4.951	0.692	0.18	0.37	0.55	0.55

Table 4-3 Coordinates and local anisotropic and ring current contributions for [9]-paracyclophane conformer (i).

Atom	x	y	z	LA	RC	LA + RC	Average
$H_{\alpha H}$	3.345	0.319	0.937	-0.49	-0.75	-1.24	-1.24
$H_{\alpha L}$	3.362	-0.103	-0.760	-0.44	-0.81	-1.25	
$H_{\beta H}$	2.574	2.244	-1.338	0.14	0.17	0.31	0.10
$H_{\beta L}$	4.103	2.221	-0.535	-0.05	-0.07	-0.12	
$H_{\gamma H}$	3.294	3.711	1.007	0.08	0.15	0.23	0.36
$H_{\gamma L}$	2.219	2.493	1.596	0.20	0.29	0.49	
$H_{\delta L}$	1.556	4.497	-0.636	0.19	0.37	0.56	0.56
$H_{\delta H}$	1.062	4.655	1.042	0.19	0.37	0.56	
H_{ε}	-0.174	2.495	0.880	0.78	1.89	2.67	2.67

Table 4-4 Coordinates and local anisotropic and ring current contributions for [9]-paracyclophane conformer (ii).

Atom	Weighted average of (LA + RC)	Predicted shift δ = 1.36-(LA + RC)
H_{α}	-1.22	2.58
H_{β}	-0.09	1.45
H_{γ}	0.66	0.70
H_{δ}	1.19	0.17
H_{ε}	0.80	0.56

Table 4-5 The weighted average local anisotropic and ring current contributions for both the conformers of [9]-paracyclophane and the predicted chemical shift, based on 1.36 ppm as standard, on the δ scale.

APPENDIX A

COMPUTER PROGRAMME LISTINGS

```
C     PROGRAMME LARC
C
C     FORTRAN PROGRAMME FOR CALCULATING THE LOCAL
C     ANISOTROPIC AND RING CURRENT CONTRIBUTIONS
C     TO THE CHEMICAL SHIFTS OF PROTONS IN BENZENE
C     AND ITS DERIVATIVES.
C
C     WRITTEN BY ARVIND AGARWAL, DEPARTMENT OF
C     CHEMISTRY, MCMASTER UNIVERSITY, HAMILTON,
C     ONTARIO, CANADA, 1976.
C
C
      DIMENSION SINE(3),COSE(3),TENCO(6),TNSOR(12),P(3),PZ(3)
      DIMENSION B(3),SIG(3),FA(30),FB(30),PHI(6)
C
C     GENERATING AND INITIALIZING CONSTANTS.
C
      EC=.1E-70
      PI=4.*ATAN(1.)
      DO 100 I=1,3
      SINE(I)=SIN((I-1)*PI/3.)
      COSE(I)=COS((I-1)*PI/3.)
100   CONTINUE
C
C     GENERATING THE COEFFICIENTS FOR THE EXPANSION
C     OF C AND E, THE ELLIPTICAL INTEGRALS OF THE
C     FIRST AND SECOND TYPE RESPECTIVELY.
C
      DO 109 MF=1,29
      N=MF-1
      F1=((FACT((2*N)+1))/((FACT(N))**2))**2
      F2=((4.**N)*((2.*N)+2.))**2
      FA(MF)=F1/F2
      FB(MF)=(F1/F2)/((2*N)+1)
109   CONTINUE
C
C     THE 13C SHIELDING TENSORS ARE FED IN AS AN ARRAY
C     CALLED TNSOR. THE FIRST 3 CORRESPOND TO H AS
C     SUBSTITUENT; NEXT 3 TO CH AS SUBSTITUENT;
C     NEXT 3 TO CH2 AS SUBSTITUENT; AND LAST
C     3 TO CH3 AS SUBSTITUENT. THE TENSORS ARE USED
C     FOR LOCAL ANISOTROPY CALCULATION.
C
      DATA TNSOR/153.,73.,-19.,177.,32.,-20.,178.,36.,-20.,
     1179.,40.,-20./
C
C     INPUT: NH = NUMBER OF HYDROGEN POSITIONS FOR
C     WHICH CALCULATIONS ARE DESIRED; ARRAY TENCO
C     BEING THE CODE FOR THE SUBSTITUENT ON THE
C     CARBON, 1=H,2=CH,3=CH2,4=CH3; ARRAY PHI IS FOR
C     THE ANGLE EACH CARBON IS BENT OUT OF PLANE .
C
      WRITE(6,1000)
1000  FORMAT(2X,'WRITE THE NUMBER OF HYDROGEN SHIFT TO BE CALCULATED',/)
      READ(5,1010) NH
```

```
1010  FORMAT(I3)
      WRITE(6,1050)
1050  FORMAT(2X,'WRITE THE TENSOR CODE FOR EACH CARBON.'/,2X,
     1'FIELD OF 1 COLUMN FOR EACH VALUE.'/)
      READ(5,1060) (TENCO(I),I=1,6)
1060  FORMAT(6(I1))
      WRITE(6,1110)
1110  FORMAT(2X,'GIVE THE ANGLE BY WHICH EACH CARBON IS BENT.'/,
     12X,'BENDING UP IS POSITIVE. FIELD OF 6 COLUMNS.'/)
      READ(5,1120) (PHI(I), I=1,6)
1120  FORMAT(6F6.2)
C
C     OUTERMOST LOOP STARTS, NUMBER OF ITERATIONS
C     EQUAL TO NUMBER OF HYDROGEN POSITIONS.
C
      DO 105 I=1,NH
C
C     INPUT: X,Y,Z, THE COORDINATES OF THE HYDROGEN
C     WITH RESPECT TO THE CENTER OF THE RING.
C
      WRITE(6,1020)
1020  FORMAT(////2X,'WRITE THE COORDINATES OF H'./,2X,
     1'FIELD OF 7 COLUMNS FOR EACH COORDINATE.'/)
      READ(5,1030) X,Y,Z
1030  FORMAT(3F7.3)
C
C     OUTPUT: COORDINATES AND TABLE HEADINGS.
C
      WRITE(6,1040) I,X,Y,Z
1040  FORMAT(2X,20HTHE COORDINATES OF H,I3,5H  ARE,/(2X,2HX=,F7.3,
     13H Y=,F7.3,3H Z=,F7.3),/)
      WRITE(6,1070)
1070  FORMAT(/2X,'C',1X,'TNC',6X,'SIG1',10X,'SIG2',10X,
     1'SIG3',9X,'SIGMA')
C
C     INITIALIZING VARIABLES: NC=NUMBER OF CARBONS;
C     TLA=TOTAL LOCAL ANISOTROPY.
C
      NC=1
      TLA=0.0
C
C     FOR LOCAL ANISOTROPY CALCULATIONS, THE
C     COORDINATES HAVE TO BE TRANSFORMED SO AS TO
C     BE CENTERED ON THE CARBON ITSELF. ALSO THE AXES
C     HAVE TO BE ROTATED BY 60 DEGREES FOR EACH
C     CARBON SO AS TO BRING THE CIRCULATIONS INTO
C     PROPER ORIENTATION. SYMMETRY OF THE RING IS USED
C     SO THAT THE AXES HAVE TO BE ROTATED FOR
C     3 CARBONS ONLY.
C
      DO 101 J=1,2
      IF(J.EQ.1) CX=1.39
      IF(J.EQ.2) CX=-1.39
      CY=0.0
      CZ=0.0
      DO 101 K=1,3
```

```
      HX=X*COSE(K)-Z*SINE(K)
      HY=Y
      HZ=X*SINE(K)+Z*COSE(K)
C
C     TEST FOR PLANARITY OF THE RING.
C
      IF(PHI(NC).EQ.0.0) GOTO 111
C
C     DIVERSION IF THE RING IS BENT.
C
      IF(J.EQ.1) GOTO 112
      IF(J.EQ.2) GOTO 113
112   CBX=0.695
      HX=HX-0.695
      RPHI=PI*PHI(NC)/180.
      GOTO 114
113   CBX=-0.695
      HX=HX+0.695
      RPHI=-PI*PHI(NC)/180.
114   HBX=HX*COS(RPHI)+HY*SIN(RPHI)
      HBY=HY*COS(RPHI)-HX*SIN(RPHI)
      HBZ=HZ
      DELX=ABS(HBX-CBX)
      DELY=ABS(HBY-CY)
      DELZ=ABS(HBZ-CZ)
      GOTO 115
C
C     MAIN PROGRAMME FOR PLANAR RING.
C
111   DELX=ABS(HX-CX)
      DELY=ABS(HY-CY)
      DELZ=ABS(HZ-CZ)
C
C     THE P'S AND PZ'S ARE THE RADIAL AND
C     PERPENDICULAR DISTANCES OF THE HYDROGEN TO
C     THE CIRCULATION LOOPS AROUND EACH CARBON.
C     CIRCULATION IN XZ PLANE=1;XY=2;YZ=3.
C
115   P(1)=SQRT(DELX**2+DELZ**2)
      P(2)=SQRT(DELX**2+DELY**2)
      P(3)=SQRT(DELY**2+DELZ**2)
      PZ(1)=DELY
      PZ(2)=DELZ
      PZ(3)=DELX
C
C     A IS THE RADIUS OF CIRCULATION AROUND A CARBON
C     FOR THE LOCAL ANISOTROPY; NR IS THE NUMBER OF
C     CIRCULATIONS TO BE CALCULATED. NR ALSO SERVES AS
C     THE BRANCHING CONDITION FOR ANISOTROPY OR
C     RING CURRENT CALCULATIONS.
C
      A=0.47
      NR=3
      CONST=A/PI
      GOTO 107
C
```

```
C     THE VARIABLES FOR RING CURRENT CALCULATIONS ARE
C     DEFINED NOW.
C
106   A=1.39
      NR=1
      CONST=8.979
      P(1)=SQRT(X**2+Z**2)
      PZ(1)=ABS(Y)
C
C     CALCULATION OF THE MAGNETIC FIELD DUE TO A
C     LOOP OF CIRCULATING ELECTRONS.
C
107   DO 102 L=1,NR
      W=(A+P(L))**2+PZ(L)**2
      R=4.*A*P(L)/W
      G=1.
      FA=1.
      DO 103 M=1,29
      G=G+(FA(M)*(R**M))
      FB=FB(M)*(R**M)
      IF(FB.LT.FC) GOTO 110
      FA=FA-FB
103   CONTINUE
110   C=PI*G/2.
      E=PI*FA/2.
      S=A**2-P(L)**2-PZ(L)**2
      T=(A-P(L))**2+PZ(L)**2
      B(L)=(CONST/SQRT(W))*(C+S*E/T)
102   CONTINUE
C
C     BRANCHING. NOW FOR RING CURRENT.
C
      IF(NP.EQ.3) GOTO 108
      WRITE(6,1100) B(1)
1100  FORMAT(/2X,'THE RING CURRENT=',E14.5)
      GOTO 105
C
C     FOR LOCAL ANISOTROPY.
C
108   IF(TENCO(NC).EQ.1) II=0
      IF(TENCO(NC).EQ.2) II=3
      IF(TENCO(NC).EQ.3) II=6
      IF(TENCO(NC).EQ.4) II=9
      SIGMA=0.0
      DO 104 JJ=1,3
      SIG(JJ)=B(1)*TNSOR(JJ+II)
      SIGMA=SIGMA+(SIG(JJ)/3.)
104   CONTINUE
      TLA=TLA+SIGMA
      WRITE(6,1090) NC,TENCO(NC),(SIG(KK),KK=1,3),SIGMA
1090  FORMAT(2X,I1,2X,I1,4(E14.5))
      NC=NC+1
101   CONTINUE
      WRITE(6,1090) TLA
1090  FORMAT(/2X,'THE TOTAL LOCAL ANISOTROPY=',E14.5)
      GOTO 106
```

```
C
C       RETURN TO BEGINING FOR NEXT HYDROGEN.
C
105     CONTINUE
        STOP
        END
C
C       THE FUNCTION FOR CALCULATING FACTORIALS.
C
        FUNCTION FACT(L)
        X=1.0
        DO 100 I=1,L
        X=X*I
100     CONTINUE
        FACT=X
        RETURN
        END
```

```
C      PROGRAMME LOAN
C
C      FOR LOCAL ANISOTROPIC CONTRIBUTION
C      CALCULATION ON A FLAT RING ONLY.
C
       DIMENSION SINE(3),COSE(3),TENCO(6),TNSOR(12),P(3),PZ(3)
       DIMENSION B(3),SIG(3),FA(30),FB(30)
       EC=.1E-70
       PI=4.*ATAN(1.)
       DO 100 I=1,3
       SINE(I)=SIN((I-1)*PI/3.)
       COSE(I)=COS((I-1)*PI/3.)
100    CONTINUE
       DO 109 MF=1,29
       N=MF-1
       F1=((FACT((2*N)+1))/((FACT(N))**2))**2
       F2=((4.**N)*((2.*N)+2.))**2
       FA(MF)=F1/F2
       FB(MF)=(F1/F2)/((2*N)+1)
109    CONTINUE
       DATA TNSOR/153..73.,-19.,177.,32.,-20.,178.,36.,-20.,
      1179.,40.,-20./,A/.47/
       WRITE(6,1000)
1000   FORMAT(2X,'WRITE THE NUMBER OF HYDROGEN SHIFT TO BE CALCULATED',/)
       READ(5,1010) NH
1010   FORMAT(I3)
       WRITE(6,1050)
1050   FORMAT(2X,37HWRITE THE TENSOR CODE FOR EACH CARBON,/)
       READ(5,1060) (TENCO(I),I=1,6)
1060   FORMAT(6(I1))
       DO 105 I=1,NH
       WRITE(6,1020)
1020   FORMAT(////2X,'WRITE THE COORDINATES OF H',/'X IN COLUMNS 1-7;
      1Y IN 8-14; Z IN 15-21',/)
       READ(5,1030) X,Y,Z
1030   FORMAT(3F7.3)
       WRITE(6,1040) I,X,Y,Z
1040   FORMAT(2X,20HTHE COORDINATES OF H,I3,5H  ARE,/(2X,2HX=,F7.3,
      13H Y=,F7.3,3H Z=,F7.3),/)
       WRITE(6,1070)
1070   FORMAT(/2X,'C',1X,'TNC',6X,'SIG1',10X,'SIG2',10X,
      1'SIG3',9X,'SIGMA')
       NC=1
       TLA=0.0
       DO 101 J=1,2
       IF(J.EQ.1) CX=1.39
       IF(J.EQ.2) CX=-1.39
       CY=0.0
       CZ=0.0
       DO 101 K=1,3
       HX=X*COSE(K)-Z*SINE(K)
       HY=Y
       HZ=X*SINE(K)+Z*COSE(K)
       DELX=ABS(HX-CX)
       DELY=ABS(HY-CY)
```

```
      DELZ=ABS(H7-CZ)
      P(1)=SQRT(DELX**2+DELZ**2)
      P(2)=SQRT(DELX**2+DELY**2)
      P(3)=SQRT(DELY**2+DELZ**2)
      PZ(1)=DELY
      PZ(2)=DELZ
      PZ(3)=DELX
      DO 102 L=1,3
      W=(A+P(L))**2+PZ(L)**2
      R=4.*A*P(L)/W
      G=1.
      EA=1.
      DO 103 M=1,29
      G=G+(FA(M)*(R**M))
      EB=FB(M)*(R**M)
      IF(EB.LT.0.0) GOTO 110
      EA=EA-EB
  103 CONTINUE
  110 C=PI*G/2.
      E=PI*EA/2.
      S=A**2-P(L)**2-PZ(L)**2
      T=(A-P(L))**2+PZ(L)**2
      B(L)=((A/PI)/SQRT(W))*(C+S*E/T)
  102 CONTINUE
      IF(TENCO(NC).EQ.1) II=0
      IF(TENCO(NC).EQ.2) II=3
      IF(TENCO(NC).EQ.3) II=6
      IF(TENCO(NC).EQ.4) II=9
      SIGMA=0.0
      DO 104 JJ=1,3
      SIG(JJ)=B(JJ)*TNSOR(JJ+II)
      SIGMA=SIGMA+(SIG(JJ)/3.)
  104 CONTINUE
      TLA=TLA+SIGMA
      WRITE(6,1080) NC,TENCO(NC),(SIG(KK),KK=1,3),SIGMA
 1080 FORMAT(2X,I1,2X,I1,4(E14.5))
      NC=NC+1
  101 CONTINUE
      WRITE(6,1090) TLA
 1090 FORMAT(/2X,'THE TOTAL LOCAL ANISOTROPY=',E14.5)
  105 CONTINUE
      STOP
      END
      FUNCTION FACT(L)
      X=1.0
      DO 100 I=1,L
      X=X*I
  100 CONTINUE
      FACT=X
      RETURN
      END
```

```
C      PROGRAMME TABLA
C
C      FOR GENERATING TABLES OF LOCAL ANISOTROPY
C      VALUES FOR FLAT BENZENE. VARIOUS MODIFICATIONS
C      USED FOR THE DIFFERENT PLANES PLOTTED.
C
       DIMENSION SINE(3),COSE(3),TENCO(6),TNSOR(12),P(3),PZ(3)
       DIMENSION B(3),SIG(3),TLA(10),FA(30),FB(30)
       EC=.1E-70
       PI=4.*ATAN(1.)
       DO 100 I=1,3
       SINE(I)=SIN((I-1)*PI/3.)
       COSE(I)=COS((I-1)*PI/3.)
100    CONTINUE
       DO 109 MF=1,29
       N=MF-1
       F1=((FACT((2*N)+1))/((FACT(N))**2))**2
       F2=((4.**N)*((2.*N)+2.))**2
       FA(MF)=F1/F2
       FB(MF)=(F1/F2)/((2*N)+1)
109    CONTINUE
       DATA TNSOR/153.,73.,-19.,177.,32.,-20.,178.,36.,-20.,
      1179.,40.,-20./,A/.47/
       DATA TENCO/1.1,1.1,1.1/
       Y=0.0
       DISPLAY"  "
       DISPLAY"  "
       DISPLAY"Y=",Y
       Z=0.0
       DO 106 IZ=1,60
       DISPLAY"  "
       DISPLAY"Z=",Z
       X=0.0
       DO 105 IXX=1,6
       DO 107 IX=1,10
       NC=1
       TLA(IX)=0.0
       DO 101 J=1,2
       IF(J.EQ.1) CX=1.39
       IF(J.EQ.2) CX=-1.39
       CY=0.0
       CZ=0.0
       DO 101 K=1,3
       HX=X*COSE(K)-Z*SINE(K)
       HY=Y
       HZ=X*SINE(K)+Z*COSE(K)
       DELX=ABS(HX-CX)
       DELY=ABS(HY-CY)
       DELZ=ABS(HZ-CZ)
       P(1)=SQRT(DELX**2+DELZ**2)
       P(2)=SQRT(DELX**2+DELY**2)
       P(3)=SQRT(DELY**2+DELZ**2)
       PZ(1)=DELY
       PZ(2)=DELZ
       PZ(3)=DELX
```

```
      DO 102 L=1,3
      W=(A+P(L))**2+PZ(L)**2
      R=4.*A*P(L)/W
      G=1.
      EA=1.
      DO 103 M=1,29
      G=G+(FA(M)*(R**M))
      EB=FB(M)*(R**M)
      IF(EB.LT.EC) GOTO 110
      EA=EA-EB
103   CONTINUE
110   C=PI*G/2.
      E=PI*EA/2.
      S=A**2-P(L)**2-PZ(L)**2
      T=(A-P(L))**2+PZ(L)**2
      B(L)=((A/PI)/SQRT(W))*(C+S*E/T)
102   CONTINUE
      IF(TENCO(NC).EQ.1) II=0
      IF(TENCO(NC).EQ.2) II=3
      IF(TENCO(NC).EQ.3) II=6
      IF(TENCO(NC).EQ.4) II=9
      SIGMA=0.0
      DO 104 JJ=1,3
      SIG(JJ)=B(JJ)*TNSOR(JJ+II)
      SIGMA=SIGMA+(SIG(JJ)/3.)
104   CONTINUE
      TLA(IX)=TLA(IX)+SIGMA
      NC=NC+1
101   CONTINUE
      X=X+0.1
107   CONTINUE
      DISPLAY (TLA(IT),IT=1,10)
105   CONTINUE
108   CONTINUE
      Z=Z+0.1
106   CONTINUE
      STOP
      END
      FUNCTION FACT(L)
      X=1.0
      DO 100 I=1,L
      X=X*I
100   CONTINUE
      FACT=X
      RETURN
      END
```

```
C      PROGRAMME RICU
C
C      FOR CALCULATING THE RING CURRENT.
C
       DIMENSION FA(30),FB(30)
       PI=4.*ATAN(1.)
       A=1.39
       DO 109 MF=1,29
       N=MF-1
       F1=((FACT((2*N)+1))/((FACT(N))**2))**2
       F2=((4.**N)*((2.*N)+2.))**2
       FA(MF)=F1/F2
       FB(MF)=(F1/F2)/((2*N)+1)
109    CONTINUE
       DISPLAY "WRITE NUMBER OF HYDROGENS"
       READ(5,*) N
       DO 104 J=1,N
       DISPLAY "GIVE H COORDINATES"
       READ(5,*) X,Y,Z
       DISPLAY "THE COORDINATES OF H ",J,"ARE"
       DISPLAY "  ","X=",X,"Y=",Y,"Z=",Z
       P=SQRT(X**2+Z**2)
       PZ=ABS(Y)
       W=(A+P)**2+PZ**2
       R=4.*A*P/W
       G=1.
       EA=1.
       DO 103 M=1,29
       G=G+(FA(M)*(R**M))
       EA=EA-(FB(M)*(R**M))
103    CONTINUE
       C=PI*G/2.
       E=PI*EA/2.
       S=A**2-P**2-PZ**2
       T=(A-P)**2+PZ**2
       B=(8.970/SQRT(W))*(C+S*E/T)
       DISPLAY "THE RING CURRENT IS=",B
104    CONTINUE
       STOP
       END
       FUNCTION FACT(L)
       X=1.0
       DO 100 I=1,L
       X=X*I
100    CONTINUE
       FACT=X
       RETURN
       END
```

```
C       PROGRAMME TABRC
C
C       FOR CALCULATING RING CURRENTS.
C       GENERATING THE TABLE IN THE XY PLANE.
C
        DIMENSION B(10),FA(30),FB(30)
        PI=4.*ATAN(1.)
        A=1.39
        DO 109 MF=1,29
        N=MF-1
        F1=((FACT(2*N)*1))/((FACT(N))**2))**2
        F2=((4.**N)*((2.*N)+2.))**2
        FA(MF)=F1/F2
        FB(MF)=(F1/F2)/((2*N)+1)
109     CONTINUE
        X=0.0
        DISPLAY "X=",X
        Y=0.0
        DO 104 J=1,60
        DISPLAY " "
        DISPLAY "Y=",Y
        Z=0.0
        DO 101 K=1,6
        DO 102 L=1,10
        P=SQRT(X**2+Y**2)
        PZ=ABS(Y)
        W=(A+P)**2+PZ**2
        R=4.*A*P/W
        G=1.
        FA=1.
        DO 103 M=1,29
        G=G+(FA(M)*(R**M))
        FA=FA-(FB(M)*(R**M))
103     CONTINUE
        C=PI*G/2.
        E=PI*FA/2.
        S=A**2-P**2-PZ**2
        T=(A-P)**2+PZ**2
        B(L)=(8.970/SQRT(W))*(C+S*E/T)
        Z=Z+0.1
102     CONTINUE
        DISPLAY (B(L),L=1,10)
101     CONTINUE
        Y=Y+0.1
104     CONTINUE
        STOP
        END
        FUNCTION FACT(L)
        X=1.0
        DO 100 I=1,L
        X=X*I
100     CONTINUE
        FACT=X
        RETURN
        END
```

```
C
C     PROGRAMME SQPLOT
C
C     FOR PLOTING A SINGLE QUADRANT.
C
      DIMENSION X(90),Y(90)
      CALL DATE(THEDATE)
      CALL LETTER(0,.25,90.,.5,1.0,6HARVIND)
      CALL LETTER(10,.25,90.,1.0,1.0,THEDATE)
      CALL PLOT(1.5,2.0,-3)
      CALL PLTIN(1.0,1.0,-1.0,-1.0,-1.0,7.0,-1.0,7.0)
      CALL PLOT(.0,1.0,3)
      CALL PLOT(8.0,1.0,2)
      CALL PLOT(1.0,.0,3)
      CALL PLOT(1.0,8.0,2)
      XD=7.0
      DO 10 I=1,7
      CALL PLOT(XD,1.0,3)
      CALL PLOT(XD,0.75,2)
10    XD=XD-1.0
      YD=7.0
      DO 20 I=1,7
      CALL PLOT(1.0,YD,3)
      CALL PLOT(0.75,YD,2)
20    YD=YD-1.0
      READ(5,*) N
      DO 40 II=1,N
      READ(5,*) M
      READ(5,*) (X(I),I=1,M)
      READ(5,*) (Y(I),I=1,M)
      CALL PLTMPL(X,Y,M)
40    CONTINUE
      CALL PLOT(10.,.0,-3)
      CALL PLOT(10.,.0,999)
      STOP
      END
```

```
C
C     PROGRAMME FQPLOT
C
C     FOR PLOTING IN ALL FOUR QUADRANTS.
C
      DIMENSION X(90),Y(90),X1(90),Y1(90),X2(90),Y2(90),X3(90),Y3(90)
      CALL DATE(THEDATE)
      CALL LETTER(5.,.25,90.,.5,1.0,6HARVIND)
      CALL LETTER(10.,.25,90.,1.0,1.0,THEDATE)
      CALL PLOT(1.5,2.0,-3)
      CALL PLTIN(2.0,2.0,-7.0,-7.0,-7.0,7.0,-7.0,7.0)
      CALL PLOT(.0,3.5,3)
      CALL PLOT(7.0,3.5,2)
      CALL PLOT(3.5,.0,3)
      CALL PLOT(3.5,7.0,2)
      XD=6.5
      DO 10 I=1,13
      CALL PLOT(XD,3.5,3)
      CALL PLOT(XD,3.25,2)
10    XD=XD-0.5
      YD=6.5
      DO 20 I=1,13
      CALL PLOT(3.5,YD,3)
      CALL PLOT(3.25,YD,2)
20    YD=YD-0.5
      READ(5,*) N
      DO 40 II=1,N
      READ(5,*) M
      READ(5,*) (X(I),I=1,M)
      READ(5,*) (Y(I),I=1,M)
      DO 30 I=1,M
      X1(I)=-X(I)
      Y1(I)=Y(I)
      X2(I)=X1(I)
      Y2(I)=-Y1(I)
      X3(I)=X(I)
30    Y3(I)=-Y(I)
      CALL PLTMPL(X,Y,M)
      CALL PLTMPL(X1,Y1,M)
      CALL PLTMPL(X2,Y2,M)
      CALL PLTMPL(X3,Y3,M)
40    CONTINUE
      CALL PLOT(10.,.0,-3)
      CALL PLOT(10.,.0,999)
      STOP
      END
```

APPENDIX B

TABLES OF LOCAL ANISOTROPIC AND RING CURRENT CONTRIBUTIONS

y \ x	0.0	1.0	2.0	3.0	4.0	5.0	6.0
0.0	-11.262	179.375	-51.672	-1.314	-0.333	-0.139	-0.073
1.0	- 1.678	1.609	1.018	-0.337	-0.201	-0.107	-0.062
2.0	0.592	0.809	0.567	0.105	-0.035	-0.047	-0.038
3.0	0.450	0.427	0.302	0.134	0.034	0.004	-0.014
4.0	0.263	0.242	0.181	0.106	0.048	0.016	0.001
5.0	0.157	0.146	0.116	0.079	0.046	0.023	0.009
6.0	0.099	0.093	0.078	0.058	0.038	0.023	0.012

Table B-1 Local anisotropic contribution for the xy plane with z = 0.0 Å.

y \ z	0.0	1.0	2.0	3.0	4.0	5.0	6.0
0.0	-11.262	-24.465	-2.820	-0.655	-0.257	-0.124	-0.069
1.0	- 1.678	1.836	1.349	-1.441	-0.157	-0.096	-0.059
2.0	0.592	0.811	0.582	0.127	-0.023	-0.042	-0.036
3.0	0.450	0.427	0.303	0.136	0.036	-0.003	-0.014
4.0	0.263	0.242	0.181	0.107	0.049	0.016	0.001
5.0	0.157	0.146	0.116	0.079	0.046	0.023	0.009
6.0	0.099	0.093	0.078	0.058	0.038	0.023	0.012

Table B-2 Local anisotropic contributions in the yz plane with x = 0.0 Å.

x \ z	0.0	1.0	2.0	3.0	4.0	5.0	6.0
0.0	- 11.262	- 24.465	- 2.820	-0.655	-0.257	-0.124	-0.069
1.0	179.375	102.135	-10.077	-0.834	-0.260	-0.120	-0.067
2.0	- 51.672	- 1.871	- 1.243	-0.517	-0.211	-0.105	-0.060
3.0	- 1.314	- 0.680	- 0.367	-0.236	-0.137	-0.080	-0.050
4.0	- 0.333	- 0.266	- 0.180	-0.126	-0.086	-0.058	-0.039
5.0	- 0.139	- 0.125	- 0.099	-0.075	-0.056	-0.041	-0.030
6.0	- 0.073	- 0.069	- 0.059	-0.048	-0.038	-0.030	-0.023

Table B-3 Local anisotropic contribution for xz plane with y = 0.0 Å.

x \ z	0.0	1.0	2.0	3.0	4.0	5.0	6.0
0.0	-6.770	2.096	0.688	-0.463	-0.228	-0.116	-0.066
1.0	-5.702	17.714	-2.077	-0.628	-0.232	-0.113	-0.064
2.0	-1.754	- 0.216	-0.796	-0.432	-0.192	-0.099	-0.058
3.0	-0.922	- 0.514	-0.309	-0.213	-0.128	-0.077	-0.048
4.0	-0.293	- 0.237	-0.164	-0.118	-0.082	-0.056	-0.038
5.0	-0.130	- 0.118	-0.094	-0.072	-0.054	-0.040	-0.030
6.0	-0.070	- 0.066	-0.057	-0.047	-0.037	-0.030	-0.023

Table B-4 Local anisotropic contributions in the xz plane with y = 0.5 Å.

x \ z	0.0	1.0	2.0	3.0	4.0	5.0	6.0
0.0	-1.678	1.836	1.349	-0.144	-0.157	-0.096	-0.059
1.0	1.609	3.142	0.322	-0.273	-0.165	-0.094	-0.057
2.0	1.018	0.653	-0.194	-0.256	-0.147	-0.084	-0.052
3.0	-0.337	-0.219	-0.183	-0.156	-0.105	-0.067	-0.044
4.0	-0.201	-0.169	-0.126	-0.097	-0.071	-0.050	-0.035
5.0	-0.107	-0.098	-0.080	-0.063	-0.049	-0.037	-0.028
6.0	-0.062	-0.059	-0.051	-0.043	-0.035	-0.027	-0.022

Table B-5 Local anisotropic contribution in the xz plane with y = 1.0 Å.

x \ z	0.0	1.0	2.0	3.0	4.0	5.0	6.0
0.0	0.200	1.175	0.887	0.051	-0.082	-0.069	-0.048
1.0	1.162	1.386	0.526	-0.037	-0.092	-0.069	-0.047
2.0	0.819	0.601	0.088	-0.101	-0.093	-0.064	-0.043
3.0	-0.016	-0.016	-0.067	-0.091	-0.076	-0.054	-0.038
4.0	-0.106	-0.094	-0.080	-0.070	-0.056	-0.042	-0.031
5.0	-0.077	-0.071	-0.061	-0.051	-0.041	-0.032	-0.025
6.0	-0.050	-0.048	-0.043	-0.037	-0.030	-0.025	-0.020

Table B-6 Local anisotropic contributions in the xz plane with y = 1.5 Å.

x \ z	0.0	1.0	2.0	3.0	4.0	5.0	6.0
0.0	0.592	0.811	0.582	0.127	-0.023	-0.042	-0.036
1.0	0.809	0.813	0.435	0.071	-0.034	-0.044	-0.035
2.0	0.567	0.453	0.170	-0.006	-0.046	-0.043	-0.034
3.0	0.105	0.078	0.009	-0.038	-0.047	-0.039	-0.030
4.0	-0.035	-0.035	-0.039	-0.043	-0.040	-0.033	-0.026
5.0	-0.047	-0.045	-0.041	-0.037	-0.032	-0.027	-0.021
6.0	-0.038	-0.036	-0.033	-0.029	-0.025	-0.021	-0.017

Table B-7 Local anisotropic contributions for the xz plane with $y = 2.0$ Å.

x \ z	0.0	1.0	2.0	3.0	4.0	5.0	6.0
0.0	0.450	0.427	0.303	0.136	0.036	-0.003	-0.014
1.0	0.427	0.389	0.261	0.113	0.028	-0.005	-0.014
2.0	0.302	0.262	0.161	0.064	0.010	-0.010	-0.015
3.0	0.134	0.114	0.066	0.021	-0.004	-0.014	-0.015
4.0	0.034	0.027	0.012	-0.003	-0.012	-0.015	-0.015
5.0	-0.004	-0.006	-0.009	-0.013	-0.015	-0.015	-0.014
6.0	-0.014	-0.015	-0.015	-0.015	-0.014	-0.013	-0.012

Table B-8 Local anisotropic contributions in the xz plane with y = 3.0 Å.

x \ z	0.0	1.0	2.0	3.0	4.0	5.0	6.0
0.0	0.263	0.242	0.181	0.107	0.049	0.016	0.001
1.0	0.242	0.221	0.163	0.095	0.043	0.014	0.000
2.0	0.181	0.164	0.119	0.068	0.030	0.009	-0.002
3.0	0.106	0.095	0.069	0.039	0.016	0.003	-0.004
4.0	0.048	0.043	0.031	0.016	0.005	-0.002	-0.006
5.0	0.016	0.014	0.009	0.003	-0.002	-0.005	-0.006
6.0	0.001	0.000	-0.002	-0.004	-0.005	-0.006	-0.007

Table B-9 Local anisotropic contributions in the xz plane with y = 4.0 Å.

x \ z	0.0	1.0	2.0	3.0	4.0	5.0	6.0
0.0	0.157	0.146	0.116	0.079	0.046	0.023	0.009
1.0	0.146	0.136	0.108	0.073	0.042	0.021	0.008
2.0	0.116	0.108	0.085	0.058	0.033	0.017	0.006
3.0	0.079	0.073	0.058	0.039	0.023	0.011	0.003
4.0	0.046	0.042	0.034	0.023	0.013	0.006	0.001
5.0	0.023	0.021	0.017	0.011	0.006	0.002	-0.001
6.0	0.009	0.008	0.006	0.004	0.001	-0.001	-0.002

Table B-10 Local anisotropic contributions in the xz plane with y = 5.0 Å.

y \ x	0.0	1.0	2.0	3.0	4.0	5.0	6.0
0.0	20.273	35.352	-7.400	-1.324	-0.491	-0.238	-0.134
1.0	10.844	7.819	0.107	-0.597	-0.342	-0.193	-0.117
2.0	3.768	2.736	0.898	0.061	-0.100	-0.099	-0.076
3.0	1.506	1.216	0.639	0.222	0.039	-0.020	-0.034
4.0	0.717	0.621	0.408	0.210	0.086	0.024	-0.003
5.0	0.390	0.352	0.263	0.165	0.090	0.042	0.015
6.0	0.233	0.217	0.175	0.124	0.079	0.046	0.024

Table B-11 Ring current contributions in the xy plane with z = 0.0 Å.

REFERENCES

1. A. Cotton and H. Mouton; Compt. rend., 141, 317, 349 (1905).
2. P. Langevin; Compt. rend., 151, 475 (1910).
3. C. V. Raman and K. S. Krishnan; Proc. Roy. Soc. (London), A113, 511 (1927).
4. K. S. Krishnan, B. C. Guha and S. Banerjee; Phil. Trans. Roy. Soc. London, A231, 235 (1933).
5. K. S. Krishnan; Nature, 130, 698 (1932).
6. K. S. Krishnan and S. Banerjee; Phil. Trans. Roy. Soc. London, A234, 265 (1935).
7. K. Lonsdale and K. S. Krishnan; Proc. Roy. Soc. (London), A156, 597 (1936).
8. K. Lonsdale; Proc. Roy. Soc. (London), A159, 149 (1937).
9. K. Lonsdale; Proc. Roy. Soc. (London); A171, 541 (1939).
10. R. C. Shaney, S. L. Aggarival and M. Singh; J. Indian Chem. Soc., 23, 335 (1946).
11. P. J. Garratt; Aromaticity, McGraw Hill, 1971, p. 25.
12. P. Ehrenfest; Physica, 5, 388 (1925).
13. C. V. Raman; Nature, 123, 945 (1929).
14. L. Pauling; J. Chem. Phys., 4, 673 (1936).
15. F. London; J. Chem. Phys., 5, 837 (1937).
16. F. London; J. Phys. Radium, 8, 397 (1937).
17. R. M. Lynden-Bell and R. K. Harris; Nuclear Magnetic Resonance Spectroscopy; Nelson, U.K., 1969.
18. L. M. Jackman and S. Sternhell; Applications of Nuclear Magnetic Resonance Spectroscopy in Organic Chemistry, 2nd Edition; Pergamon Press, London, 1969.

19. J. A. Pople, W. G. Schneider and H. J. Bernstein; High-resolution Nuclear Magnetic Resonance; McGraw Hill, New York, N. Y., 1959.

20. J. R. Dyer; Applications of Absorption Spectroscopy of Organic Compounds; Prentice Hall Inc., Englewood Cliffs, N. J., 1965.

21. W. E. Lamb; Phys. Rev., 60, 817 (1941).

22. N. F. Ramsey; Phys. Rev., 78, 699 (1950).

23. A. Saika and C. P. Slichter; J. Chem. Phys., 22, 26 (1954).

24. J. A. Pople; J. Chem. Phys., 24, 1111 (1956).

25. H. M. McConnell; J. Chem. Phys., 27, 226 (1957).

26. J. A. Pople; Proc. Roy. Soc. (London), A239, 541 (1957).

27. J. A. Pople; Proc. Roy. Soc. (London), A239, 550 (1957).

28. B. P. Dailey and J. N. Shoolery; J. Am. Chem. Soc., 77, 3977 (1955).

29. E. D. Becker; High Resolution NMR, Academic Press, New York, N. Y., 1969.

30. P. T. Narasimhan and M. T. Rogers; J. Phys. Chem., 63, 1388 (1959).

31. H. F. Hameka; Rev. Mod. Phys., 34, 87 (1962).

32. J. A. Pople; J. Chem. Phys., 37, 53 (1962).

33. J. A. Pople; J. Chem. Phys., 37, 60 (1962).

34. J. Guy and J. Tillieu; J. Chem. Phys., 24, 1117 (1956).

35. J. Tillieu; Ann. Phys., 2, 471, 631 (1957).

36. H. J. Bernstein, W. G. Schneider and J. A. Pople; Proc. Roy. Soc. (London), A236, 515 (1956).

37. F. Sondheimer; Pure Appl. Chem., 7, 363 (1963).

38. J. S. Waugh and R. W. Fessenden; J. Am. Chem. Soc., 79, 846 (1957).

39. W. R. Smyth; Static and Dynamic Electricity, 3rd Edition, p. 290, McGraw Hill Book Company Inc., New York, N. Y., 1968.

40. J. P. Blewett; J. Appl. Phys., 18, 968 (1947).

41. A. Agarwal, J. A. Barnes, J. L. Fletcher, M. J. McGlinchey and B. G. Sayer; Submitted for publication.

42. C. E. Johnson and F. A. Bovey; J. Chem. Phys., 29, 1012 (1958).

43. J. Hoarau; Ann. Chim. (Paris), 1, 560 (1956).

44. B. P. Dailey; J. Chem. Phys., 41, 2304 (1964).

45. J. A. Pople; Mol. Phys., 1, 175 (1958).

46. R. McWeeny; Mol. Phys., 1, 311 (1958).

47. G. G. Hall and A. Hardisson; Proc. Roy. Soc. (London), A268, 328 (1962).

48. P. J. Black, R. D. Brown and M. L. H. Heffernan; Australian J. Chem., 20, 1305, 1325 (1967).

49. C. W. Haigh and R. B. Mallion; Mol. Phys., 22, 945, 955 (1971).

50. C. W. Haigh and R. B. Mallion; Org. Magn. Reson., 4, 203 (1974).

51. R. B. Mallion; Mol. Phys., 25, 1415 (1973).

52. H. G. Ff. Roberts; Mol. Phys., 27, 843 (1974).

53. J. I. Musher; Adv. Magn. Reson., 2, 177 (1966).

54. J. M. Gaidis and R. West; J. Chem. Phys., 46, 1218 (1967).

55. J. I. Musher; J. Chem. Phys., 46, 1219 (1967).

56. R. C. Haddon, V. R. Haddon and L. M. Jackman; Top. Curr. Chem., 16, 103 (1971).

57. G. Berthier, M. Mayot, A. Pullman and B. Pullman; J. Phys. Radium, 13, 15 (1952).

58. K. G. Kidd, G. Kotowycz and T. Schaefer; Can. J. Chem., 45, 2155 (1967).

59. D. J. Wilson, V. Boekelheide, R. W. Griffin; J. Am. Chem. Soc., 82, 6302 (1960).

60. N. Jonathan, S. Gordon and B. P. Dailey; J. Chem. Phys., 36, 2443 (1962).

61. I. J. Maddox and R. McWeeny; J. Chem. Phys., 36, 2353 (1962).

62. J. D. Memory; J. Chem. Phys., 38, 1341 (1963).

63. R. J. Abraham; Mol. Phys., 4, 145 (1961).

64. G. Wagniere and M. Gouterman; Mol. Phys., 5, 621 (1962).

65. G. G. Hall, A. Hardisson and L. M. Jackman; Disc. Farad. Soc., 34, 15 (1962).

66. G. G. Hall, A. Hardisson and L. M. Jackman; Tetrahedron, 19, Suppl. 2, 101 (1963).

67. G. T. Robillard, C. E. Tarr, F. Vosman and H. J. C. Berendsen; Nature, 262, 363 (1976).

68. R. Benassi, P. Lazzeretti, I. Moretti, F. Faddei and G. Torre; Org. Magn. Reson., 5, 391 (1973).

69. K. W. Blake and B. Jaques; J. Chem. Soc. Perkin II, 1660 (1973).

70. F. J. Koer and C. Altona; Rev. Trav. Chim., 93, 147 (1974).

71. R. Korenstein, K. A. Muszkat and S. Sharafy-Ozeri; J. Am. Chem. Soc., 95, 6177 (1973).

72. C. F. G. C. Geraldes, V. M. S. Gil and D. H. Eargle; J. Chem. Phys., 59, 1166, 1171 (1973).

73. J. A. Pople; J. Chem. Phys., 41, 2559 (1964).

74. A. Pines, M. G. Gibby and J. S. Waugh; Chem. Phys. Lett., 15, 373 (1972).

75. S. Pausak, A. Pines and J. S. Waugh; J. Chem. Phys., 59, 591 (1973).

76. S. Pausak, J. Tegenfeldt and J. S. Waugh; J. Chem. Phys., 61, 1338 (1974).

77. M. Barfield, D. M. Grant and D. Ikenberry; J. Am. Chem. Soc., 97, 6956 (1975).

78. H. Eyring, J. Walter and G. E. Kimball; Quantum Chemistry, p. 163, John Wiley and Sons Inc., New York, N. Y., 1944.

79. J. A. Barnes; personal communication.

80. Handbook of Chemistry and Physics, 50th Ed., p. A-199, The Chemical Rubber Co., Cleveland, Ohio, 1969.

81. R. Ditchfield; Mol. Phys., 27, 789 (1974).

82. Sadtler Standard Spectra, Sadtler Research Laboratory, Philadelphia, Pennsylvania.

83. G. E. Maciel', J. W. McIver, N. S. Ostlund and J. A. Pople; J. Am. Chem. Soc., 92, 1 (1970).

84. The Aldrich Library of NMR Spectra, Aldrich Chemical Company Inc., Milwaukee, Wisconsin.

85. B. G. Sayer; personal communication.

86. N. L. Allinger; personal communication.

87. D. J. Cram and M. Goldstein; J. Am. Chem. Soc., 85, 1063 (1963).